Science Bulletin 62 (2017) 1388–1426

Contents lists available at ScienceDirect

Science Bulletin

journal homepage: www.elsevier.com/locate/scib

Science Bulletin
www.scibull.com

Review

# A review of concentrated photovoltaic-thermal (CPVT) hybrid solar systems with waste heat recovery (WHR)

Xing Ju [a], Chao Xu [a,*], Zhirong Liao [a], Xiaoze Du [a], Gaosheng Wei [a], Zhifeng Wang [b], Yongping Yang [a]

[a] Key Laboratory of Condition Monitoring and Control for Power Plant Equipment of Ministry of Education, School of Energy Power and Mechanical Engineering, North China Electric Power University, Beijing 102206, China
[b] Key Laboratory of Solar Thermal Energy and Photovoltaic Systems, Institute of Electrical Engineering, Chinese Academy of Sciences, Beijing 100190, China

ARTICLE INFO

*Article history:*
Received 17 August 2017
Received in revised form 26 September 2017
Accepted 30 September 2017
Available online 9 October 2017

*Keywords:*
Hybrid solar system
Waste heat recovery
Photovoltaic/thermal
Concentration
Concentrator photovoltaic/thermal

ABSTRACT

In conventional photovoltaic (PV) systems, a large portion of solar energy is dissipated as waste heat since the generating efficiency is usually less than 30%. As the dissipated heat can be recovered for various applications, the wasted heat recovery concentrator PV/thermal (WHR CPVT) hybrid systems have been developed. They can provide both electricity and usable heat by combining thermal systems with concentrator PV (CPV) module, which dramatically improves the overall conversion efficiency of solar energy. This paper systematically and comprehensively reviews the research and development of WHR CPVT systems. WHR CPVT systems with innovative design configurations, different theoretical evaluation models and experimental test processes for several implementations are presented in an integrated manner. We aim to provide a global point of view on the research trends, market potential, technical obstacles, and the future work which is required in the development of WHR CPVT technology. Possibly, it will offer a generic guide to the investigators who are interested in the study of WHR CPVT systems.

© 2017 Science China Press. Published by Elsevier B.V. and Science China Press. All rights reserved.

## 1. Introduction

Solar energy, as the radiant light and heat from the Sun, is deemed as an important renewable energy source. The annual potential of solar energy is 1,575–49,837 exajoules (EJ), which is 1.8–58 times over the estimated future world energy consumption of 860 EJ in 2040 [1,2]. Solar energy can be harnessed using a range of ever-evolving technologies, such as PV, concentrated solar power (CSP), solar thermal utilization, chemical process, artificial photosynthesis. From the global point of view, the PV technology and solar thermal technology for heating and cooling are more matured and commercialized than other technologies. During 2016, at least 75 GWdc of solar PV capacity and 31 GWth solar thermal capacity were added worldwide. Presently, the cumulative global solar PV and thermal capacity has increased to 303 GWdc and 456 GWth, respectively [3].

Due to the rising demand of producing electricity with alleviated pollution and reduced $CO_2$ emissions, the PV technology has been rapidly developed during the past decades. Solar PV gradually becomes the substantial power source in countries such as Honduras, Italy, Greece and Germany, covering 6%–10% national electricity demand. On the other hand, solar thermal technology, the history of which is much longer than the PV technology, has undergone a stable and rapid growth over many years. The solar thermal system usually uses the evacuated tube or flat-plate to collect solar radiation, and it is extensively used to provide domestic hot water, to heat and cool space, to dry crops, to cook, to distillation, and to provide heat, steam or refrigeration for other industrial or commercial processes. Despite these achievements, the global solar thermal market has faced challenging times during recent years, because the traditional mass markets of China and Europe are shrinking under market pressure from heat pumps and PV systems [4].

Although there is a competition in markets between PV and solar thermal, some researchers are striving to combine these two technologies. Though PV cells have hit a conversion efficiency record of 46.0% [5], conversion efficiencies of commercial PV modules are 14%–20% for silicon cells and 25%–30% for III-V multijunction cells [6]. Most of the remaining part of solar energy, which is dissipated as heat in PV techniques, can be harnessed by combining thermal systems. As the two technologies are complementary to each other, the PV/thermal (PVT) hybrid system has obtained a great interest in both solar thermal and PV research community. The advantage of PVT system is that not only the conversion efficiency of solar energy is improved [7], but also the utilization of

* Corresponding author.
*E-mail address:* mechxu@ncepu.edu.cn (C. Xu).

https://doi.org/10.1016/j.scib.2017.10.002
2095-9273/© 2017 Science China Press. Published by Elsevier B.V. and Science China Press. All rights reserved.

**Nomenclature**

*Symbols*

| | |
|---|---|
| $C_o$, suns | Optical CR |
| $C_g$, suns | Geometrical CR |
| $T_{in}$, °C | Inlet temperature |
| $T_{out}$, °C | Outlet temperature |
| $\Delta T$, °C | Temperature difference between $T_{in}$ and $T_{out}$ |
| $\eta_E$, % | Electrical efficiency |
| $\eta_T$, % | Thermal efficiency |
| $\eta_O$, % | Overall efficiency |

*Abbreviations*

| | |
|---|---|
| AHP | Absorption heat pump |
| ANU | Australian National University |
| BI | Building integrated |
| CFD | Computational fluid dynamics |
| COP | Coefficient of performance |
| CPC | Compound parabolic concentrator |
| CPV | Concentrator photovoltaic |
| CPVT | Concentrator photovoltaic/thermal |
| CR | Concentration ratio |
| CSP | Concentrated solar power |
| CST | Concentrating solar thermal |
| DA-CPV | Dense array concentrated photovoltaic |
| DNI | Direct Normal Irradiance |
| DWC | Solid desiccant wheel cycle |
| EDF | Energy distribution fitting |
| EJ | Exajoules |
| EX | Experimental |
| FEM | Finite element method |
| GJ | Gigajoules |
| HCPV | High concentrated photovoltaic |
| HCPVT | High concentration WHR CPVT system |
| HTF | Heat transfer fluid |
| LCoE | Levelized cost of energy |
| LCPVT | Low concentration WHR CPVT system |
| MCPVT | Medium concentration WHR CPVT system |
| MCT | Micro-Concentrator |
| MD | Membrane distillation |
| MED | Multiple effect distillation |
| MEED | Multi-effect evaporation desalination |
| MEMD | Multi-effect membrane distillation |
| NIR | Near-infrared |
| NM | Not mentioned |
| ORC | Organic Rankine cycle |
| PA | Patent |
| PCM | Phase change material |
| PMMA | Polymethyl methacrylate |
| PTC | Parabolic trough concentrator |
| PV | Photovoltaic |
| PVT | Photovoltaic/thermal |
| RO | Reverse osmosis |
| SBS | Spectral beam splitting |
| T&E | Theoretical and experimental |
| TCT | Total cross tied |
| TH | Theoretical |
| TPV | Thermo-photovoltaic |
| UV | Ultraviolet |
| VCC | Vapor compression cycle |
| VIS | Visible |
| WHR | Waste heat recovery |

solar energy is expanded as it produces both heat and electricity simultaneously [8,9]. As the flat stationary PV panel dominates the PV market, many of the studies are engaged in flat-plate PVT hybrid systems. These investigations are reviewed in many papers [10–14], including glazed/unglazed liquid/air flat-plate PVT modules. The integration of flat-plate PV and thermal collector reduces the production and installation costs, and it is scalable for different applications demanding both electricity and heat. As thus, the flat-plate PVT systems are quite practical, especially for integrating with building rooftop and façade [15]. However, considering the big drop between the theoretical and practical efficiencies and the costs, there is still a margin to improve the flat-plate PVT. Furthermore, since solar cells cannot be used as an efficient thermal absorber due to their large emissivity of the encapsulation material, the flat-plate PVT system usually generates low temperature heat, which is hard to use in most applications. Thence, the commercial flat-plate PVT systems usually focus on the solar cell cooling only, and the thermal energy is considered as a byproduct. As an alternative, the CPVT system uses low-cost optical elements to replace the expensive semiconductor materials of solar cells (typically silicon and III-V materials such as GaAs). The use of optical concentrators can increase the illumination on PV cells. On one hand, for the PV system, the output power of PV modules rises within a proper concentration ratio (CR) range along with the conversion efficiency [16]. The ohmic loss would also be reduced in series connected solar cells. Since the solar cell area is saved, expensive III-V multi-junction solar cells can be used to achieve higher efficiencies. On the other hand, for the thermal system, the thermal receiver area decreases, inherently reducing the thermal losses to circumstance. The thermal system can achieve an acceptable thermal efficiency and a higher thermal yield temperature than the flat-plate PVT, which expands the application area of the hybrid system.

Despite the aforementioned advantages, the CPVT hybrid system faces several challenges. Due to the precise 1-axis or 2-axis tracking system of concentrators, additional costs may be introduced in CPVT systems. The maintenance costs also rise because of the system complexity. The mismatch loss in PV modules, which occurs when the electrical parameters of one solar cell are significantly altered from those of the remaining devices, may deteriorate due to the non-uniform illumination and shading of the framework. Under non-uniform illumination, the inherent non-uniform temperature on PV cells also causes mismatch losses and hot-spot heating. High-heat flux heat-exchangers, which are employed to keep PV modules operating at a low and uniform temperature, are also crucial in CPVT systems. Moreover, the reliability and weatherability problems, including stagnation temperature, thermal shock and electrical insulations, are also more difficult when combining with concentrators.

The PV and PVT systems can be categorized as shown in Fig. 1. Presently, there are diverse configurations of CPVT system. Based on the distribution method and conversion sequence of energy flux, CPVT systems can be classified into three types: the WHR CPVT, the spectral beam splitting (SBS) CPVT, and the energy distribution fitting (EDF) CPVT. Similar to the CPV systems, as the system configuration is mainly affected by the CR of optical concentrators, WHR CPVT systems could be further categorized into three types: low CR system ($CR \leq 10x$) which is named as low concentration WHR CPVT system (LCPVT), medium CR system ($10x < CR \leq 100x$) which is named as medium concentration WHR

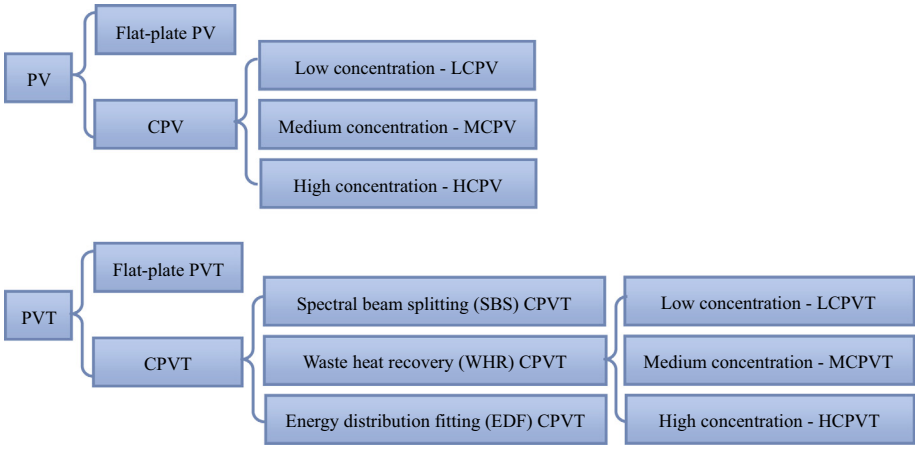



**Fig. 1.** (Color online) The category of PV and PVT systems.

CPVT system (MCPVT), and high CR system (CR > 100x) which is named as high concentration WHR CPVT system (HCPVT).

The system configurations and energy flux of WHR, SBS, and EDF CPVT systems are shown in Fig. 2 and described as follows.

(1) The WHR CPVT system is developed based on the conventional flat-plate PVT system. As shown in Fig. 2a and b, the thermal subsystem is the cooling system of PV modules and is usually active cooling on the module backside. In addition, there are other cooling methods, such as immersion cooling, passive cooling, and phase change cooling, that may also be adopted. During operation, all incident solar energy is firstly received by PV modules. Part of the radiation with energy near the bandgap of PV cells is converted into electricity in PN junction, while the majority of the rest part is converted to heat through the thermalization process. After that, the cooling system absorbs the heat for further utilization such as domestic hot water or space heating. From an energy conversion point of view, this process is based on cascade utilization of solar energy.

(2) The SBS CPVT system is based on the notion that solar energy can be utilized according to its spectral wavelength. The spectral beam of solar radiation is ranging from 200–4000 nm, corresponding to photon energy 0.31–6.20 eV. As only photons with energy over the solar cell bandgap can be converted by PV cells, photons with lower energy are directed to the thermal receiver for heat generation. As bandgaps of silicon and GaAs solar cells are 1.11 and 1.43 eV, respectively, the solar radiation is usually split into ultraviolet + visible (UV + VIS) part and near-infrared (NIR) part. As thus, the SBS CPVT system can make full utilization of solar energy in a broad solar spectrum wavelength range. As shown in Fig. 2c and d, an additional optical element for spectral beam splitting is necessary, and the spectral beam splitter could be a dichroic filter, a liquid or solid absorptive filter, a holographic filter, a luminescent filter, etc. [17]. Compared with the WHR CPVT system in which the temperature of the thermal subsystem is limited by PV cells' operating temperature, the SBS CPVT system has thermally decoupled PV and thermal subsystems, which means the thermal yield can achieve a higher temperature over the operating temperature limitation of PV cells.

(3) The EDF CPVT system is an emerging concept. As shown in Fig. 2e and f, the EDF CPVT system is specially designed for non-uniform concentrated solar radiation, such as the Gaussian distribution of point focused concentrators. This type of CPVT design aims to make full use of the spillage loss of the truncated energy profile. The edge part of concentrated illumination, which is usually discarded, is recovered in this type of CPVT. Under the non-uniform concentrated illumination, the facula area with different CRs can be adequately received by PV and thermal receiver separately.

The WHR and SBS CPVT systems have been developed since 1970s and 1980s [18], respectively, and they have been reviewed in several documents [18–31]. However, most of these papers mainly concern the examinations of flat-plate PVT systems, and discussions on CPVT systems are not quite profound and comprehensive. Only a few reviews are completely concerned for the CPVT, including the reviews of Sharaf and Orhan [19,20], Zhang et al. [21], and Ju et al. [32]. The scientific basics, the technological fundamentals, characteristics, design considerations, advances, solar components, energy and exergy models, performance assessment methods, and application areas of CPVT systems were summarized. As an emerging concept, researches on EDF CPVT is not enough. A typical research was recently presented by Meng et al. [33], in which an annular PV receiver is deployed outside of a thermal receiver. As thus, the central high concentrated illumination is received by the thermal receiver, and the remaining is converted by PV module. Reversed designs using high concentration area for PV and low concentration area for the thermal receiver were also proposed by Ju et al. [34] and Han et al. [35,36] for CPVT or CPV-CSP hybrid systems. Combinations of these three solar energy harness approaches may inspire novel designs and better performance, such as the combination of EDF and WHR concept [34–36], and the combination of interference/absorption SBS and WHR concept [37–39].

The above three types of CPVT differ greatly from each other. Most of the review papers are not concerned with a specified type of CPVT. Especially for WHR CPVT, although it seems simpler than the other two types of CPVT, it's design and operation constraints are much tighter. The system designs and performance characteristics are quite different from that of SBS and EDF CPVT systems. Studies on WHR CPVT techniques have not been systematically and comprehensively reviewed yet. A review particularly on WHR CPVT researches would be helpful to achieve better understanding on this kind of CPVT technology.

This paper aims to provide an up-to-date comprehensive review of the research and development of CPVT systems using WHR technologies. Basic conceptions and the purpose of this paper are introduced in Section 1. Section 2 provides brief profiles of the research documents on different types of WHR CPVT systems, including the CPVT systems using low, medium and high concentration solar collectors, and the researches mainly concerning applications. The special components and system configurations, system characteristics, application fields, advantages and disadvantages of these WHR CPVT systems are presented in detail. Section 3 summarizes

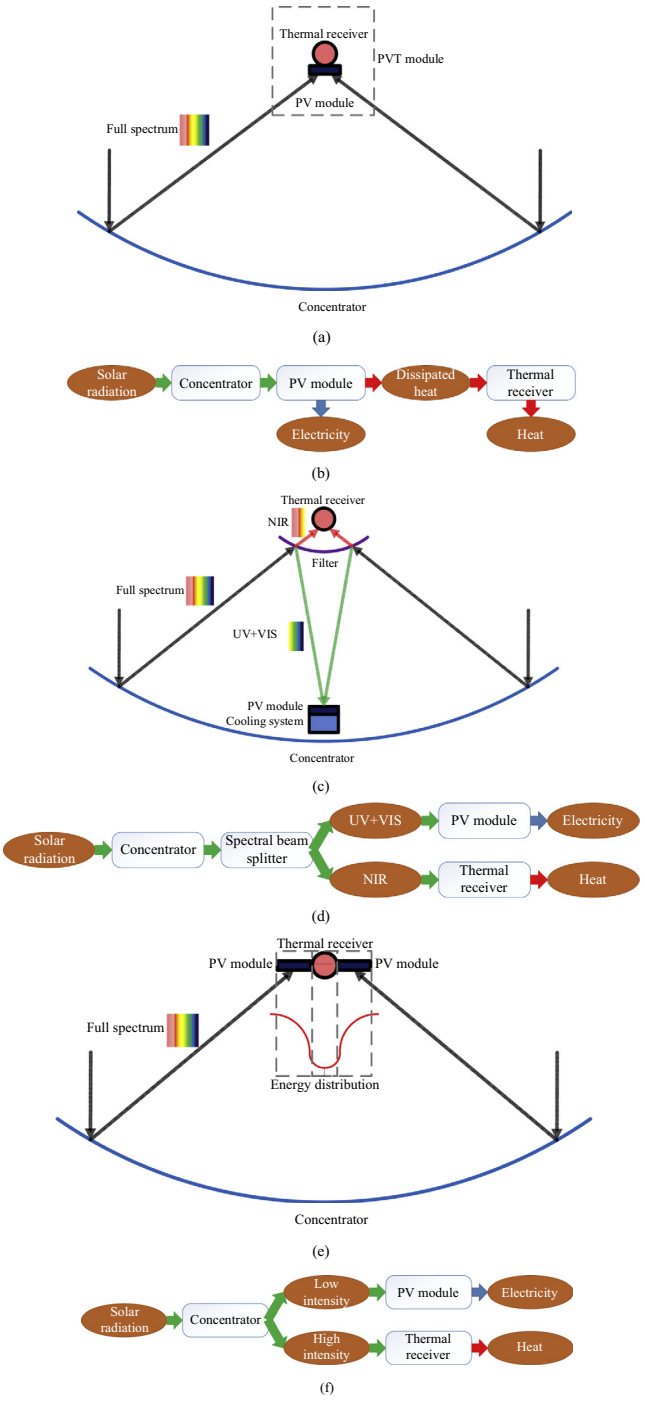



**Fig. 2.** (Color online) The classification of CPVT system: (a) basic system configuration of WHR CPVT; (b) energy flux of WHR CPVT; (c) basic system configuration of SBS CPVT; (d) energy flux of SBS CPVT; (e) basic system configuration of EDF CPVT; (f) energy flux of EDF CPVT.

the research development status. The characteristics of different WHR CPVT systems, including the research method, system efficiency, CR, HTF temperature, application area, type of optical elements and solar cell, and heat recovery materials, are compared in this section. The performances of WHR CPVT systems are also compared to the results from the SBS CPVT review paper [32]. Finally, Section 4 makes a conclusion on the development of this technology, involving the research trends, market potentials, technical obstacles, and the future work required.

## 2. Studies of the WHR CPVT systems in the literature

Different optical systems are applied in the thermally coupled WHR CPVT systems, including flat specular/diffuse reflectors, compound parabolic concentrators (CPCs), linear Fresnel reflectors, parabolic troughs, dish reflectors, tower-heliostats, Fresnel lenses and so on. The CR of the optical system is a key parameter of system configuration, and it influences significantly the thermal system design, the type of solar cells, the adoption of tracking systems, the electrical and thermal performance, and the system costs. What's more, the CPVT system can be used for various applications, and some of the applications do not have to be combined with complex auxiliary systems, such as to provide heat or hot water for buildings, to cook food, and to dry crops. As these researches mainly involved CPVT systems itself, we discuss them according to the three types of WHR CPVT system: LCPVT, MCPVT, and HCPVT. Other examinations concerning the application systems, including desalination, air-conditioning, polygeneration, and absorption cooling, are discussed in an independent section.

### 2.1. Low concentration WHR CPVT system (LCPVT) (CR = 1–10x)

The LCPVT systems of CR < 10x are the simplest type of CPVT approaches. Flat specular/diffuse reflectors and CPCs are the typical optical configurations of LCPVT systems, and parabolic reflectors and linear (2D) Fresnel lenses have also been applied in LCPVT systems.

#### 2.1.1. Flat plate reflector/V-trough

For CPVT systems of CR $\leq$ 4x, both the flat-plate reflector (or more precisely the booster) and V-trough can be used as the concentrator. As flat reflectors usually combine with stationary PV modules, the orientation of flat reflectors and PV absorbers should be optimized to obtain the maximal concentration of solar radiation intensity. Solar panels or PV cells connected in a row and bonded into flat-reflector/V-troughs are used as solar receivers. Water/air flows in pipes or tubes under the solar cells to harvest the wasted heat from solar cell modules.

(1) Flat specular reflector

Configurations of typical LCPVT systems using flat-plate reflectors are shown in Fig. 3. The flat-plate boosters can be mounted on one side, or both top and bottom sides of the PVT panel. The system is usually stationary, since the tracking system would introduce an uncompensated cost increase. Al-Baali [40] tested a stationary solar panel that utilized a reflecting mirror and a water circulation. The reflecting mirror was mounted on the topside of solar panel (Fig. 3a). Under low concentrated illumination of 0.12 W/cm$^2$, the measured data showed the one-side mirror configuration would increase the power output by about 25%, and the increase in cooling water temperature was 13 °C, namely from 29 to 42 °C. A LCPVT module with a bottom booster and an active PVT air collector was tested by Haddad et al. [41]. They compared the performance of various system configurations, containing separate PV panel and PVT panel with and without aluminum plate reflectors. Compared to the separate PV panel, the PVT with finned channels and aluminum plate reflectors showed a better performance. Studies of Garg et al. [42] discussed the solar panels combining solar air heaters for drying. The panels with different booster structures (no booster, top booster, bottom booster, and both boosters (Fig. 3b) were theoretically compared. The results showed that the solar cell area can be reduced by using flat-plate boosters, and the costs can be saved.

The passive cooling design can be a viable option for the flat-plate LCPVT systems. As shown in in Fig. 4, Ziapour et al. [43] proposed a passive cooling LCPVT system with a finned

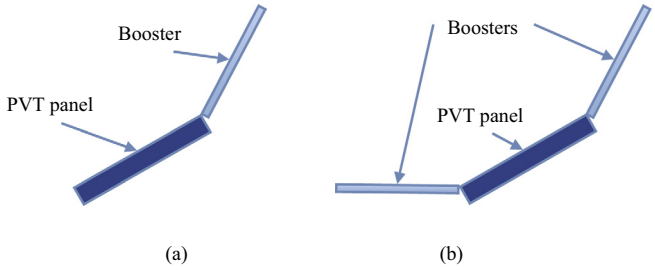



**Fig. 3.** (Color online) The LCPVT system using flat-plate boosters as the concentrator: (a) top booster; (b) top and bottom booster.

cooling chamber and aluminum plates. The simulated results illustrated that the hybrid system with fins in the absorber plate backside shows a better performance than the hybrid system without fins [44].

Except for the stationary configurations, some researches in this field adopted tracking techniques. Segmented flat mirrors were usually applied to increase the CR and thus reduce the costs. As shown in Fig. 5, Du et al. [45] measured the performance of a 2-axis tracking CPVT system with segmented flat mirrors as the reflector. The system CR achieved 8.5x, which led to 4.7–5.2 times of output power over the fixed cells, and the thermal and electrical efficiencies were 45% and 8.2%, respectively. Using finite-volume computational fluid dynamics (CFD) method and discrete ordinates (DO) radiation model, Chaabane et al. [46] simulated the performance of such system with different cooling configurations, including the connected pipes (the configuration of 2-connected pipes is the same as the cooling system presented by Du et al. [45]) and rectangular channel. The rectangular channel cooling system performs better in lessening the hot spots of CPV, and achieves theoretical thermal and electrical efficiencies of 74.2% and 9.3%, respectively.

Bifacial PV panels were also used in the LCPVT system to increase the total power output. Robles-Ocampo et al. [47] constructed and studied a bifacial PV module. As shown in Fig. 6, the bifacial PV module combined a water-filled transparent solar collector and two additional pairs of reflecting wings. Water layer on the upper face of bifacial PV panel absorbed light of the infrared region above 1100 nm, and the illumination on the rear face was enhanced by the stainless-steel planes. The water temperature increase of about 15–20 °C was measured, and the thermal and electrical efficiencies of the system were estimated to be 50% and 16.4%, respectively. Bifacial receiver CPVT system can also adopt 1-axis tracking, as the prototype of Ibrahim and Khalil [48]. The geometrical CR of the bottom PV module was 4x. The measured results demonstrated that the power produced by pc-Si cells was nearly 3 times compared to a normal module, and the cooling water temperature rose from 22.4 to 53 °C.



**Fig. 5.** (Color online) The LCPVT system with segmented flat mirrors and a 2-axis tracking system. Reprinted with permission from Ref. [45]. Copyright © 2012 Elsevier.

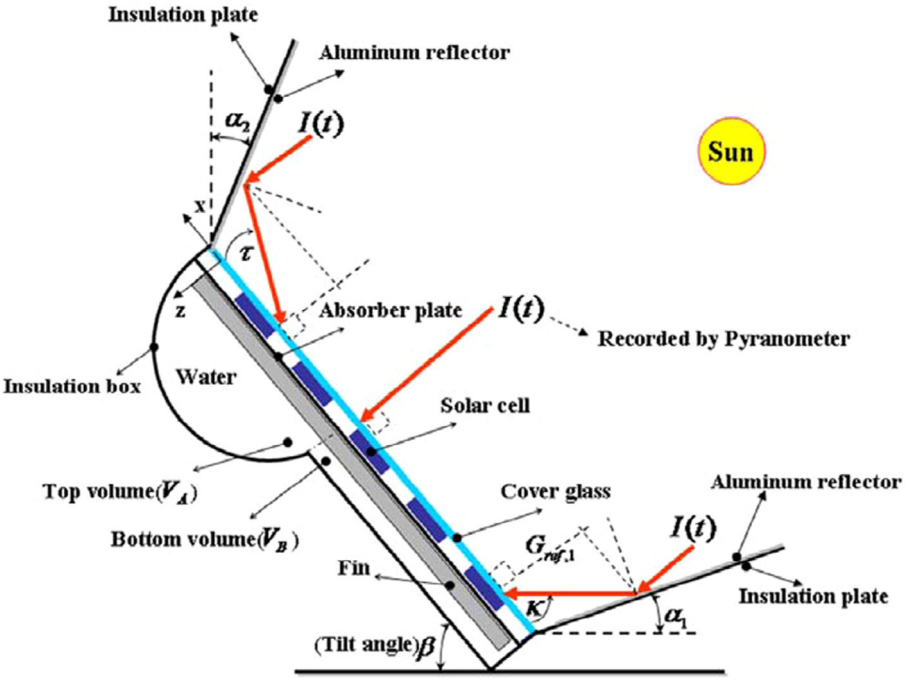



**Fig. 4.** (Color online) The passive cooling LCPVT system with a finned cooling chamber. Reprinted with permission from Ref. [43]. Copyright © 2016 Elsevier.



**Fig. 6.** (Color online) The stationary LCPVT system with a bifacial receiver. Reprinted with permission from Ref. [47]. Copyright © 2007 Elsevier.

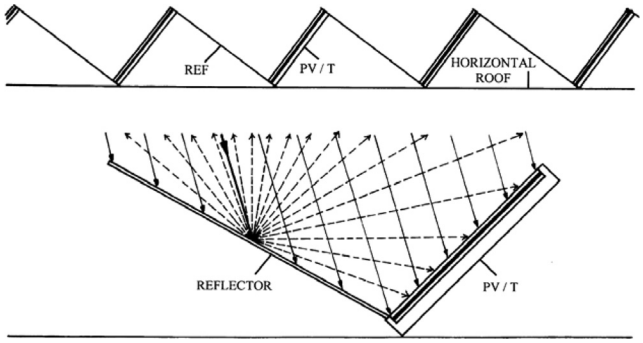



**Fig. 7.** The BI-LCPVT system with a booster diffuse reflector. Reprinted with permission from Ref. [50]. Copyright © 2002 Elsevier.

The light funnel flat-plate concentrator was also utilized in LCPVT designs. Gurel [49] designed and tested a CPVT system with a sphere PVT receiver. The receiver was placed at the focal point of a light funnel concentrator consisting of 4 mirrors, and filled with paraffin wax as the phase change material (PCM), which was different from other researches usually using water or air as the coolant. Even at concentrated radiations, the average PV cell temperature still kept at about 30 °C. The average electrical efficiency of PV cells was calculated as 14.67%. Using paraffin wax was considered as an efficient cooling and thermal energy storage method.

(2) Flat diffuse reflector

Different from the specular reflectors, the flat diffuse reflectors could achieve smoother solar radiation distributions on the PV surface. Although the CR on the surface of PV modules is usually lower than that of specular reflectors, the diffuse reflectors are cheaper and can be easily combined with typical size PV modules.

Fig. 7 shows the building integrated LCPVT (BI-LCPVT) system proposed by Tripanagnostopoulos et al. [50,51]. The system used flat aluminum plates as the booster diffuse reflectors. The reflectors were mounted onto one side of pc-Si / a-Si PV panel, resulting in an optical CR of 1.35x. The experimental results showed that the system achieved an electrical output increase of about 16% compared with the basic PVT systems, and also gave a remarkable thermal heat extraction efficiency of 30% for air as the HTF and 60% for water.

Tripanagnostopoulos et al. [52] also presented and studied several designs of BI-LCPVT, including rooftop or façade integrated diffuse/specular boosters, V-troughs, symmetric/asymmetric CPCs. For these proposed stationary systems, the CRs were lower than 2.5x. The tests showed that the use of 2.5x concentrated diffuse and specular reflectors resulted in 24% and 113% increases in electricity output, respectively. For 1.5x concentrated diffuse and specular boosters, the electricity output increased by 16% and 75%, respectively. As thus, the reflector length was more significant for the specular reflector than the diffuse one. They also proposed novel designs of BI-CPVT, in which large stationary CPCs were integrated into the walls or roofs, and the moving PVT module was used for tracking.

Kostić et al. [53] discussed the optimal position of flat-plate reflectors theoretically and experimentally. They also compared the energy-saving efficiency [54] of the LCPVT system with or without aluminum plates mounted in both sides of a c-Si PV module as the diffuse reflectors. The results indicated that although the energy-saving efficiency of LCPVT collector decreased slightly with the CR of solar radiation, the total thermal and electric energy generated by the LCPVT with reflectors in the optimal position was significantly higher than that generated by the PVT collector without reflectors. They also compared the influence of flat-plate concentrators with different reflectances (aluminum sheet and foil) [55]. Since aluminum foil has a better specular reflectance, the LCPVT system with aluminum foil showed better performance than the one with aluminum sheet in all reflector positions.

(3) V-trough

V-trough CPVT systems can be regarded as a discrete type of flat-plate LCPVT. Solar panels are replaced by linear solar cells on the bottom of V-trough. Compared with the LCPVT systems with flat-plate boosters, the optical losses would be reduced due to the shorter distance between cells and reflectors. After developing the LCPVT with flat specular reflectors [42], Garg et al. [56] developed a LCPVT system with stationary V-trough and thermosiphon water heating. Various electrical and thermal experiments were carried out to study the performances. Künnemeyer et al. [57] presented theoretical and experimental studies on a stationary V-trough CPVT system. The basic unit of the V-trough solar receiver is shown in Fig. 8. The reflectors were fabricated from specular stainless-steel sheets to meet the design life in New Zealand's corrosive maritime climate. The stainless steel plate, rather than the more reflective aluminum, would still offer 25% increase in the incident radiation over a typical year. The optical CR near the equinoxes was about 1.6x, but it was lower near the solstices. The peak combined thermal and electrical efficiency of the collector was about 35%, which was much lower than the designed peak efficiency (70%) because of the increased heat losses by radiation and convection in the absence of a glazing layer. Except for the stationary V-trough CPVT systems, a V-trough solar collector adopting a 2-axis tracking was also patented [58].

### *2.1.2. Compound parabolic concentrator*

CPC is a non-imaging optical device that uses parabolic mirrors to guide the light to the receiver. The studies on LCPVT systems with CPC is summarized as follows.

(1) Symmetrical CPC trough

The symmetrical CPC trough is the most widely used concentrator for LCPVT systems. Many researches had investigated the performance of CPC-LCPVT systems. Hedayatizade et al. [59] developed detailed energy balance and electrical model for a CPC-LCPVT system with finned-tube, and the simulation results were in good agreement with the experimental results of Huang et al. [54]. The thermal and electrical model developed by Cheng et al. [60] was also used to predict the performance of such LCPVT systems. Despite these modelling investigations, the CPC-LCPVT system was usually compared with flat-plate PVT systems, both

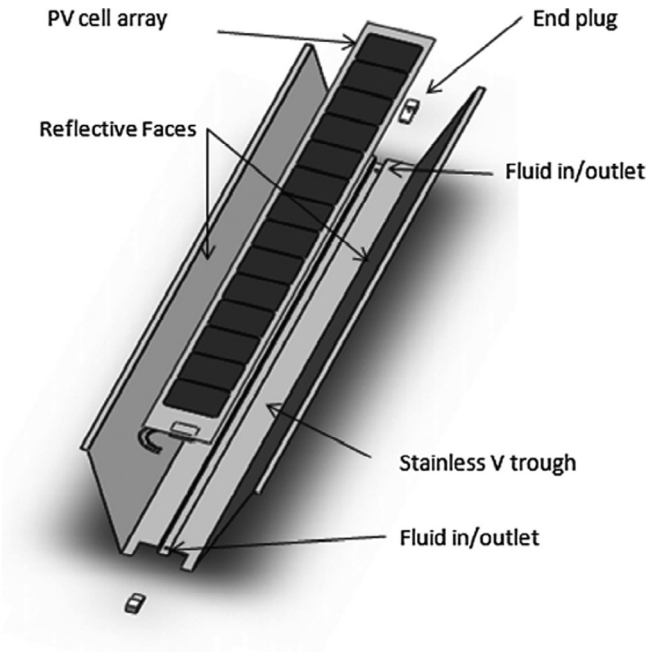



**Fig. 8.** The V-trough LCPVT system with active cooling. Reprinted with permission from Ref. [57]. Copyright © 2014 Elsevier.

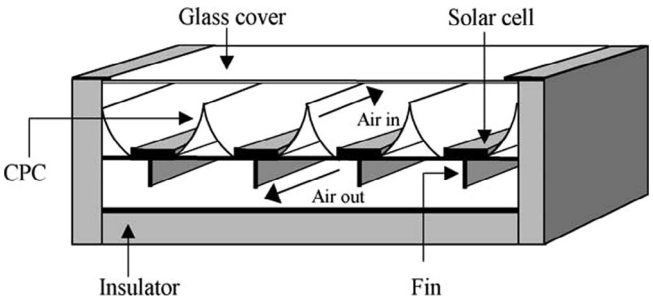



**Fig. 9.** The double-pass air LCPVT system with a symmetrical CPC. Reprinted with permission from Ref. [64]. Copyright © 2005 Elsevier.

theoretically and experimentally. Garg and Adhikari [61] investigated an LCPVT system that coupled CPC and air heating collector. The CPC trough was designed for 2.88 suns [62]. The parametric study showed that the thermal and electrical output increased with the collector length, air mass flow rate and packing fraction, but decreased with the increase in duct depth. According to the research, the system coupled with CPC always performed better in terms of both the thermal and electrical output than the hybrid system without CPC. A contrary opinion was proposed by Redpath et al. [63]. They compared a flat-plate PVT with a CPC-LCPVT using a heat-pipe. It was experimentally demonstrated that the CPC-LCPVT had a lower thermal efficiency (54%) than the flat-plate PVT (67%). However, the heat-pipe cooled CPC-LCPVT system responded much more rapidly, and thus was more suitable for transient climatic conditions.

Researches on designs of CPC-LCPVT systems focused on its two critical components: the energy conversion component (PVT module), and the energy collection component (CPC trough). Normal designs of the PVT module are PV cells with channels or tubes underneath, which are not different from PVT modules mentioned before, but there also exist special designs considering the speciality of objects. If using air as the HTF, the thermal systems can be designed to a double-pass configuration. Othman et al. [64] designed and fabricated a prototype double-pass PVT solar air collector with CPC and fins. As shown in Fig. 9, air flows through the upper channel formed by the glass cover and the PV panel and is heated directly by the sun. Then it enters the lower channel formed by the PV panel and the back plate with fins. Both the indoor test and the steady-state theoretical analysis demonstrated that, at solar irradiance of 500 W/m$^2$, the system of 1.86x concentration achieved an overall efficiency of over 60%, and it produced a hot air of over 50 °C when the inlet air temperature was 31–32 °C. A transient model simulation [65] and an experimental test [66] were also carried out to investigate the performance of a single-pass PVT solar air collector. The measured results showed that, at a solar irradiance of 400 W/m$^2$, the overall efficiency ranged from 27.5% to 40.0%. The double-pass CPC-LCPVT systems with and without fins were compared for a selected case at Dhahran, Saudi Arabia [67]. The CPC-LCPVT with fins had more than 3% thermal and 8% electrical gain than that without fins, and the CPC-LCPVT showed better performance than the flat PVTs. The materials (including aluminum, copper, brass, and nickel) and shapes (including rectangular, triangular, and parabolic) of fins were also investigated, among which the copper rectangular fin noted the best performance. A similar system with a 2x geometrical CR was also investigated by Sun and Shi [68,69], Sun and Wang [70]. It was illustrated that the electrical efficiency boosted, but both the thermal efficiency and the total efficiency declined when increasing the packing fraction.

Although most of PVT receivers are fully covered by PV cells, it can be otherwise partially covered by PV. Therefore, the energy proportion of PV and thermal subsystem is adjustable. Atheaya et al. [71] theoretically compared the partially covered CPC-LCPVT (Fig. 10a) with fully covered CPC-LCPVT and fully/partially covered flat-plate systems. The 25% partially covered CPC-LCPVT achieved the highest overall exergy efficiency, and the fully covered CPC-LCPVT was most suitable to meet the electrical and thermal energy demand. Exergy analysis for a constant collection temperature of 50 °C was also carried out [72]. The outlet fluid temperature, electrical efficiency, thermal energy, electrical energy and overall exergy efficiency of the systems were presented. Designs of partially covered CPC-LCPVT with inverted glazed and unglazed absorbers (Fig. 10b) were also compared [73]. The glazed one was more suitable for higher thermal energy, while the inverted one was more cost-effective. The system performance was detailed analyzed in Refs. [74–76], including the energy and exergy efficiencies, economics, and $CO_2$ emission for different Indian climatic conditions. The use of different HTFs (e.g., Molten salt and water) was also compared [77]. The 25% PV covered CPC-LCPVT collector using molten salt as the HTF achieved higher fluid temperature and overall thermal energy, and thus was more suitable for high steam cooking. At geometrical CR of 2x, the molten salt outlet temperature can achieve about 190 °C at January.

There also exists a special design of the PVT module. In most of the WHR CPVT systems, solar cells are directly used as the thermal absorber. However, compared to the vacuum tube and selective coating applied in solar thermal systems, the heat losses would be much higher, because of the large emissivity of PV encapsulation material. Jiang et al. [78] and Jiang and Winston [79] proposed a CPVT system using a vacuum encapsulated thin film cell to minimize heat losses. As displayed in Fig. 11, an external CPC was employed as the concentrator, and the absorber was embedded in a glass evacuated tube to lock the heat [80]. The transparent conductive oxide electrode of the thin-film solar cell was transparent in visible light and reflective beyond infrared, such that the heat loss could be minimized. The simulation results of a thermosyphon system applying this configuration demonstrated that the whole surface of tube wall can heat up, and negative effect of hot spot on the thermal efficiency can be neglected.

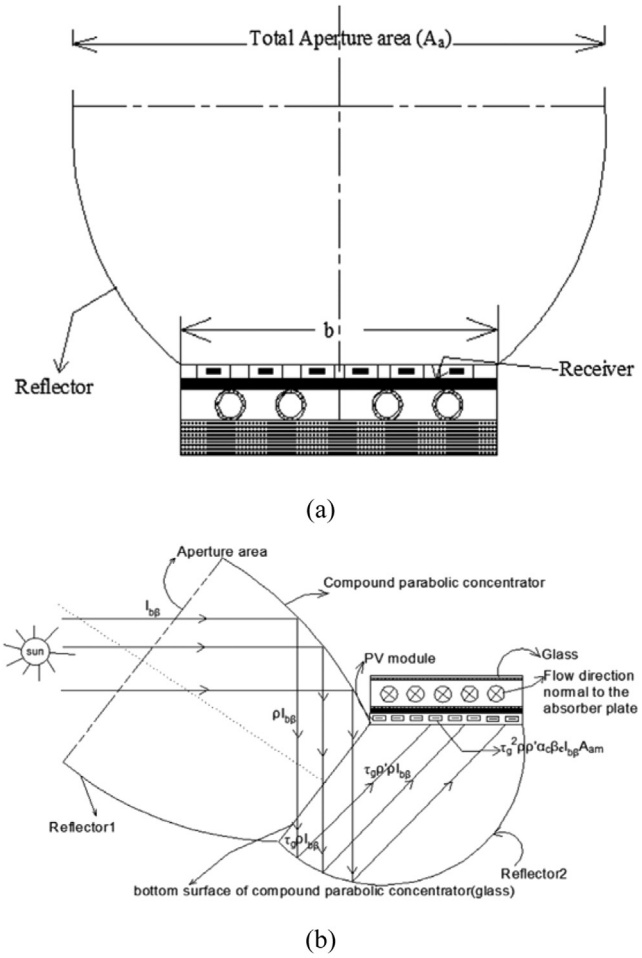



**Fig. 10.** The LCPVT system with partially covered CPCs. (a) the horizontal configuration; (b) the glazed inverted configuration. Reprinted with permission from Refs. [71,73]. Copyright © 2015 and 2016 Elsevier.

The thermal subsystem is a critical issue for designing a PVT module. It should be designed to efficiently remove the dissipated heat and achieve uniform temperature distribution on solar cells. Li et al. [81] proposed a thermal subsystem design with a U-type pipe as the thermal collector. The temperature uniformity on the whole absorber and cells would benefit from the U-type pipe design, such that the solar cells can simultaneously produce electricity at the same temperature. Proell et al. [82] studied the optimum operating temperature of a PVT collector. Based on the exergy analysis and carbon emission reduction analysis, they suggested that a 60–80 °C outlet temperature was optimum. After that, a 3x concentrated CPC-CPVT prototype was tested at different incident angles and fluid temperatures. The influence of non-uniform illumination on the electrical efficiency of different PVT absorbers was presented. The temperature distribution of PVT absorber was also experimentally and theoretically investigated [83]. It was noted that the aluminum absorber with multi-channels performed better than the conventional copper plate with a central fluid pipe. The PCM can also be applied in thermal systems [84]. As shown in Fig. 12, under the absorber plate and copper pipes, a thin layer of paraffin as the PCM to store the generated heat. A 1-axis tracking CPC trough with a maximum CR of 1.82x was mounted on the collector. Outdoor experiments were carried out in the winter season, and the results proved that the overall efficiency of the PVT collector was between 55% and 63% for clear day and around 46%–55% for semi-cloudy day. The corresponding top heat loss value was around 3 W/(m$^2$ °C) for clear day and around 2.5 W/(m$^2$ °C) for semi-cloudy day.

There are also margins to improve the design of the energy collection component (CPC trough). Studies on the optical elements of CPC-LCPVT have developed various methodologies to improve the optical performance and reduce the costs. Brogren et al. [85,86] built a 4x concentrated CPC LCPVT system in a high latitude location (Alvkarleby, Sweden). The system optical efficiency using bright anodized aluminum reflectors was 71%, which was limited because of the mismatch between the reflectance and the bandgap of silicon solar cell. It was suggested that the antireflection-treated glazing and optimized reflectors such as silvered thin glass mirror and interference coated aluminum mirror could further increase the electrical output by 20%.

As the height of conventional CPC increases greatly with increasing the geometrical CR, problems of large reflector consumption and deteriorative optical performance would be encountered. Xie et al. [87,88] designed new-type truncated CPCs eliminating multiple reflections. A truncated CPC with the highest truncation position was tested and showed improvements in the tradeoff between cost reduction and optical performance. The CPC with the lowest truncation position was also investigated. The results of material consumption assessment and Monte-Carlo simulation showed that the material consumption of CPC with lowest truncation position was about 80% of the highest one while the optical performance was almost the same, indicating that CPC with lowest truncation position has more extensive application potential.

Li et al. [89–91] proposed a novel CPC optical element, as shown in Fig. 13. The concentrator was composed of a mirror CPC and lens-walled structure, which can make full use of the total internal

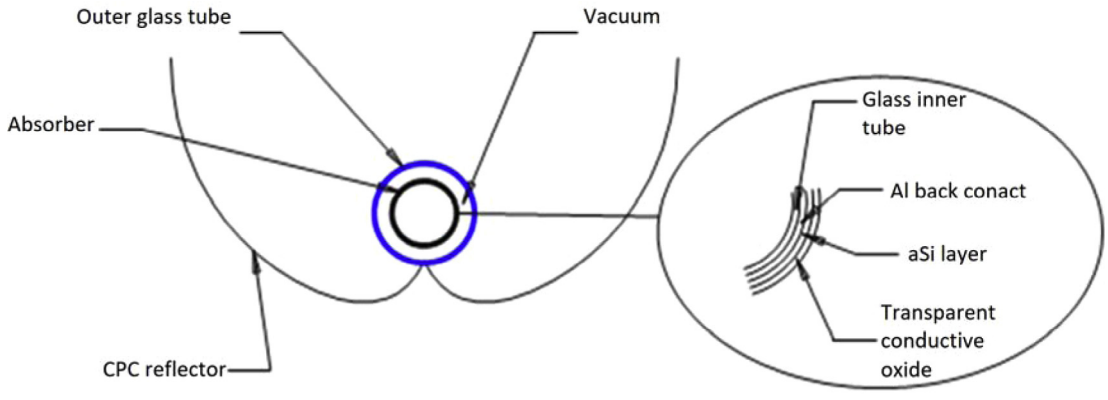



**Fig. 11.** (Color online) The LCPVT system with an external CPC and an outer glass tube. Reprinted with permission from Ref. [80].

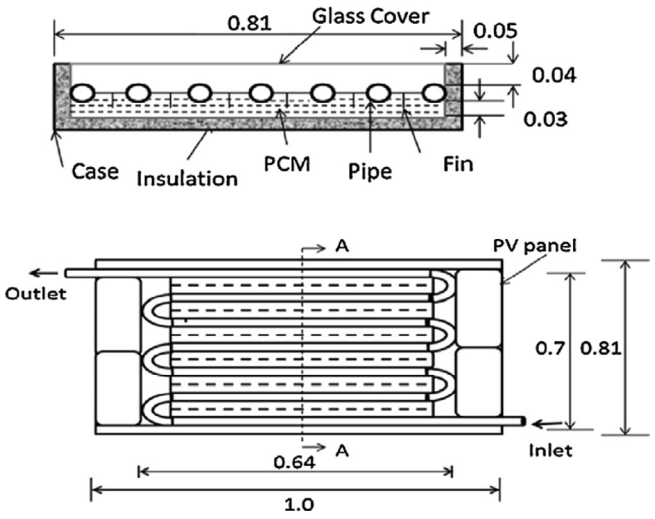



**Fig. 12.** The LCPVT system with a PCM thermal energy storage. Reprinted with permission from Ref. [84]. Copyright © 2016 Elsevier.

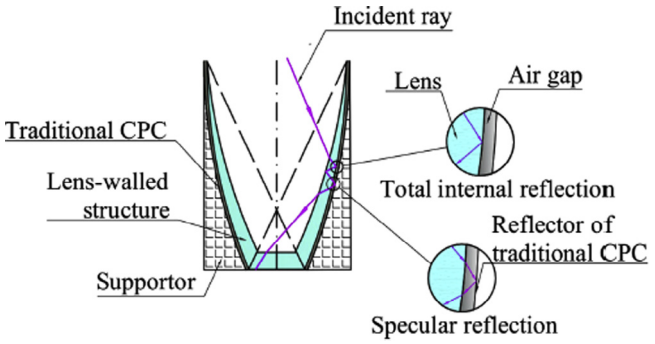



**Fig. 13.** (Color online) The novel LCPVT system with a lens-walled CPC mirror. Reprinted with permission from Ref. [89]. Copyright © 2016 Elsevier.

reflection and specular reflection. The theoretical optical efficiency was ranged between 56% and 70%, depending on the application conditions, and the experimental optical efficiency values were similar to the theoretical ones. The tested electrical and thermal efficiencies were 6.0% and 35.0%, respectively, and the final water temperature achieved 70 °C.

Another research used a quasi-CPC-LCPVT system consisting of multiple flat mirror segments to avoid the use of expensive curved mirror which is usually used in standard CPC [92]. The overall efficiency of the CPVT system was measured to be above 70%, indicating that the design had the potential of reducing the costs without greatly reducing the conversion efficiency.

(2) Asymmetric CPC trough

Unlike the symmetrical CPC troughs, the two segments of the asymmetric CPC consist of two different lengths of parabola, such that the concentrator has a wider acceptance angle, and both direct and a significant component of diffuse insolation is concentrated. For that reason, the asymmetric CPC systems were usually designed for BI-LCPVT and high latitude locations. As shown in Fig. 14a, different MaReCo (Maximum Reflector Collector) hybrid systems [93] were set up in Lund, Sweden, to evaluate the long term performance. The measurements showed that the front reflector collected most of the irradiation in the summer, and the back reflector in the spring and fall. The reflector materials were also experimentally investigated, and the tested anodized aluminum and aluminum laminated steel showed no significant difference in yearly output. The steel based reflector seemed an interesting option, although it was considered to be less effective in the previous work [57]. As suggested in Ref. [94], although the optimal placement of PV cells is facing the front reflector, having cells on both sides is in most cases the best option because of the solar cell's low price. This asymmetrical CPC trough was redesigned and optimized for better performances [94]. As shown in Fig. 14b, the receiver consisting of two PV strings at both front and back sides was placed on the receiver top. Influences of the incidence angle in both the longitudinal and transversal directions were tested. At peak hours, the measured efficiency was 20.9% per cell area and 13.9% per active glazed area. Several prototypes of the CPVT collector (with reflective/transparent end gables and different cell sizes) were further tested and compared [95], in order to minimize the impact of shading at oblique solar incidence angles. The measured results showed that, at large incident angles, the system with transparent end gables and larger cells performed better. Furthermore, the best configuration of cell string layout was also discussed [96], and the reliability with consideration of shading was proved.

Chaabane et al. [97] also designed and tested an asymmetrical CPC-LCPVT system for a given spring climatic condition of the Tunisian Saharan city Tozeur. Compared to the CPV system, although the hybrid system was simplified and cost-reduced, the combined thermal and electrical efficiency still reached 26%.

*2.1.3. Parabolic reflector and trough*

Parabolic reflectors use truncated parabolic mirrors to concentrate solar radiation, and could be considered as a special design of parabolic troughs. Brogren et al. [98] developed a ready-to-use façade element, including parabolic aluminum reflectors, Cu(In, Ga)$Se_2$-based Siemens ST5 thin-film PV modules and an EPS insulation. After that, the thin film module presented above was exchanged by a PVT hybrid module using c-Si solar cells as the receiver [99], as illustrated in Fig. 15. This design was found to be attractive for building integration at high latitudes. Similar concentrator design was applied in a building-integrated multifunctional PVT solar window [100], as shown in Fig. 16. This solar window can replace installations of PV modules, solar thermal collectors and sun shades. The solar window can annually produce about 35% more electric energy per unit cell area compared to a vertical flat PV module. It also can produce more heat per absorber area than a flat-plate solar collector placed on the roof at 20° tilt angle (Solgarden, Sweden). It should be noticed that about 40% of the annual electrical energy produced in the window is due to diffuse radiation.

The Solar-8 CPVT system [101,102] constructed in Lund, Sweden consisted of two separate parabolic reflectors, a PVT absorber in the middle and a 1-axis tracking system. The geometrical CR of Solar-8 was 10x. It was noticed through the simulation results that the thermal output in Madrid Spain is over 2 times of that in Lund Sweden, and the electrical output is over 6 times, which is due to the lower ratio of direct radiation in Northern Europe.

For the purpose of developing CPVT standard testing procedure and evaluation methodology, a complete methodology to characterize, simulate and evaluate CPVT hybrids has been proposed by Bernardo et al. [103]. The test bench applied a similar optical system as the Solar-8 system. The CR was reduced to 7.8x, since the bifacial flat PVT absorber was replaced by a triangle PVT absorber. The hybrid electrical efficiency was 6.4% while the optical efficiency was 45% and the U-value was 1.9 W/($m^2$ °C). Such values were much lower than conventional PV modules. Moreover, the beam irradiation incident on a north-south axis tracking surface was 20%–40% lower than the global irradiation incident on a fixed surface at the optimal tilt. These factors make the studied hybrid

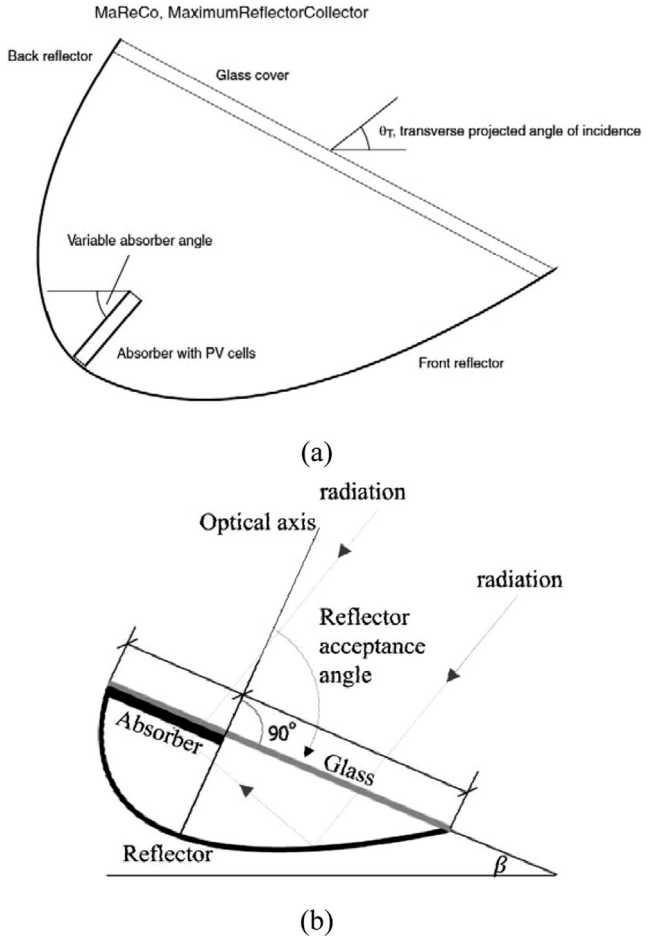



**Fig. 14.** The LCPVT system with an asymmetrical CPC collector: (a) MaReCo system; (b) redesigned MaReCo system. Reprinted with permission from Refs. [93] and [94]. Copyright © 2007 and 2014 Elsevier.

difficult to compete with conventional PV modules and flat-plate collectors.

*2.1.4. Linear (2D) Fresnel lens*

The linear Fresnel (2D) lens has gained more attention than the circular Fresnel (3D) lens as it only demands 1-axis tracking and can easily combine with the PVT system. However, optical losses of linear Fresnel lens are usually high, mainly because of the reflection, diffraction, absorption and chromatic aberration, which result from the structure and material of lenses. Since the lenses can separate direct and diffuse solar radiation, this advantage makes them suitable for the combined demands of electricity, heat and illumination in greenhouses and buildings.

Tripanagnostopoulos et al. [104,105] performed an experimental study on a 2x concentrated linear Fresnel solar system in buildings and greenhouses, which could provide cooling, heating, lighting control and power generation based on the CPVT concept. As shown in Fig. 17, the linear Fresnel lenses were mounted stationarily on the building sunspace roof and combined with PVT receivers. The incident beam solar radiation was concentrated on the tracking PVT absorbers and can be taken away from the illuminated area. In high intensity solar radiation, the PVT absorber can help the sunspace to avoid overheating of the interior space, and in low intensity solar radiation, the absorbers can be out of focus leaving the light to come in the interior space and keeping the irradiation at an acceptable level for the plants.

Chemisana et al. [106] developed a CPVT system with a two-stage concentrator leading to 2.5–10 suns. A domed linear Fresnel

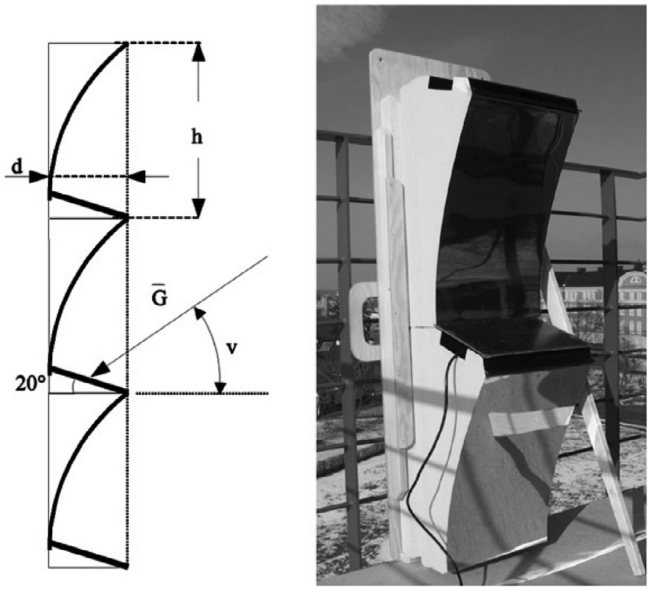



**Fig. 15.** The BI-LCPVT wall elements with a parabolic reflector. Reprinted with permission from Ref. [98]. Copyright © 2003 Elsevier.

lens and a compound parabolic reflector were used as the primary and secondary concentrators, respectively. A simulation model was established and validated experimentally to predict the electrical and thermal performance. A Reynolds number in the range between 200 and 250 was found to satisfy the requirements for a thermal collector giving a temperature step above 6 °C and a PV cell temperature around 55 °C.

Chemisana et al. [107] also performed an analysis on the fluid flow fields and temperature contours of greenhouses with linear Fresnel lenses based on the CFD method. The system also applied the concept of stationary linear Fresnel lens and moving PVT receiver (tracking the focal point of the Fresnel lens). The system can cover a great part of greenhouse thermal and electrical load. To achieve a better understanding of this kind of LCPVT greenhouse, Chemisana et al. [108] also proposed a TRNSYS simulation study. Effects of different weather conditions and tilt angles on Fresnel concentrator performance were investigated. An equation for the optimization of the annual yield was proposed. For the climatic conditions of Barcelona, an improvement above 5% can be achieved when the optimum tilt angle is adopted.

An LCPVT system proposed by Kong et al. [109] is shown in Fig. 18. The optical elements were similar to the two-stage concentrator, based on a compound concentrator with linear Fresnel lens and flat mirror reflectors. Since the CPVT system using single crystalline silicon solar cells had an optimal CR of 4.23x [110], the geometrical CR was designed to be 5 suns to reach an optimal efficiency. The experimental results showed that on a clear day the electrical efficiency and the thermal efficiency were about 10% and 56%, respectively.

*2.1.5. Hyperbolic concentrator*

In order to increase the acceptance angle of BI-LCPVT systems, Adeilla et al. [111] replaced the habitually adopted Fresnel lenses by the hyperbolic lenses. The hyperbolic concentrator can lessen the gained solar radiation and enhance natural day lighting in buildings. The fabricated prototype was divided into two sections to compare the heat transfer of different configurations. As observed in Fig. 19, the first section was PMMA configured with longitudinal aluminum plates and the second section was a flat aluminum plate. The results showed that the water temperature rise of flat aluminum plate was slightly higher than that of PMMA plus longitudinal aluminum plates.

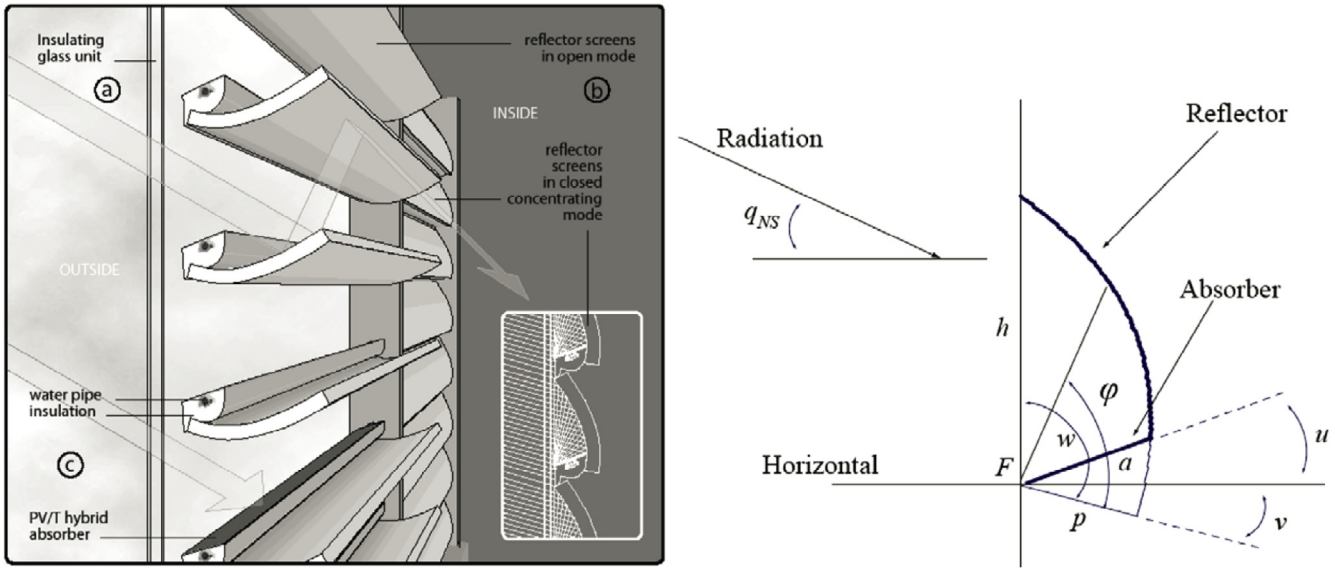



**Fig. 16.** The BI-LCPVT solar window. Reprinted with permission from Ref. [100]. Copyright © 2010 Elsevier.

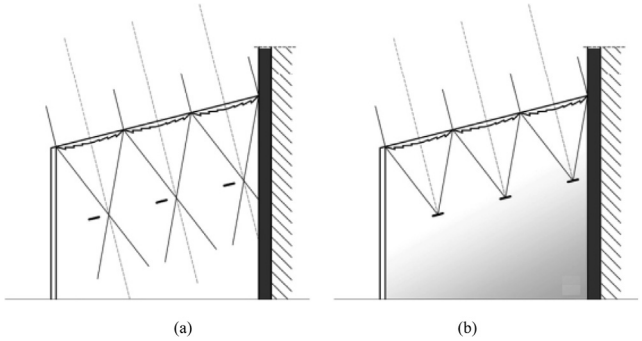



**Fig. 17.** Lighting effect of the BI-LCPVT with linear Fresnel lenses: (a) the absorbers out of focus and no shading effect; (b) on focus with shading effect. Reprinted with permission from Ref. [104]. Copyright © 2007 Elsevier.

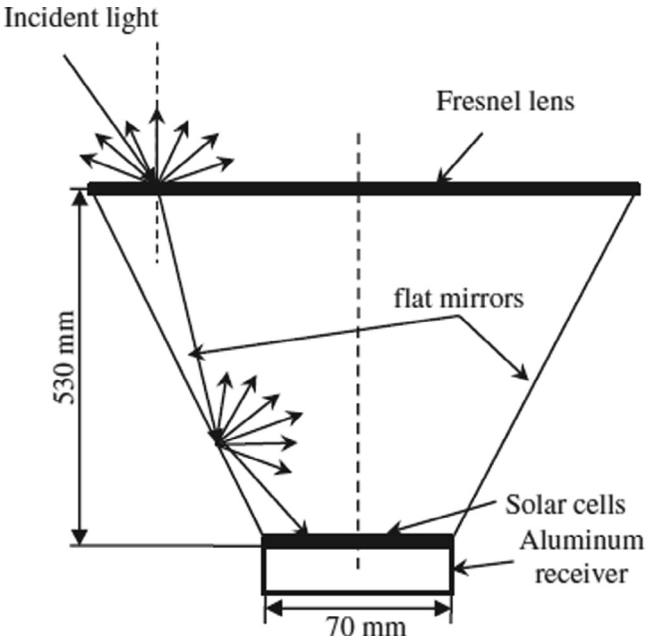



**Fig. 18.** The LCPVT system with a Fresnel lens and flat mirror reflectors. Reprinted with permission from Ref. [109]. Copyright © 2013 Elsevier.

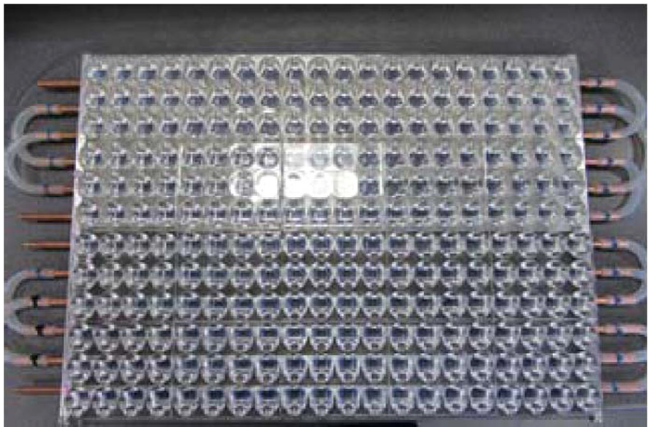


**Fig. 19.** (Color online) The BI-LCPVT with hyperbolic lenses. Reprinted with permission from Ref. [111]. Copyright © 2016 IEEE.

*2.1.6. Linear Fresnel reflector*

The linear Fresnel reflector, consisting of a series of planar reflective mirrors with different tilt angles, is a type of cost-effective concentrator. Several researches on LCPVT used the linear Fresnel reflector as the concentrator. At 1986, Sharan et al. [115] theoretical analyzed an actively cooled CPVT system with a fin-type receiver. The variations of overall electrical output, thermal output, temperatures of cells and water, and effect of various design and operational parameters were studied. Based on the research, they tested a prototype [108], which showed that a total 0.02 $m^2$ receiver area could provide a thermal output power of 100 W and an electrical output power of 4 W at 5 suns. The tubular absorber was also investigated under higher concentrations to determine the design parameters [112]. Effects of different absorber shapes, including flat horizontal, flat vertical and tubular, were also discussed [113].

Xu et al. [114] studied the application of constant volume refrigeration method in LCPVT systems. The prototype consisted of 2-axis tracking Fresnel reflectors and PVT receivers with cooling tubes. The outdoor experiment in Nanjing showed that the thermal and electrical efficiencies achieved 39.4% and 14.1%, respectively. The LCPVT system with constant flow refrigeration showed better

efficiencies, while the constant volume refrigeration led to saving of auxiliary heater at the outlet.

*2.1.7. Summary of LCPVT*

Details of the LCPVT systems mentioned before are listed in Table 1. It can be observed that there are several important distinguishing features for the WHR LCPVT systems.

(1) Features of the optical system

The flat-plate reflectors and the CPC optical systems can provide geometrical CRs lower than 4 suns and optical CRs lower than 2.5 suns. The systems prefer to be stationary to avoid the expensive tracking systems. At a higher CR of $4 < C_g < 10$, the linear focused system with 1-axis tracking is more widely accepted. The integration of LCPVT system with building and greenhouse highly depends on its CR.

In the WHR LCPVT systems, 1-axis tracking systems can be employed with East-West oriented axis or North–South oriented axis. For systems with North–South oriented axis, an automatic tracking system is necessary, but for systems with East-West oriented axis, it is an economic option to adjust the collector manually.

The diffuse radiation plays an important role in the LCPVT systems. Even for low concentrated tracking systems, the diffuse radiation would provide a non-negligible portion of incident radiation [103].

(2) Features of the PV subsystem

At CR lower than 10 suns, the commercially available silicon solar cells, including monocrystalline, polycrystalline and amorphous silicon (c-Si, pc-Si and a-Si) solar cells, are usually selected in the LCPVT for economic reasons. The typical conversion efficiency of these solar cells is lower than 20%. For LCPVT systems using flat specular or diffuse reflectors, the solar panels are directly applied, which would be easy to assemble. But for systems with V-trough, CPC trough, parabolic reflector and linear Fresnel lens solar collectors, the solar cells are connected linearly to make up the PVT absorber.

(3) Features of the thermal subsystem

Water or air is adopted as the main HTF in studies. Flowing through a tube/channel with or without fins, the coolant temperature increases to 40–60 °C for tap water or local heating. Several systems can also provide illumination for greenhouse or buildings.

Despite the fact that the cells with such a low heat flux do not need to be actively cooled, passive cooling systems or thermosiphon systems are not commonly used in LCPVT systems, since active cooling systems can provide more convenient and controllable solutions.

If it is necessary to store the thermal energy, a water tank would be a regular solution. Other methods, including PCM heat storage, are still in the early stage.

*2.2. Medium concentration WHR CPVT system (MCPVT) (CR = 10–100x)*

For MCPVT systems with CRs of 10–100 suns, solar tracking and more effective cooling must be taken into account, which makes the systems more complex than LCPVT systems. The MCPVT systems usually utilize parabolic troughs, linear Fresnel lenses and reflectors as the concentrators.

*2.2.1. Linear (2D) Fresnel lens*

A planar Fresnel lens MCPVT system of CR = 25x was applied for claddings of greenhouses [117]. It helps to block up the direct radiation which is about 77% of the global radiation. The Fresnel lenses were stationary, and the PVT module was kept in the focus point by a tracking system. The measurements showed that the incoming direct radiation resulted in a thermal efficiency of 56% and an electric efficiency of 11%. The up-scaled 50x concentrated MCPVT greenhouse was also experimentally investigated by Sonneveld et al. [118,119] and Swinkels et al. [112]. The systems would lead to electrical and thermal energy output from the excessive solar energy entering a greenhouse. A 480 $m^2$ greenhouse with stationary Fresnel lens and the tracking PVT receiver would provide an electric power of 30 $W/m^2$ at global radiation of 870 $W/m^2$. And 20% of the total incident direct radiation would be collected as thermal yield.

The domed/curved linear Fresnel lens may provide a more efficient and compact design for solar systems [32]. Using the domed linear Fresnel lens, Kerzmann and Schaefer [113,120,121] proposed a 2-axis tracking, medium concentrated (80x) system, as shown in Fig. 20. An energy model was developed, and the simulation results showed that under solar and climate conditions of Phoenix, Arizona, a 6.2 kWp system could provide about 380 L hot water (49 °C) and 38.9 kWhe averaged electricity production per day [121], which is enough for the electricity and hot water demand of a 6 family residence.

Jaffré et al. [122] used tilted mirrors as the secondary optics to improve the illumination and compensate tracking errors of the MCPVT receiver using the domed linear Fresnel lens (as shown in Fig. 21). Performances of the components, such as the transmission spectrum of optical elements, illumination distribution, and variations of the CR with incidence angle and focal length, were tested. Based on the measurements, and taking into account the 77% optical efficiency, the electrical and thermal efficiencies were 8.5% and 38.5%, respectively.

Based on the design of domed Fresnel lens, Feng et al. [123] designed and studied a CPVT system using wedge-shaped cycloidal Fresnel lens. The performance of the optical system was analyzed based on the Monte Carlo ray-tracing method. A CPVT prototype using GaAs cells was tested in clear weather and hazy weather. The results showed that, at noon time of clear weather, the maximum power generating efficiency was about 18%, and the total energy efficiency achieved more than 55%. It was also shown that the hazy weather had a great influence on the electrical efficiency but the thermal efficiency was less affected.

*2.2.2. Linear Fresnel reflector*

Similar to the parabolic troughs and linear Fresnel lenses, although some of the researches use the linear Fresnel reflectors to provide a low concentrated solar radiation, the reflector is more intensively used in MCPVT systems. Rosell et al. [124] coupled a linear Fresnel reflector with a channel PVT collector. As shown in Fig. 22, the system was 2-axis tracking and of 11x optical CR. Without electrical production, the measured thermal performance was over 60%. The theoretical analysis further confirmed that the thermal conduction between the PV cells and the absorber plate is a critical parameter. After that, a 20x concentrated CPVT system was developed for commercial applications (The CIDEM rewards a group of entrepreneurs of the UdL for a solar energy project. @ http://www.udl.cat/, accessed March 28th, 2017).

The design of linear Fresnel reflectors can be more compact and modularized to achieve a better market performance. A formerly commercially available CPVT system was co-developed by Australian National University (ANU) and Chromasun Inc. for domestic applications [125–128]. As presented in Fig. 23, the novel system, which is called Micro-Concentrator (MCT), consisted of a fully sealed enclosure which housed 2 linear Fresnel reflectors and 2 hybrid PVT receivers. A single module of MCT system (aperture 3.5 $m^2$) provided an electrical output of more than 300 W, and a thermal output of more than 1500 W at 950 $W/m^2$ DNI. The total efficiency of MCT was up to 70%. Over the span of a day, the MCT achieved an average electrical efficiency of 8% and thermal efficiency of 50%–60% [129]. The design philosophy of MCT is to

**Table 1**
System details cited in the literature of LCPVT systems.

| General information[a] | | | Concentrator[b] | | | | | PV subsystem | | Thermal subsystem[c] | | | | | | Efficiency[d] | | |
|---|---|---|---|---|---|---|---|---|---|---|---|---|---|---|---|---|---|---|
| Year | Author | Method | Type | Details | $C_o$ (suns) | $C_g$ (suns) | Tracking | Cells | Package | Structure | HTF | $T_{in}$ (°C) | $T_{out}$ (°C) | $\Delta T$ (°C) | Application | $\eta_E$ (%) | $\eta_T$ (%) | $\eta_O$ (%) |
| 2016 | Ziapour et al. [43] | TH | Flat reflector | Mirror and Aluminum reflector | / | / | Stationary | / | Panel | Channel, passive cooling | Water | 25 | 45.9 | / | Domestic hot water | 12.55 | 36.15 | / |
| 1986 | Al-Baali [40] | EX | Flat reflector | / | 1.41 | / | Stationary | Si | Panel | / | Water | 29 | 42 | / | / | 11–13 | / | / |
| 2016 | Haddad et al. [41] | EX | Flat reflector | Aluminum plate | / | / | Stationary | c-Si | Panel | Finned channel | Air | / | 36 | / | / | / | / | / |
| 1991 | Garg et al. [42] | TH | Flat reflector | / | 1.13–1.21 | / | Stationary | Si | Panel | Channel | Air | / | / | 10–20 | Drying | 7–9 | 30–60 | / |
| 2012 | Du et al. [45] | EX | Flat reflector | Segmented flat mirror | / | 8.5 | 2-axis | c-Si | Linear | Pipe | Water | 31–32 | 56–60 | / | / | 7.4–8.3 | 44–47 | / |
| 2015 | Chaabane et al. [46] | TH | Flat reflector | Segmented flat mirror | / | 8.5 | 2-axis | c-Si | Linear | Channel | Water | 31 | 43 | / | / | 9.3 | 74.2 | / |
| 2007 | Robles-Ocampo et al. [47] | EX | Flat reflector | Stainless steel | 1.8 | / | Stationary | c-Si | Bifacial panel | Channel | Water | 24–30 | 35–40 | 10–20 | / | 16.4 | 50 | 60 |
| 2014 | Ibrahim and Khalil [48] | EX | Flat reflector | / | / | 4 | 1-axis | pc-Si | Bifacial panel | Tube | Water | 22.4 | 53 in tank | / | / | / | / | / |
| 2016 | Gurel [49] | TH | Flat funnel reflector | / | / | / | Stationary | c-Si | Sphere | Paraffin wax phase change thermal energy storage | Paraffin wax | / | / | / | / | 14.67 | / | / |
| 2002; 2005 | Tripanagnostopoulos et al. [50,51] | EX | Flat reflector | Diffused aluminum plate | 1.35 | / | Stationary | pc-Si, a-Si | Panel | / | Air or water | / | / | / | Rooftop | 12 (air); 13 (water) | 30 (air); 70 (water) | / |
| 2009 | Tripanagnostopoulos et al. [52] | T&E | Symmetric/ asymmetric CPC, booster, V-trough | Specular Aluminum/glass; diffused stainless steel | / | 2.5 (V-trough); 1.5 (booster) | Stationary or moving receiver | c-Si | Panel | Tubes | Water | / | / | / | Building (with illumination) | / | / | / |
| 2010(2) | Kostić et al. [53,55] | T&E | Flat reflector | Diffused aluminum plate | 1.5 | / | Stationary | c-Si | Panel | Pipe | Water | / | / | / | / | 3.69 | 36.98 | 40.66 |
| 2014 | Künnemeyer et al. [57] | T&E | V-trough | Mirror-finished stainless steel | 1.2–1.6 | 2.36 | Stationary | Si | Linear | Tube | / | / | / | / | / | 1 | / | 30 |
| 1994 | Garg et al. [56] | T&E | V-trough | Aluminum foils | / | 2.1 | Stationary | c-Si | Linear | Channel, thermosyphon | Water | 28 | 57 | / | / | 3.35 | 33.5 | / |
| 2010 | Gilbert [58] | PA | V-trough | / | / | 3 | 2-axis | / | Linear | Pipe | Water | / | / | / | / | / | / | / |
| 2013 | Hedayatizade et al. [59] | TH | Symmetrical CPC | / | 2 | / | Stationary | / | Linear | Finned-tube | Water | 29.9 | / | / | / | 8.0 | 47.3 | 68.5 |
| 2007 | Cheng et al. [60] | TH | Symmetrical CPC | / | 1–30 | / | / | / | / | / | Water | 25 | 50 | / | / | 14–16 | 71–73 | / |
| 1998; 1999 | Garg and Adhikari [61,62] | TH | Symmetrical CPC | / | / | 2.88 | / | / | Linear | Duct | Air | / | / | / | / | / | 40–50 (selective absorber); 30–45 (non-selective absorber) | / |
| 2012 | Redpath et al. [63] | EX | Symmetrical CPC | Low iron glass | / | 1.8 (NM) | Stationary | pc-Si | Linear | Heat pipe | Water | 38 | 56 | / | / | 8 | 44 | 54 |
| 2005 | Othman et al. [64] | T&E | Symmetrical CPC | / | / | 1.86 | Stationary | / | Linear | Double-pass & fins | Air | 31 | 52 | / | / | 1–3 | 37–70 | 39–72 |
| 2007; 2008 | Alfegi et al. [65,66] | TH, EX | Symmetrical CPC | / | / | 1.86 | Stationary | / | Linear | Single-pass & fins | Air | 30 | 38 | / | / | / | / | 27.5–40 |
| 2015 | Elsafi and Gandhidasan [67]. | TH | Symmetrical CPC | / | / | 1.86 | Stationary | Si | Linear | Double-pass & fins | Air | / | / | / | / | 13 | 66 | / |
| 2009(2); 2012 | Sun and Shi [68,69]; Sun and Wang [70] | TH | Symmetrical CPC | / | 2 | / | Stationary | / | Linear | Fin | Air | 25 | 67–88 | / | / | 7 | 68 | 75 |
| 2015; 2016 | Atheaya et al. [71,72] | TH | Symmetrical CPC | / | / | 2 | Stationary | / | Partially covered panel | Tube | Water | / | 25–87 | / | / | 10–13 | 32–42 | / |
| 2016 | Atheaya et al. [73] | TH | Symmetrical CPC | / | / | 2 | Stationary | / | Partially covered converted absorber panel | Tube | Water | / | 24–123 | / | / | 6.5–12.5 | 47–59 | / |
| 2016(3) | Tripathi et al. [74–76] | TH | Symmetrical CPC | / | / | 2 | Stationary | / | Partially covered panel | Tube | Water | / | >110 | / | / | 8–13 | / | / |
| 2016 | Tripathi and Tiwari [77] | TH | Symmetrical CPC | / | / | 2 | Stationary | / | Partially covered panel | Tube | Molten salt | 20 | 55–190 | / | Steam cooking | / | / | / |
| 2012(2) | Jiang et al. [78,79] | TH | Symmetrical CPC | Vacuum encapsulated | / | 3.45 | Stationary | a-Si thin film | Linear | Vacuum tube, thermosyphon | / | / | / | / | / | / | / | / |
| 2016 | Al Imam et al. [84] | EX | Symmetrical CPC | Glass | / | 1.82 (NM) | 1-axis | / | Panel | Pipes, fins and paraffin PCM | Water | / | / | / | Rooftop | / | 35–50 | 46–63 |

| | | | | | | | | | | | | | | | | | |
|---|---|---|---|---|---|---|---|---|---|---|---|---|---|---|---|---|---|
| 2012 | Li et al. [81] | TH | Symmetrical CPC | / | 1–2.5 | / | Stationary | c-Si | Linear | U-pipe | Water | 20 | 42–65 | / | / | 10–12 | 57 | / |
| 2011; 2014 | Proell et al. [82]; Proell and Hilt [83] | T&E | Symmetrical CPC | / | / | 3 | Stationary | / | Linear | / | / | / | 60–80 | / | / | 14 | / | / |
| 2001; 2004 | Brogren et al. [85]; Brogren [86] | EX | Symmetrical CPC | / | / | 4 | Stationary | c Si | Linear | Pipe & fins | Water | / | / | / | / | 29.5(35°C); 33(65°C) | / | / |
| 2016(2) | Xie et al. [87,88] | TH | Symmetrical CPC | / | / | 4 (NM) | 2-axis | / | / | / | / | / | / | / | / | / | / | / |
| 2014; 2015(2) | Li et al. [89–91] | T&E | Symmetrical CPC | Lens-walled CPC mirror | / | 2.4 | Stationary | c-Si | Linear | Pipe | Water | 25 | 70 in tank | / | Building | 6 | 35 | 41 |
| 2012 | Cui et al. [92] | EX | Quasi symmetrical CPC | Segmented flat mirror | 1.86 | 3.48 | Stationary | c-Si | Linear | Parallel channels | Water | 35 | / | / | / | 9 | >50 | >70 |
| 2006; 2007 | Pihl et al. [101]; Nilsson et al. [93] | TH | Asymmetrical CPC | Anodized aluminum /steel with aluminum coating | / | 3.5 (front); 2.5 (back) | Stationary | c-Si on both sides of receiver | Linear | Pipe | Water | / | 50 | / | / | / | / | / |
| 2013; 2014; 2016 | Bernardo et al. [95]; Gomes et al. [94]; Fernandes et al. [96] | EX | Asymmetrical CPC | Anodized aluminum | <1.5 | / | 1-axis | c-Si | Linear | Channel | Water | / | 20-–40 | / | Rooftop | 15 | 80 | / |
| 2013 | Chaabane et al. [97] | T&E | Asymmetrical CPC | Stainless steel | / | 6.7 | Stationary | c-Si | Linear | Pipe | Water | / | / | 4 | / | 8 | 13 | 21 |
| 2002; 2003 | Brogren and Karlsson [99]; Brogren et al. [98] | EX | Parabolic reflector | Anodized aluminum | / | 2.3, 3 | Stationary | c-Si | Linear | / | Water | / | / | / | Building (with illumination) | / | / | / |
| 2010 | Davidsson et al. [100] | T&E | Parabolic reflector | Anodized aluminum | 1.33 | 2.45 | Stationary | / | Linear | Pipe | Water | / | / | / | Building (with illumination) | / | / | / |
| 2006; 2008 | Pihl et al. [101] Bernardo et al. [102] | T&E | Parabolic reflector | Low iron glass | 5.81–7.1 | 10 | 1-axis | c-Si, pc-Si | Linear | / | Water | / | / | / | Building | 12.5 (simulation) | 71.6 (simulation) | / |
| 2011 | Bernardo et al. [103] | EX | Parabolic reflector | Plastic film with silver coating | / | 7.8 | 1-axis | c-Si | Linear | / | Water | 28 | 39 | / | Domestic hot water | 6.4 | 45 | / |
| 2004; 2007 | Tripanagnostopoulos et al. [104,105] | EX | Linear Fresnel lens | Glass | 1.6 | 2 | Moving receiver | pc Si | Linear | / | Water | / | 50 | / | Greenhouse; Building (with illumination) | / | / | 40 |
| 2011 | Chemisana et al. [106] | T&E | Domed linear Fresnel lens and CPC (Two-stage concentrator) | / | 7–10 | 10 | Moving receiver | c-Si | Linear | Channels | Water | 24 | 33 | / | Building | / | / | / |
| 2012(2) | Chemisana et al. [107,108] | TH | Linear Fresnel lens | / | 1.6 | 2 | Moving receiver | / | Linear | Pipe | Water | / | / | / | Greenhouse | / | / | / |
| 2013 | Kong et al. [109] | T&E | Linear Fresnel lens and Flat mirror booster reflector (Two-stage concentrator) | / | / | 5 | Stationary | c-Si | Linear | / | Water | / | / | / | / | 10 | 56 | / |
| 2016 | Adeilla et al. [111] | EX | Hyperbolic funnel reflector | PMMA | / | / | Stationary | Si | Separated | Pipe | Water | 19.5 | / | 3.3–7.3 | Building | / | / | / |
| 2012 | Xu et al. [114] | EX | Linear Fresnel reflector | Glass | 5.2 | 10 | 2-axis | / | Linear | Pipe | Water | / | 40 | / | / | 14.1 | 39.4 | 53.5 |
| 1986 | Sharan et al. [115] | TH | Linear Fresnel reflector | / | / | 6.4 | 1-axis | / | Linear | Tube | Water | / | 25–32 | / | / | / | / | / |
| 1992 | Sharan and Kandpal [116] | EX | Linear Fresnel reflector | / | / | 5 | 1-axis | / | Linear | Tube | Water | / | 26 | / | / | 8 | / | / |

[a] EX: experimental, TH: theoretical, T&E, theoretical and experimental, PA: patent.
[b] $C_o$: optical CR, $C_g$: geometrical CR; NM: not mentioned, treated as the geometrical CR; $C_g$ is considered as a primary factor on CPVT system classification if it is available in documents.
[c] $T_{in}$: inlet temperature, $T_{out}$: outlet temperature; $\Delta T$: temperature difference between the inlet and outlet of thermal system.
[d] $\eta_O$: overall efficiency, $\eta_E$: electrical efficiency, $\eta_T$: thermal efficiency. In case that both theoretical and experimental results are available in the literature, experimental results are adopted.

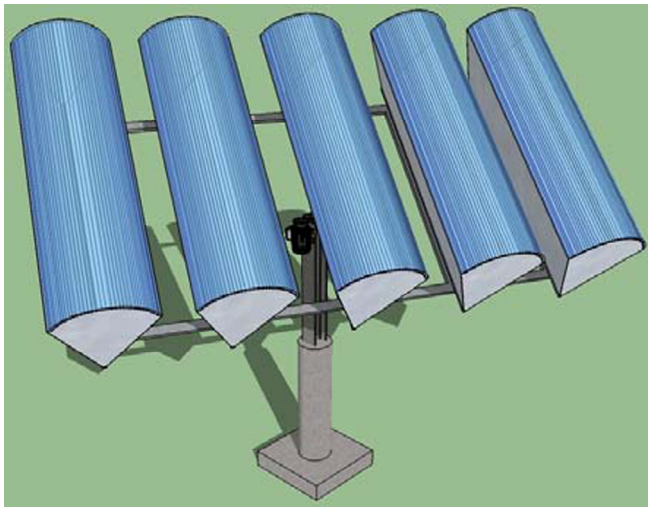


**Fig. 20.** (Color online) The 2-axis tracking MCPVT system with domed linear Fresnel lenses. Reprinted with permission from Ref. [121]. Copyright © 2012 Elsevier.

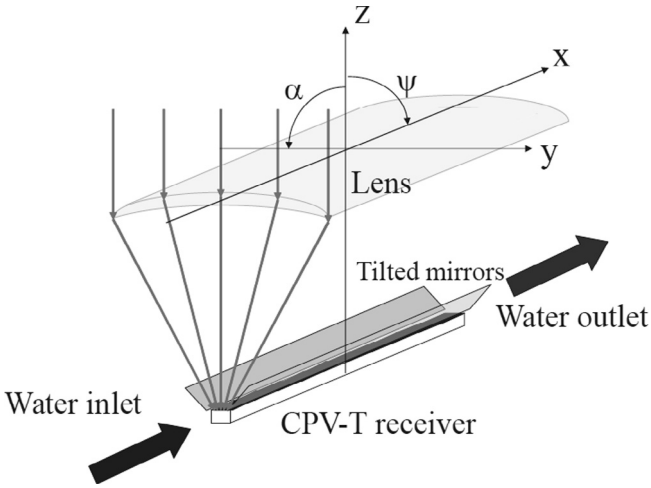



**Fig. 21.** The 2-axis tracking MCPVT module with a secondary concentrator. Reprinted with permission from Ref. [122].



**Fig. 22.** (Color online) The MCPVT system with a linear Fresnel reflector. Reprinted with permission from Ref. [124]. Copyright © 2005 Elsevier.

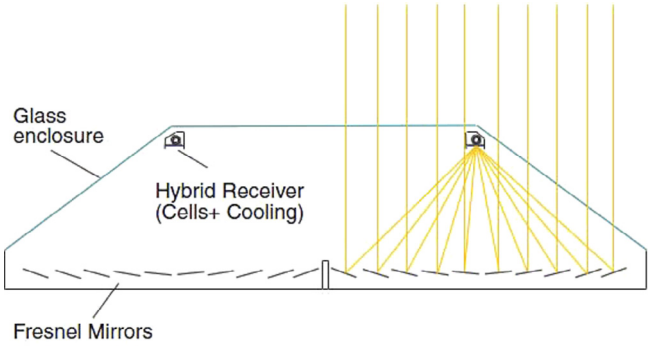



**Fig. 23.** (Color online) The MCT system developed by ANU and Chromasun Inc. Reprinted with permission from Ref. [125]. Copyright © 2012 John Wiley & Sons, Ltd.

provide a reliable, cost-effective and flexible end product. Early evaluation of the physical and mechanical properties of receiver components has been demonstrated to improve the receiver design process and the reliability of the end product [128,130]. Unlike the open-loop tracking system in conventional solar concentrators, the MCT employed a closed-loop 1-axis tracking system [131]. Solid-state temperature sensors were located on each edge of the receiver to provide feedback signals. The closed-loop increased the reliability and accuracy of tracking system, while the flux uniformity at the receiver was simultaneously improved. An economic analysis indicated that the CPVT system can be grid competitive without government subsidies [132]. Compared with alternate CHP systems, including the separated PV+CST (concentrating solar thermal) and bio-gas engines, the CPVT system has a lower levelized cost of energy (LCoE) and a shorter payback period.

The Fresnel reflectors can easily be integrated into buildings. Chemisana et al. [133] also designed a transmissive Fresnel reflector to match the needs of BI-CPVT systems. As shown in Fig. 24, the linear Fresnel reflector focuses radiation in a manner analogous to a lens. The receiver remains stationary and solar tracking is achieved in a simple and effective way by rotation of the individual reflectors, of which all rotation axes are coplanar and parallel. The daily global optical efficiency can reach a value of 56.38%, and the maximum CR is predicted to be 18 suns. Considering the high values of transparency coefficient and shading coefficient, the CPVT system could also perform a useful illumination control of the building interior space. After that, the prototype of this transmissive Fresnel reflector was measured [134]. The concentrated prototype ($C_g$ = 16.67x) was compared with a non-concentration reference PVT unit. The CPV module yielded 4.5–4.7 times more power and 1.9–2.8 times more thermal production than the non-concentrated one.

Besides, by using the linear Fresnel reflectors, it is possible to combine the MCPVT with the SBS illumination conception in greenhouses. For crops in greenhouses, the NIR radiation is useless, and the solar energy received by greenhouses may surpass the required energy. As shown in Fig. 25, Sonneveld et al. [135] and Swinkels et al. [136] developed a linear Fresnel CPVT system with spectral selective mirrors for the Venlo type greenhouse. This MCPVT system was further optimized to avoid the asymmetric greenhouse construction with bended glass, the large construction for solar tracking and the high investments in the previous study using cylindrical trough as the concentrator [137]. The reflected NIR part of solar radiation was concentrated on the MCPVT module on the ridge or gutter of the greenhouse. The heat load inside the greenhouse would be reduced, and the photons with wavelength for photosynthesis process (about 400–700 nm) could be absorbed by crops. Using the ray tracing method, the flat and circular trough-

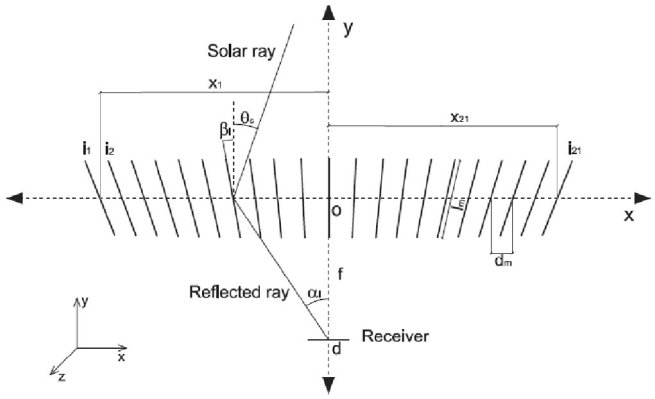



**Fig. 24.** The transmissive linear Fresnel reflector for MCPVT systems. Reprinted with permission from Ref. [133]. Copyright © 2011 Elsevier.

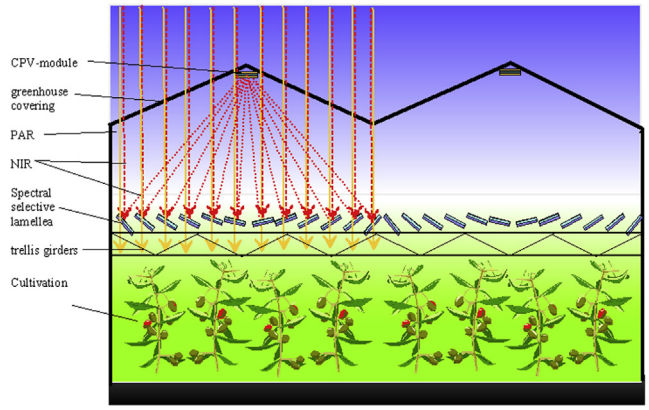



**Fig. 25.** (Color online) The MCPVT system combining a linear Fresnel NIR reflector in a Venlo greenhouse. Reprinted with permission from Ref. [135]. Copyright © 2012 ISHS.

shaped lamellas of the Fresnel reflector were investigated. The results showed that the costs of solar tracking could be lowered when adopting the circular trough because it achieved a higher CR with fewer lamellas.

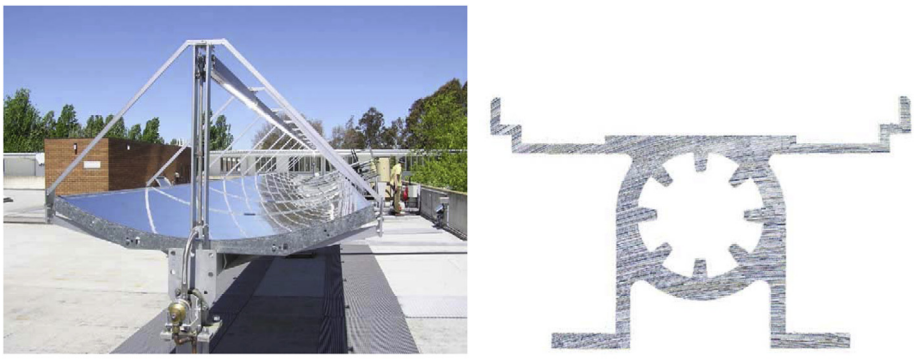
### 2.2.3. Parabolic/cylindrical trough concentrator

The parabolic trough concentrator (PTC) is a commercialized optical equipment for CSP plants. It also offers an affordable and scalable solution for CPVT concept. To demonstrate the technical feasibility, Gibart [138] theoretically studied a 1-axis tracking CPVT system with PTCs and tested the realized prototype. The results showed that the peak electrical efficiency of the hybrid prototype reached 71% of the classic flat PV collector. The peak thermal efficiency of the prototype was better than the flat thermal collector, but lower than the parabolic thermal collector.

In ANU, Coventry et al. [139] constructed 2 different prototype parabolic trough CPVT systems. The first was 2-axis tracking, with a 1.6 m long collector and CR = 25x. The second was 1-axis tracking, with a 15 m long collector and CR = 35x. Early test resulting from the first collector showed the thermal efficiency around 50% and electrical efficiency up to 10%. A TRNSYS component for dynamic modelling of the CPVT collector [140] was also written for simulation. The accuracy of the TRNSYS component was validated by a 30x concentration parabolic trough CPVT collector. The simulated annual performance of the domestic 2-axis tracking CPVT prototype (the first mentioned before) was compared with a separate solar hot water system and a separate PV system with the equivalent size. The results proved that the annual heat output is similar to one of the best flat-plate solar hot water collectors, and the annual electrical energy output is similar to one of the highest efficiency of PV modules. Thereafter, as shown in Fig. 26a, a parabolic trough CPVT system with a geometrical CR of 37 suns and peak flux intensities around 100 suns [141] was set up to investigate the impact of non-uniform illumination on the solar cells. The CPVT system showed a thermal efficiency around 58% and an electrical efficiency around 11%. The impact of illumination non-uniformity, which was due to the shape error, receiver support post shading and gaps between the mirrors, was shown to have a significant effect on the overall electrical performance. The extruded aluminum receiver (Fig. 26b) was applied to cool the cells and collect thermal energy. Internal fins were incorporated in the fluid conduit to increase the heat transfer surface in order to minimize the operating temperature difference between the cells and the fluid. For the purpose of demonstrating a real world system and sorting out the bugs, a 300 $m^2$ system was installed [142]. The projected annual generating capacity of the system was 50 MWh of electricity and 360 GJ of hot water.

Li et al. [110,143,144] compared the performances of several different types of solar cell arrays for a 10 $m^2$ parabolic trough CPVT system, including the mc-Si, pc-Si, Super Cell, and triple junction GaAs solar cells. The CPVT test bench is illustrated in Fig. 27. The geometrical CR and optical CR of the system were 30.8 and 20 suns, respectively. The reflecting mirror was made of aluminum alloy with high reflectivity of 0.69. It was demonstrated experimentally and theoretically that the triple junction GaAs cells performed better electrical performance than other types of solar cells. And the polysilicon cells exhibited poor electrical performance in CPVT systems. The optimum CRs for the solar cells were experimentally studied, and it was found that GaAs solar cells can work at a much higher CR. The effect of series resistance was also investigated in their work. The high solar cell series resistance would lead to high power loss and output performance reduction of the solar cell arrays. The instantaneous electrical efficiency and thermal efficiency of the GaAs system were 9.88% and 49.84%, respectively. Whereas that of the system using the low-cost concentrating silicon cell array were 7.51% and 42.4%, respectively. Another measurement in this 10 $m^2$ trough [145] showed that the maximum power output with the Super cell array, the GaAs cell array and the concentrating silicon cell array increased 7.66, 17.85, and 13.10 times than those in the non-concentrating irradiance, respectively. The average electrical efficiencies of the system with the three types of solar cell arrays were 3.63%, 8.94%, and 3.67%, respectively, and the thermal efficiencies were 45.17%, 41.69%, and 34.53%, respectively. Thereafter, they investigated the effect of mirror reflectivity on the performance of the MCPVT systems. The experimental results showed that the reflectivity of the parabolic mirror was an important factor to determine the CPVT system efficiency. Li et al. [143] and Ji et al. [146] also investigated a 2 $m^2$ PTC system with an optical CR of 10.27 suns. For the 4 types of solar cell arrays, the electrical performance of GaAs module was better than that of crystal silicon modules, but the thermal performances of the mc-Si and pc-Si modules were better. The superior output performance of the GaAs cell array mainly benefited from its lower series resistance.

Based on the researches aforementioned, Tan et al. [147] and Ji et al. [148] tested a two-stage MCTPV system based on a PTC. As shown in Fig. 28, a metal cavity heating stage was added after the PVT stage, which can be used to increase the temperature of outlet water without sacrificing the solar cell efficiency. The test results from the experimental platform, with a 1.8 $m^2$ PVT stage and a 30 $m^2$ heating stage, showed that the temperature of water in the tank can be increased by 28.7 °C within 30 min. Under solar radiation of 978 W/$m^2$, the measured electrical and thermal efficiencies were 2.06% and 47.26%, respectively.



(a) (b)

**Fig. 26.** (Color online) The parabolic trough MCPVT system: (b) the prototype CPVT system; (a) aluminum spine. Reprinted with permission from Ref. [141]. Copyright © 2005 Elsevier.



**Fig. 27.** (Color online) The parabolic trough MCPVT system test bench. Reprinted with permission from Ref. [110]. Copyright © 2011 Elsevier.

Besides the planar PVT receiver as implemented in the previous researches, the triangle and rectangle PVT receiver would be another viable option [149]. As shown in Fig. 29, PV cells can be secured to planar surfaces facing the parabolic reflector. Even the top surface facing the sun could be covered by solar cells or absorbing coatings to increase the electrical or thermal output, such as the design of Menova's Power-Spar module [150] and Calise and Vanoli [151].

Calise et al. [152] presented a finite-volume model to study the MCPVT system with a PTC and a linear triangular receiver (Fig. 30). The calculated electrical efficiency is around 22%, whereas the thermal efficiency is about 63%. The evaluated exergetic efficiency is slightly higher than 78%. It slightly decreases along the CPVT axis, which is the consequence of the temperature increase. They also suggested using triple-junction InGaP/InGaAs/Ge solar cells in the CPVT system, because the electrical efficiency can be further improved and the cells have a good performance at high operating temperatures [151].

Reatti et al. [153] studied the shading effects on a series of linear parabolic CPVT collectors. As shown in Fig. 31, the collectors consisted of semi-parabolic mirrors concentrating the solar irradiation towards a string of c-Si cells operated at 20x suns. Due to the rotation of the collector during the sun tracking, each collector shades the subsequent collector. As thus, the system energy production decreases. A new model was presented to investigate the relations of the system performance and the distance between collectors. The model was validated by the measured data on a prototype. The geometry of water channel was also discussed for this MCPVT system [154]. When applying the U-turn cooling channel to a single trough, the maximum outlet temperature was limited, because during the return way the water transfers heat to the cold zone of the receiver. A one-way double-channel solution could be preferred for higher temperature. After that, some practical issues of system design were discussed [155], involving the electrical layout of the bypass diodes for minimizing the end losses, and the

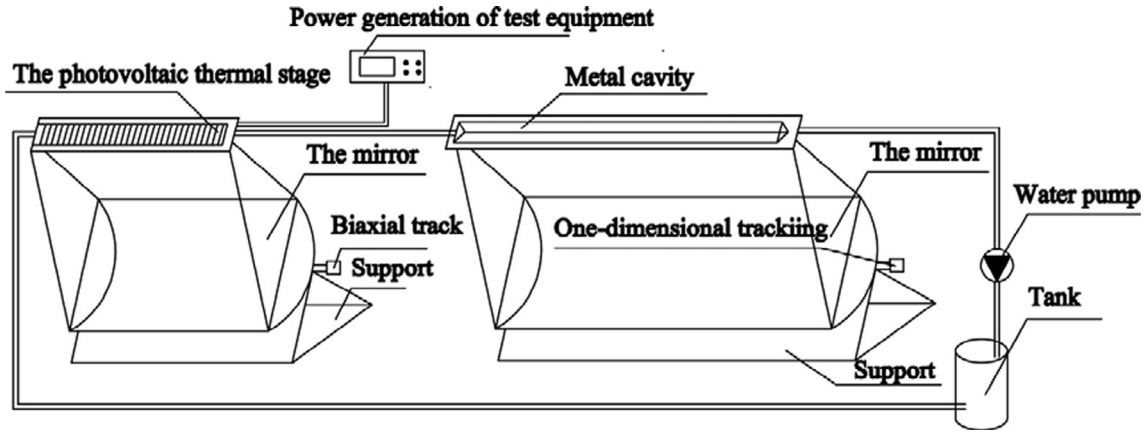



**Fig. 28.** The structure of a two-stage MCPVT system. Reprinted with permission from Ref. [147]. Copyright © 2014 Elsevier.

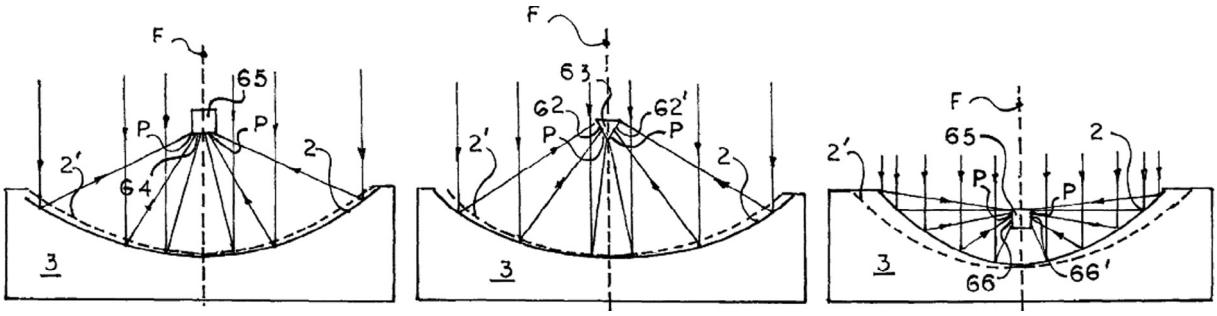



**Fig. 29.** Different configurations of parabolic trough MCPVT systems. Reprinted with permission from Ref. [149].

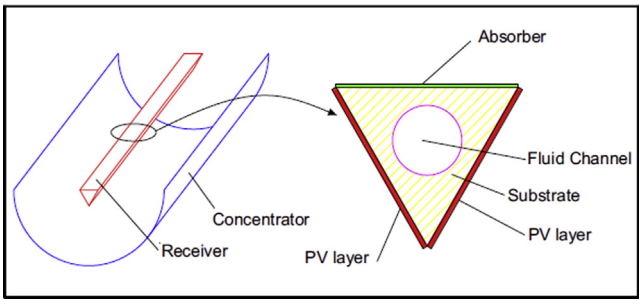



**Fig. 30.** (Color online) The MCPVT system consisting of a PTC and a linear triangular receiver. Reprinted with permission from Ref. [152]. Copyright © 2012 Elsevier.

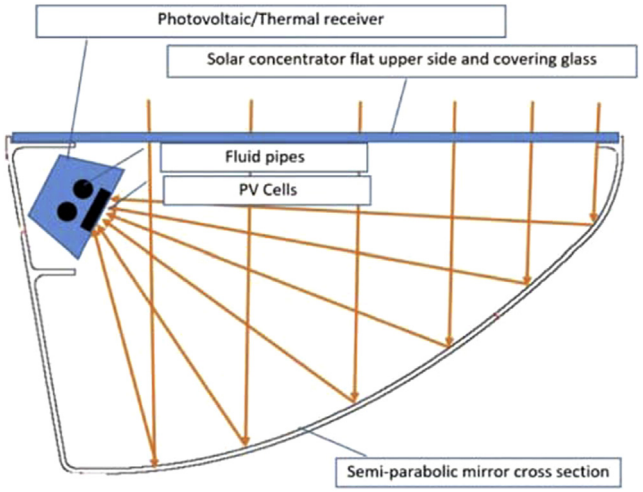



**Fig. 31.** (Color online) The MCPVT system with parabolic concentrators Reprinted with permission from Ref. [155]. Copyright © 2016 IEEE.

estimation method of solar cell operating temperature on the basis of electrical measurements. The overall efficiency, electrical efficiency and thermal efficiency of the system were 61.5%, 51.3% and 10.2%, respectively.

Geng et al. [156] developed and tested a MCPVT system with oscillating heat pipe heat exchanger for honeysuckle drying. Two full-scale experiments including the natural sun drying and 65–80 °C hot air drying were conducted. The hot air showed a much greater drying rate than the natural sun drying, and thus benefited the dry honeysuckle quality. The measured data showed that the overall efficiency of CPVT was 50%–57% during the 5 drying hours.

Besides the parabolic trough, the cylindrical trough was also adopted in MCPVT researches. A feasibility analysis performed by Sonneveld et al. [137] showed the potential of a cylindrical trough

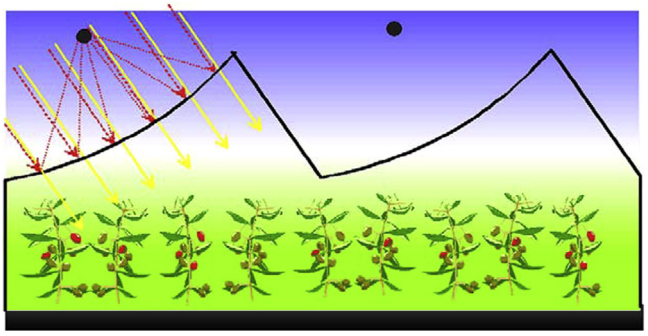


**Fig. 32.** (Color online) A cylindrical trough MCPVT system integrated with greenhouses by combining the SBS technology. Reprinted with permission from Ref. [137]. Copyright © 2010 Elsevier.

WHR CPVT system integrated with greenhouses (Fig. 32). Compared with the parabolic trough, the cylindrical trough does not have to track the sun, and thus it can be easily integrated into the covering of the greenhouse. In this system, the notion of SBS illumination was also adopted. The visible part of solar energy which is required for plant growth transmits through the film, while the NIR part is reflected to PV cells. After that, they constructed a prototype greenhouse with a moving PVT receiver to track the focal line of the cylindrical trough [157]. Under 900 W/m$^2$ illumination, the estimated electrical and thermal peak power were 30 and 121 W/m$^2$, respectively. Under Dutch weather conditions, the annual electric and thermal yield can satisfy over 60% of the energy demand of greenhouses, and this CPVT system was expected to cover all energy demand of the greenhouse and operate independently of fossil fuel in the future.

As the majority of solar energy comes in the form of visible light, investigations on WHR CPVT usually use thin-film cells, silicon cells, III-V cells or multi-junction cells, and other types of solar cells are seldom used. However, there is a research using the thermo-photovoltaic (TPV) cells [158]. A preliminary design combining the natural circulation thermal system, parabolic trough, V-type cooling channel, and TPV/Thermal receiver was proposed. This research also discussed the feasibility of combining TPV in the WHR CPVT system. Since TPV cells are designed for long wavelength, infrared light emitted by hot objects, the application of TPV cells would apparently increase the energy proportion of thermal subsystem.

### *2.2.4. Parabolic dish/spot Fresnel lens concentrator*

The small-scale point focused parabolic dish was also used as the concentrator in a test bench setup by Su et al. [159]. The MCPVT module operated under high solar irradiance and high temperature difference. In order to investigate the conjugate heat transfer mechanics of the mixed convection, the influence of environmental parameters on the system efficiencies was studied. To

improve the cooling efficiency, they suggested putting the inlet near the top PV and outlet near the bottom glass.

The other usually used point focused concentrator, the spot Fresnel lens, was also used to generate medium concentrated illumination. Radwan et al. [160] theoretically proved that the microchannel heat sink is effective to recover the dissipated heat of a CPVT with the Fresnel lens. At CR of 40x, the local solar cell temperature ranges from 37 to 41 °C, whereas the electrical and thermal efficiencies achieve 18.5% and 62.5%, respectively. A comparison between different cooling systems also indicates that using a microchannel cooling technique achieves the utmost possible reduction of solar cell temperature.

*2.2.5. Summary of MCPVT*

Details of the MCPVT systems mentioned before are listed in Table 2. Several important distinguishing features for the WHR MCPVT systems are summarized as follows.

(1) Features of the optical system

The linear concentration optics, including the parabolic trough, linear Fresnel lens and reflector, can provide a CR of 10–100 suns. Since stationary ones cannot achieve such a high concentration, both 1-axis and 2-axis tracking systems are adopted. The cost of 2-axis tracking linear systems would also increase compared with the 1-axis tracking ones.

In researches using the Fresnel lens concentrator, the domed Fresnel lens seems more popular than the flat one. Domed Fresnel lens has advantages of reduced coma, minimum reflectance, shorter focal length, and so on [163].

For greenhouses and buildings with large surfaces and illumination demand, a stationary concentrator with a moving receiver is a viable choice. Tracking of the receiver is possible with the use of two motors. One is for the distance to the Fresnel lens, and the other is for the translocation parallel to the lens. This type of optical system can provide a low or medium CR for CPVT systems. The transmissive linear Fresnel reflector provides another option for the building elements with illumination.

(2) Features of the PV subsystem

The WHR MCPVT systems use crystalline silicon solar cells, as the pc-Si and a-Si cells are not quite suitable to be operated at the CR over 10 suns. With the use of linear concentrators, the cells are packed linearly in nearly all investigations.

At the CRs of over 10 suns, the uniformity of solar radiation plays an import role in the PV efficiency. The system performance can be improved by better mirror reflectivity, and also by pursuing a suitable focal line with uniform illumination.

(3) Features of the thermal subsystem

Thermal load on MCPVT systems increases, and passive cooling or thermosiphon methods are no longer suitable. Channels with fins are more frequently adopted as the cooling structure, and water is considered as a primary HTF to achieve a better cooling performance.

*2.3. High concentration WHR CPVT system (HCPVT) (CR > 100x)*

For CPVT systems with CR > 100x, solar cells operate at extremely tough conditions, such as high energy flux and high temperature. This will affect the system configurations in various aspects. Researches on the HCPVT systems are described as follows.

*2.3.1. Parabolic trough concentrator*

CPVT systems with 2-axis tracking linear parabolic concentrators would achieve higher CRs than the 1-axis tracking parabolic troughs mentioned before. O'leary and Clements [164] modelled the performance of a CPVT system with 2-axis tracking PTC (Fig. 33). The model did not account for convective heat losses to the surroundings. Three different piping arrangements were discussed for best coolant flow geometry, and the single duplex-series arrangements were selected for economic reasons. Results of the further study showed a broad optimal operating region for this type of active cooling system in parabolic trough HCPVT systems. Del Col et al. [165] proposed a 2-axis parabolic trough CPVT system (Fig. 34) with a geometrical CR around 130x. They used a secondary concentrator made of two flat mirrors, which contributed to the concentrated flux on GaInP/GaAs/Ge cells. The modelled and measured data showed that the electrical efficiency of the system displayed a minor penalization with increasing reduced temperature difference (reduced temperature difference = [(HTF outlet temperature + HTF inlet temperature)/2 − ambient temperature]/DNI). It is possible to increase the operating temperature to produce heat at medium temperature (80–90 °C). The measured global system efficiency ranged between 55% and 70%.

The 2-axis tracking linear parabolic HCPVT systems are more complex than the above mentioned 1-axis tracking MCPVT systems. But the 2-axis tracking system can maximize the system performance, whereas the linear geometry releases any precision constraints for the azimuthal tracking. These facts will help to reduce the additional cost. An economic evaluation performed by Quaia et al. [166] demonstrated the viability of the 2-axis tracking PTCs. The LCoE of a 144x concentrated 2-axis tracking PTC CPVT system is 0.087 €/kWh, which is competitive compared with different commercially available PV and thermal technologies.

*2.3.2. Spot (3D) Fresnel lens*

2-Axis tracking-type spot (3D) Fresnel lenses are usually applied in high concentrated PV (HCPV) systems. The spot Fresnel lenses are comprised of PMMA, quartz, or glass materials. The PMMA Fresnel lenses can be made larger than glass lenses, as well as being much cheaper and lighter. However, the glass or quartz materials are of much lower thermal expansion coefficient and better thermal stability. The spot Fresnel lens can concentrate extremely high illumination (200–7000 suns) onto solar cells [167]. Mbewe et al. [168] developed a very simple semi-experimental model for silicon solar cells under concentrated illumination. The agreement between the predicted and tested data was shown to be within 10% for all parameters. Arab et al. [169] patented a CPVT system with two-stage solar concentration optical elements. The primary optical element could be square Fresnel lenses, parabolic dishes and so on. The sun tracking system adopts two or more linear actuators, and when the actuators extend or retract, the tilt of the solar collector can be changed.

Performance of an HCPVT system with spot Fresnel lenses was also experimentally compared with the ordinary high concentrated photovoltaic (HCPV) system under different operating conditions [170]. To minimize the heat losses, an additional internal thermo-isolation was mounted between the air gap and the PV cells. The indoor experiments showed that the efficiency of heat transfer was improved at low flow rates. But at high flow rates, even without additional isolation, the closed air gap of the module was effective enough to reduce the parasitic heat losses. On the other hand, outdoor experiments showed that the PVT module achieved a considerable increase in the total efficiency, and about 70% of the incoming solar power can be extracted from the PVT module.

Hussain and Lee [171] performed experimental and theoretical studies to discuss the maximum power generation of a CPVT system. The CPVT employed 8 Fresnel lenses as the concentrator and a U-shaped pipe with 8 solar cells as the receiver (Fig. 35). The influences of fluid flow rate, solar irradiation, and ambient temperature were discussed. The estimated electrical and thermal efficiencies were 18% and 54%, respectively. A prototype scale CPVT with similar configurations was also tested [172]. The maximum water temperature in the tank was measured to be 60–69 °C at dif-

**Table 2**
System details cited in the literature of MCPVT systems.

| General information[a] | | | Concentrator[b] | | | | | PV subsystem | | Thermal subsystem[c] | | | | | | Efficiency[d] | | |
|---|---|---|---|---|---|---|---|---|---|---|---|---|---|---|---|---|---|---|
| Year | Author | Method | Type | Details | $C_o$ (suns) | $C_g$ (suns) | Tracking | Cells | Package | Structure | HTF | $T_{in}$ (°C) | $T_{out}$ (°C) | $\Delta T$ (°C) | Application | $\eta_E$ (%) | $\eta_T$ (%) | $\eta_O$ (%) |
| 2010; 2012; 2013 | Kerzmann and Schaefer [113,120,121] | TH | Domed linear Fresnel lens | / | / | 80 | 2-axis | GaInP/ GaAs/ Ge | Linear | Channel | Water | 21 | 50 | / | Domestic hot water | 35 | / | / |
| 2014 | Jaffré et al. [122] | EX | Domed linear Fresnel lens | PMMA | 17 | 20 | 2-axis | c-Si | Linear | Channel | Water | / | <50 | / | Domestic hot water | 8.5 | 38.5 | / |
| 2011 | Sonneveld et al. [117] | EX | Linear Fresnel lens | PMMA | / | 25 | Moving receiver (2 motor) | c-Si | Linear | Pipe | Water | 20 | 60 | / | Greenhouse | 11 | 56 | 67 |
| 2011(3) | Sonneveld et al. [118,119]; Swinkels et al. [112] | EX | Linear Fresnel lens | PMMA | / | 50 | Moving receiver (2 motor) | Si | Linear | Pipe | Water | / | / | / | Greenhouse | / | / | / |
| 2016 | Feng et al. [123] | T&E | Domed linear Fresnel lens | PMMA | / | / | 1-axis | GaAs | Linear | Channel | Water | / | / | / | / | 18 | 45 | 55 |
| 1987 | Sharan et al. [161] | T&E | Parabolic trough | / | / | 1–60 | 1-axis | / | Linear | Tube | Water | / | 25–37 | / | / | / | / | / |
| 1987 | Sharan et al. [162] | TH | / | / | / | 1–50 | 1-axis | / | Linear | Tubular tube; flat vertical tube; flat horizontal tube | Water | 25 | 32 | / | / | 7 | / | / |
| 2005 | Rosell et al. [124] | T & E | Linear Fresnel reflector | / | 11.1 | 13.6 | 2-axis | Si | Linear | Channel | Water | 30 | 58 | / | / | / | >60 | / |
| 2010(3); 2011(4); 2012; 2013 | Everett et al. [126–128,131]; Walter et al. [130]; Vivar et al. [125,129]; Chatterjee et al. [132] | EX | Linear Fresnel reflector | Anodized aluminum | 15 | 30 | 1-axis, elevation can be changed | c-Si | Linear | Channel | Water | 36 | 42 | / | Rooftop | 8 | 50–60 | 70 |
| 2011 | Chemisana and Rosell [133] | TH | Transmissive linear Fresnel reflector | / | 8–11 | / | 1-axis | / | Linear | / | / | / | / | / | Building (with illumination) | / | / | / |
| 2016 | Chemisana et al. [134] | EX | Transmissive linear Fresnel reflector | / | <6 | 16.67 (cell); 10.32 (PVT) | 1-axis | c-Si | Linear | Copper pipe | Water | 25–32 | 36–52 | / | Building (with illumination) | / | / | / |
| 2011; 2012 | Swinkels et al. [136]; Sonneveld et al. [135] | TH | Linear Fresnel reflector (flat/circular mirrors) with interference filter | / | 23 | 100; 46 (effective) | 1-axis | / | Linear | / | / | / | / | / | Greenhouse | / | / | / |
| 1981 | Gibart [138] | T&E | Parabolic trough | / | / | 10–40 | 1-axis | Si | Linear | Tube | Water | 20 | 80 | / | Domestic hot water | 5.5–7.7 | 15–75 | / |
| 2005; 2006 | Coventry [141]; Smeltink and Blakers [142] | EX | Parabolic trough | Laminated glass | / | 37, 38 | 1-axis | c-Si | Linear | Tube with internal fins | Water with anti-freeze and anticorrosion additives | 25 | 65 | / | Rooftop | 11 | 58 | / |
| 2002(2) | Coventry [139,140] | TH | Parabolic trough | Laminated glass | 25 | / | 2-axis | c-Si | Linear | Tube | Water | 18 | 45 in tank | / | Rooftop | 10 | 50 | / |
| 2011; 2012 | Li et al. [143]; Ji et al. [146] | EX | Parabolic trough | Aluminum | 10.27 | 16.92 | 1-axis | Super cell; GaAs | Linear | Channel with internal fins | Water | 22.6 (Super cell); 20.1 (GaAs) | 50.1 (Super cell); 39.1 (GaAs) | / | / | 1.93–2.22 (Super cell); 5.73–5.95 (GaAs) | 34.5– 9.4 (Super cell); 41.13–41.85 (GaAs) | / |
| 2011(2); 2009 | Li et al. [110,145]; Xu et al. [144] | EX | Parabolic trough | Aluminum alloy | 20 | 30.8 | 1-axis | Super Cell; GaAs; Si | Linear | Channel with internal fins | Water | 25.8 (Super cell); 23.9 (GaAs); 18.0 (Si) | 41.2 (Super cell); 47.4 (GaAs); 41.6 (Si) | / | / | 3.63 (Super cell); 8.94 (GaAs); 3.67 (Si) | 45.17 (Super cell); 41.69 (GaAs); 34.53 (Si) | / |
| 2014; 2016 | Tan et al. [147]; Ji et al. [148] | EX | Parabolic trough | / | / | ~20 | 2-axis | c-Si | Linear | / | Water, two-stage heating | / | 62.8 in tank | 28.7 | / | 2.2–2.8 (sub) | 38.3–56.2 (sub) | / |
| 2008 | Niedermeyer [149] | PA | Parabolic trough | / | / | / | 1-axis | / | Linear | Tube | Water | / | / | / | / | / | / | / |
| 2012 | Calise et al. [152]; Calise and Vanoli [151] | TH | Parabolic trough | / | / | 10 | 1-axis | GaInP/ GaAs/ Ge | Linear | V-Channel | Water | 70 | 88 | / | / | 22 | 63 | / |
| 2015(2); 2016 | Cappelletti et al. [154,155]; Reatti et al. [153] | T&E | Semi-parabolic trough | / | / | 20 | 1-axis | c-Si | Linear | U-Pipe | Water | 18 | 22 | / | Rooftop | 10.2 | 51.3 | 61.5 |
| 2013 | Geng et al. [156] | EX | Parabolic trough | / | 5.5 | 11 | / | / | Panel | Oscillating heat pipe heat exchanger | Air | / | 65–80 | / | Crop drying | 23–30 | 24–35 | 50–57 |
| 2016 | Manokar et al. [158] | TH | Parabolic trough | Glass | / | / | 1-axis | TPV | Linear | V-channel | Water in tank, natural circulation | / | / | / | / | / | / | / |
| 2010(2) | Sonneveld et al. [137,157] | EX | Spectral selective | Dielectric | / | 30; 13.9 | Moving | Si | Linear | Rectangular | Water | / | / | / | Greenhouse | 11.3 | 65 | / |

(*continued on next page*)

**Table 2** (*continued*)

| General information[a] | | | Concentrator[b] | | | | PV subsystem | | Thermal subsystem[c] | | | | | Efficiency[d] | | |
|---|---|---|---|---|---|---|---|---|---|---|---|---|---|---|---|---|
| Year | Author | Method | Type | Details | $C_o$ (suns) | $C_g$ (suns) | Tracking | Cells | Package | Structure | HTF | $T_{in}$ (°C) | $T_{out}$ (°C) | $\Delta T$ (°C) | Application | $\eta_E$ (%) | $\eta_T$ (%) | $\eta_O$ (%) |
| | | | cylindrical trough with interference filter | multilayer Plastic film (Ebiral) | | (effective) | receiver | | | aluminum ducts | | | | | | | | |
| 2014 | Su et al. [159] | T&E | Parabolic dish | Glass | / | 22 | 2-axis | pc-Si | Dense array | Channel | Water | 26 | / | / | / | / | / | 20–45 |
| 2016 | Radwan et al. [160] | TH | Spot Fresnel lens | / | / | 1–40 | 2-axis | pc-Si | / | Rectangular microchannel | Water | 30 | 34.6–90.2 | / | / | 18.5 | 62.5 | / |

[a] EX: experimental, TH: theoretical, T&E, theoretical and experimental, PA: patent.
[b] $C_o$: optical CR, $C_g$: geometrical CR; NM: not mentioned, treated as the geometrical CR; $C_g$ is considered as a primary factor on CPVT system classification if it is available in documents.
[c] $T_{in}$: inlet temperature, $T_{out}$: outlet temperature; $\Delta T$: temperature difference between the inlet and outlet of thermal system.
[d] $\eta_O$: overall efficiency, $\eta_E$: electrical efficiency, $\eta_T$: thermal efficiency. In case that both theoretical and experimental results are available in the literature, experimental results are adopted.

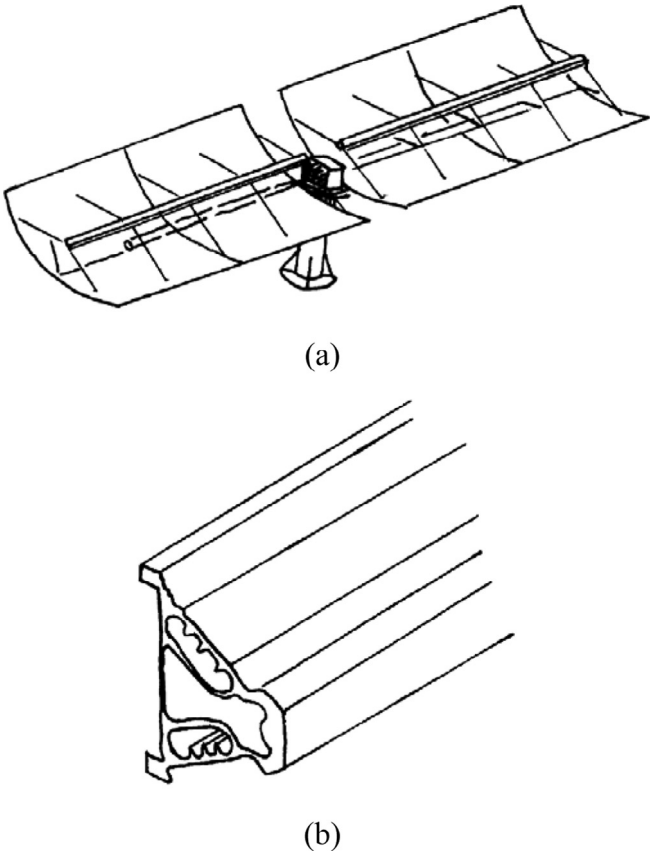



**Fig. 33.** The 2-axis tracking HCPVT system with a PTC: a) concentrator design; b) receiver with cooling channels. Reprinted with permission from Ref. [164]. Copyright © 1980 Elsevier.

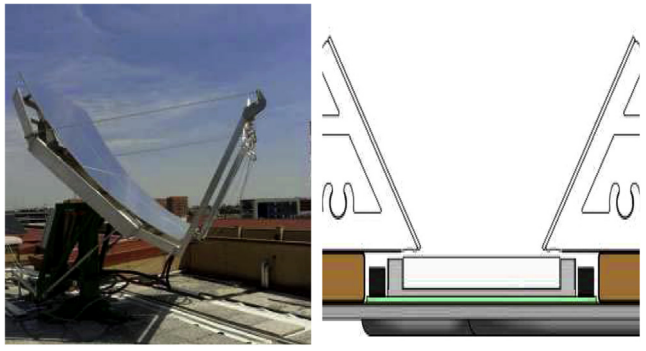



**Fig. 34.** (Color online) The 2-axis tracking HCPVT system with a PTC and a secondary optical concentrator: (a) CPVT system under testing; (b) the design of receiver with the flat-mirror secondary concentrator. Reprinted with permission from Ref. [165]. Copyright © 2014 Elsevier.

ferent flow rates, and the efficiencies would be increased when the focal length of Fresnel lens was changed. The economic viability of this system as a substitute for electricity, kerosene, and diesel for greenhouse heating was also discussed [173]. By installing a CPVT system instead of buying electricity, kerosene and diesel for greenhouse heating, the life cycle savings (LCS) were 7, 344 $, 8, 658 $ and 11, 405 $, respectively, and the relevant discounted payback periods (DPP) were 21, 16 and 11 years, respectively.

The U-shaped pipe was also applied to the CPVT system proposed by Renno and Petito [174]. As shown in Fig. 36, the system

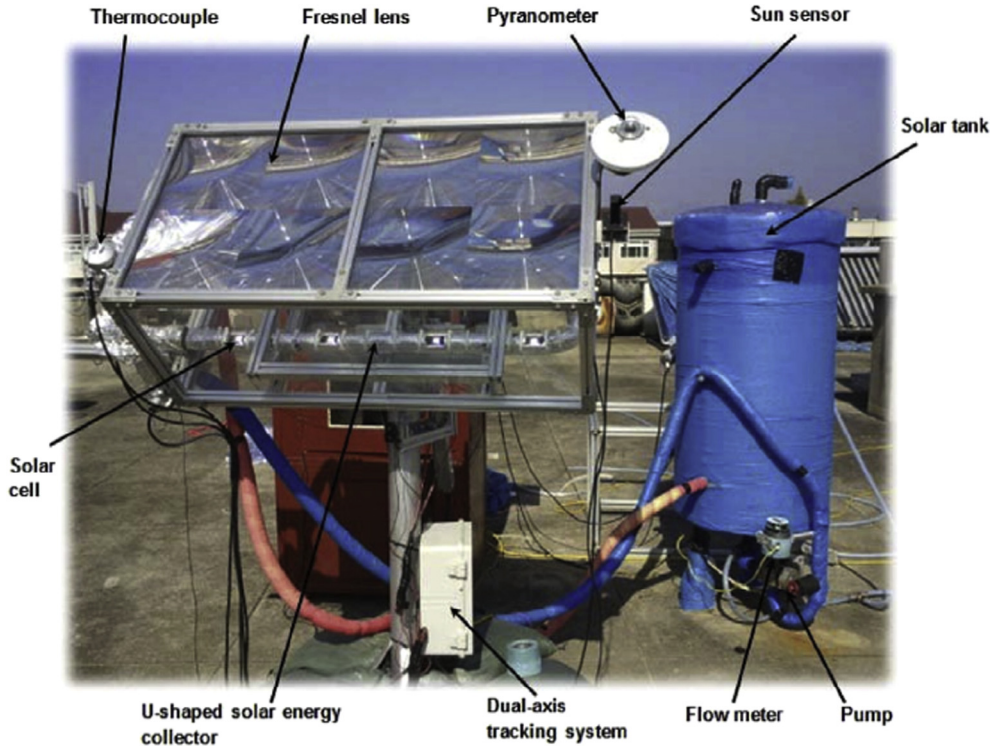



**Fig. 35.** (Color online) The HCPVT system with a U-shaped solar energy collector. Reprinted with permission from Ref. [171]. Copyright © 2015 Elsevier.

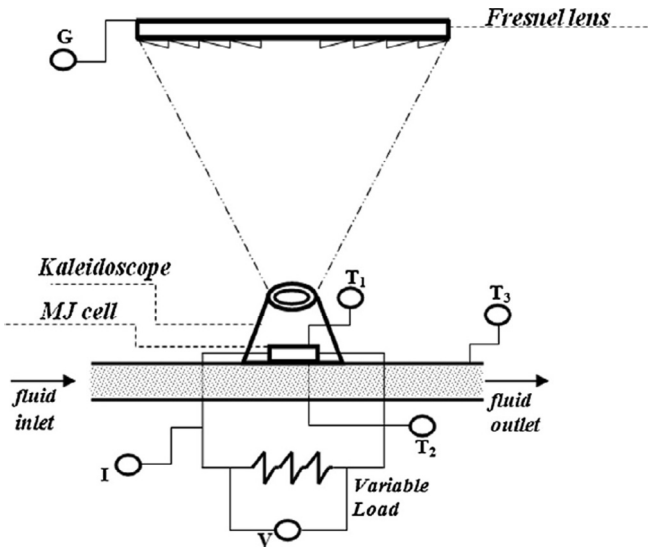



**Fig. 36.** The HCPVT system with Fresnel lenses and kaleidoscopes. Reprinted with permission from Ref. [174]. Copyright © 2016 Elsevier.

combined Fresnel lenses as the primary concentrator and Kaleidoscopes as the secondary concentrator. An experimental test was carried out to define the system configurations. The measured CR was 208.6x. Values of the experimental and theoretical electric power were compared in different operating conditions. A CFD model was used to analyze the thermal system, which showed that the fluid temperature reached about 55 °C in 4 h in the summer day.

Since non-uniformity of solar radiation on cells may cause performance reduction and solar cell damage, secondary optics were wildly used in the CPV or CPVT systems using Fresnel lenses. Xu et al. [175] proposed a Fresnel lens system using the optical prism as the secondary optic, which can provide a CR of 1090 suns. Grooved tubes were used as the thermal component. By combining the Shockley diode equation based electrical model and the two-dimensional steady-state heat transfer model, electrical and thermal efficiencies were evaluated to be 28% and 60%, respectively. After that, the model was further validated by the experimental results of the prototype. Based on the validated model, influences of different parameters on the module performance were analyzed in detail, such as the DNI, wind speed, ambient temperature, cell temperature, and water temperature.

### 2.3.3. Parabolic/spherical dish concentrator

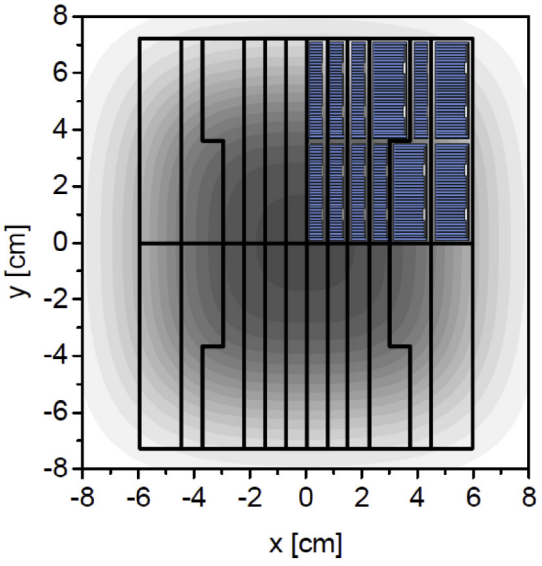
Parabolic dish is the most widely used HCPVT concentrator, as it can provide accurate 2-axis tracking, good optical performance, very high optical CR, and a scalable system size. Several prototypes were developed for the dish HCVPT system and the performances were investigated.

A miniature parabolic dish CPVT system was presented and analyzed by Kribus et al. [176]. The small dish with a reflector of 0.95 $m^2$ concentrated about 500 suns onto a GaInP/GaAs/Ge solar cell dense array, which fit for installation on rooftops close to a consumer. At coolant exit temperature of 58 °C, about 20% of the incident solar energy was captured as electric power, whereas more than 60% was converted to thermal energy. At elevated temperatures, the electrical efficiency was reduced, but most of the lost electrical energy was recaptured as thermal energy. The overall system efficiency was nearly 80% for 58–100 °C outlet water, and thus is not very sensitive to the temperature.

Chayet et al. [177,178] and Moran et al. [179] developed a parabolic dish HCPVT system of 11 $m^2$ aperture area (Fig. 37a). Multiple simple flat mirrors were mounted on the plastic dish surfaces as reflectors. A special designed heteromorphous dense array concentrated photovoltaic (DA-CPV) module with GaInP/GaAs/Ge solar cells (Fig. 37b) was applied as the receiver to even out the effects of inhomogeneous illumination [180]. The system represented



(a)




(b)

**Fig. 37.** (Color online) Zenith Solar Ltd's HCPVT system. (a) Z20 dish HCPVT system; (b) the heteromorphous DA-CPV design Reprinted with permission from Ref. [180]. Copyright © 2010 AIP.

20% electrical and 50% thermal conversion efficiency. The hot water produced was between 60 and 90 °C, suitable for domestic hot water process heat and so on. These researches were applied in the Zenith Solar Ltd's HCPVT system (3rd generation solar power up to 75% efficient combined heat & power. @ http://www.zenith-solar.com/, accessed March 38th, 2017).

Polonsky et al. [181] setup a parabolic dish CPVT system with the homogenizer and dense array metamorphic III-V solar cells. A 3 mm thick porous aluminum slab was sandwiched in the cold plate to increase the surface area for convective heat transfer. The incident solar radiation on the cells was non-uniform even though it passed though the homogenizer, leading to the high mismatch loss of seriesly connected solar cells. The best module efficiency was about 22% at concentration of about 400, indicating that there were still spaces for further improvement.

Helmers et al. [182] set up an outdoor bench for CPVT system characterization and scientific analysis. The system used a parabolic dish as the primary concentrator, and a kaleidoscope was applied as the flux homogenizer. An efficiency model, which showed good agreement with measured results, was presented. The total efficiency reaches nearly 80% when the water inlet temperature equals to the ambient temperature. It is proved that high concentration reduces the thermal losses considerably and increases the electrical efficiency. Rely on the test bench, they developed and validated a performance model [183] for yield predictions of CPVT receivers. The linear coefficients of thermal and electrical outputs were obtained from multi-linear regression on measured data, which is similar to the quasi-dynamic method EN 12975-2: 2006 applied for solar thermal collectors. The influences of solar circumsolar ratio, shading, tracking error, deviations in the shape of the parabolic surface, and the homogenizer length were simulated using the ray-tracing method [184]. It was demonstrated that if sufficient length is provided, a kaleidoscope homogenizer compensates well for non-ideality factors of the primary concentrator. The kaleidoscope homogenizer is a potential choice to improve the flux distribution of dish CPVT systems.

Zimmermann et al. [185] applied a manifold microchannel cooling system [186,187] for the purpose of providing simultaneously electricity and heat. They tested the indoor and outdoor performances of the receiver consisting of a single junction GaAs monolithic interconnected module with an ultra-high performance manifold microchannel heatsink. When combining with the heat recovery, the estimated overall conversion efficiency increased by 300% from 15% to 60%, and the overall exergy efficiency increased by 55%. The economics of the hybrid system for different utilizations were also discussed. A new metric of the enhanced economic value coefficient, which was defined as the ratio of the economic value of the energy output in the combined case of electricity and heat harvesting to the value of the maximum achievable electrical energy, was introduced to better quantify the economic value of CPVT systems.

As many parabolic dishes provide very high radiation at its focal surface, sometimes it's necessary to adjust the distance between the CPV and collector to reduce the CR. Kronland et al. [188] designed and constructed a prototype and reduced the CR from 900 to 100 suns. The testing data indicated that a theoretical overall efficiency of 45% can be achieved.

Researchers also developed many theoretical models to investigate the performance of dish HCPVT systems. Renno and Giacomo [189] proposed a CPVT dynamic model by means of the finite element method (FEM). The InGaP/InGaAs/Ge solar cells, placed on pipes where the cooling fluid (water and glycol solution) flows, convert the concentrated radiation from parabolic dishes. The obtained fluid outlet temperature can be over 85 °C at 1000 suns. Since the CPVT system configuration is strongly influenced by the domestic user energy demands, a model was proposed to evaluate different configurations with consideration of the energy and economic performance and space occupied [190]. Proper CPVT components and configurations were determined according to different load demands in southern Italy. The high concentration configurations were observed to be a better solution from the energy and economic point of view. The inefficiencies, maintenance problems, and the related costs of the CPVT system were also analyzed [191], including the maintenance problems such as the moving parts of tracking system, cell wear due to hotspot problems, and optics cleaning, that can affect the cell efficiency and energy output.

With the consideration of electrical, mechanical, and economic aspects, Gholami et al. [192] simulated and optimized a CPVT system. With a storage tank and active cooling, the thermal energy can be effectively extracted for domestic applications. The total maximum efficiency is about 85%. Using frog leap algorithm optimization, the cost can be reduced to 13.4 $/m$^2$.

Helmers et al. [193] also proposed an energy balance model and analyzed the thermal and electrical performance of a parabolic dish HCPVT system. The paper discussed the limiting cases of maximum electrical outputs and maximum thermal outputs. The thermal losses become nearly negligible for mean fluid temperatures

up to 160 °C at CR > 300x, and the overall efficiency is over 75% for CR > 500x.

Tracking systems may suffer from problems of structural instability under high wind conditions. To minimize the influence of that problem, a spherical concentrator, consisting of a stationary dish and a tracking absorber, was built and investigated in the early stage of 1980s. This type of concentrator was also investigated for the HCPVT system. Bar-lev et al. [194] analyzed the CPVT requirements, and modified the design of the receiver to generate both hot water and electricity. A special two-section polygonal cone shape PVT absorber can provide a constant illumination distribution on the receiver, and the light incidence angle on the absorber surface is closer to normal. Further investigations showed that up to 58% of the absorber surface may be unilluminated at the worst conditions, and the unilluminated surface should be used only for heat generation.

### 2.3.4. Tower-heliostat

As the tower-heliostat optical system which is usually applied in the CSP can provide a high total energy flux in a more centralized way, the CPVT system combining the tower system seems a potential method to obtain simultaneously thermal and electrical energy from the sunlight. Compared with the conventional CPVT systems, the energy of a tower-heliostat system is more centralized, resulting in the benefits that both the energy loss of pipe network and the flow control complexity are reduced. However, the complexity and difficulty of such a system prevent it from commercialization presently.

Hagfarah and Nazarinia [195] investigated a tower CPVT system which generated simultaneously electricity and thermal energy. A receiver prototype with a DA-CPV module and a microchannel heat exchanger was designed and fabricated. A simulation using the System Advisor Model (SAM) software proved the viability of tower CPVT system. The results indicated that the levelized costs of electricity and energy are 0.119 $/kWhe and 0.021 $/kWh, respectively. The water temperature is raised to 65 °C, and the cell temperature can be maintained below 90 °C.

Ju et al. [34] proposed a patent aimed to increase the fluid temperature. The design is based on tower/dish HCPVT and CPV-CSP. As shown in Fig. 38a and b, since the energy flux distribution follows a Gaussian or trapezoid profile, an annular CSP thermal receiver is mounted surrounding the DA-CPV modules with a microchannel cooling system. The coolant R134a first absorbs the wasted heat of CPV modules, and then is heated to a higher temperature in the thermal receiver. Further studies [35,36] also showed that, if the thermal energy is used for electricity generation, the overall generating efficiency can be increased by 20% at 500 suns.

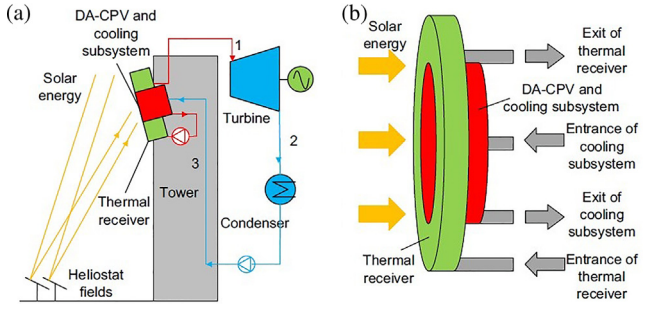



**Fig. 38.** (Color online) The CPV-CSP hybrid system with an external thermal receiver: (a) the system schematic; (b) the solar receiver. Reprinted with permission from Ref. [36].

### 2.3.5. Summary of HCPVT

Details of the HCPVT systems mentioned before are listed in Table 3. The distinguishing features for the WHR HCPVT systems are summarized as follows.

(1) Features of the optical system

WHR HCPVT systems employ concentrating optics such as dish reflectors or spot Fresnel lenses that concentrate sunlight to intensities of 100 suns or more. The systems with 2-axis tracking parabolic trough or tower-heliostat are also investigated, but they are not considered as the main research object, as the CR and cost of 2-axis tracking parabolic trough are not competitive in HCPVT systems, and the tower-heliostat system is of high complexity.

(2) Features of the PV subsystem

Multi-junction solar cells are currently favored over silicon as they are more efficient at higher CRs and temperatures. Though the cost of multi-junction GaAs solar cell is much higher than that of comparable silicon cells, the cell cost remains a small fraction of the cost of the overall HCPV system, and the system economics might still favor the multi-junction GaAs cells.

Design of DA-CPV modules becomes an important issue under non-uniform irradiation. To achieve current matching, various PV connection methods were investigated, and the total cross tied (TCT) method achieved less mismatching loss [196]. Irregularly shaped PV cells would be another option to solve this problem [180].

(3) Features of the thermal subsystem

The solar cells operating at over 100 suns require high-capacity heat sinks to prevent thermal destruction and to manage temperature related performance losses. Microchannel heat sinks have the advantages of high heat transfer performance, easy integration with moving components, light weight, and high stability, and thus are supposed to be a viable method to cope with the extremely high thermal load.

Water-glycol mixture and pressurized water can be used as the cooling fluid at temperatures above 100 °C. As the temperatures of HCPVT systems rise, water-glycol mixture and pressurized water as the HTF are increasingly studied. A closed thermal cycle and a secondary heat exchanger are necessary for these systems.

## 2.4. Researches on the application of WHR CPVT

WHR CPVT systems were suggested or applied in many intensive application fields since its appearance. On one hand, the thermal energy can be used for domestic hot water, local heating, air conditioning, absorption cooling, thermal desalination, district heat, organic Rankine cycle, and so on [197]. On the other hand, the electric energy can be used to drive the auxiliary devices of a thermal system, or to drive the processes which can easily be combined with the thermal processes. The documents mentioned above have already discussed many application fields, but the researches were mainly concerned with the development of CPVT devices. Investigations on the applications are summarized especially in this section.

### 2.4.1. Polygeneration

In polygeneration CPVT systems, the PV part provides electricity for system parasitic consumption, local electricity supply or grid demands. Simultaneously, the thermal part provides heat, used for space heating, domestic hot water and driving the absorption chiller to produce cooling energy.

Kribus and Mittelman [198] theoretically compared several configurations for polygeneration based on the WHR CPVT conception. Polygeneration leads to increased conversion efficiency, and the PV based polygenerations show better performance than the heat engine based ones. They also concluded that within the CRs investigated, the combined system with a bottoming absorption

**Table 3**
System details cited in the literature of HCPVT systems.

| General information[a] | | | Concentrator[b] | | | | | PV subsystem | | Thermal subsystem[c] | | | | | | Efficiency[d] | | |
|---|---|---|---|---|---|---|---|---|---|---|---|---|---|---|---|---|---|---|
| Year | Author | Method | Type | Details | $C_o$ (suns) | $C_g$ (suns) | Tracking | Cells | Package | Structure | HTF | $T_{in}$ (°C) | $T_{out}$ (°C) | $\Delta T$ (°C) | Application | $\eta_E$ (%) | $\eta_T$ (%) | $\eta_O$ (%) |
| 1980 | O'leary and Clements [164] | TH | Parabolic trough | / | / | / | 2-axis | Si | Linear | Channel with fins | Water-glycol | 26.7 | 47.2 | / | / | / | / | / |
| 2014 | Del Col et al. [165] | T&E | Parabolic trough & flat mirror (Two-stage concentrator) | / | / | 130 | 2-axis | GaInP/GaAs/Ge | Linear | Channel | Water | 80 | 86 | / | / | 14–20 | 40–55 | 55–73 |
| 2012 | Quaia et al. [166] | TH | Parabolic trough | Glass | 144 | / | 2-axis | / | Linear | / | Water | / | / | / | / | / | / | 56 |
| 1985 | Mbewe et al. [168] | TH | Spot Fresnel lens | / | 1–1000 | / | NA | Si | Separate | Channel | Water | / | / | / | / | / | / | / |
| 2011 | Arab et al. [169] | PA | Parabolic dish / Spot Fresnel lens & secondary optics (Two-stage concentrator) | Plastic, acrylic material; quartz, glass, metal; semiconductor material; films and fluid-filled structures | / | / | 2-axis | / | Separate | / | / | / | / | / | Domestic hot water; water purification; absorption air conditioning; engine | / | / | / |
| 2014 | Rumyantsev et al. [170] | EX | Spot Fresnel lens | Glass | / | 867 | 2-axis | InGaP/GaAs/Ge | Separate | Chamber | Water | 8–12 | 25–44 | / | / | 22–24 | 47–48 | 70 |
| 2015(2); 2016 | Hussain and Lee [171–173] | T&E | Spot Fresnel lens | Glass | / | 600 | 2-axis | InGaP/GaAs/Ge | Separate cells in the tube | U-shape tube | Water | 30 | 40–75 | / | / | 18 | 54 | 76 |
| 2016 | Renno and Petito [174] | T&E | Spot Fresnel lens | / | 208.6 | / | 2-axis | InGaP/InGaAs/Ge | Cells on the pipes | U-pipe | Water-glycol | ~10 | 42–55 | / | Air heating and cooling | 28.9 | / | / |
| 2016 | Xu et al. [175] | T&E | Spot Fresnel lens | / | / | 1090 | 2-axis | InGaP/GaAs/Ge | Cells on the pipes | Grooved U-pipe | Water | 35 | 70 | / | / | 28 | 60 | / |
| 2006 | Kribus et al. [176] | T&E | Parabolic dish | Low-iron glass | / | 500 | 2-axis | GaInP/GaAs/Ge | Dense array | Channel | Water | / | 58–100 | / | / | 20 | 60 | 80 |
| 2010; 2011; 2012 | Chayet et al. [177,178]; Moran et al. [179] | EX; PA | Parabolic dish | Flat mirrors | / | 600 | 2-axis | GaInP/GaAs/Ge | Dense array & heteroideus solar cells | Microchannel | Water | / | 60–90 | / | / | 20 | 50 | 70 |
| 2013 | Polonsky et al. [181] | EX | Parabolic dish & homogenizer | / | / | 400–500 | 2-axis | GaInP/GaInAs/Ge | Dense array | Porous aluminum | Water | / | / | / | / | 19.5–21.6 | / | / |
| 2011; 2013(2) | Helmers et al. [182–184] | T&E | Parabolic dish & homogenizer | Glass | 132–795 | / | 2-axis | 2-junction GaAs | Dense array | Microchannel | Water | 13–109 | 120 | / | / | 25 | 53 | 80 |
| 2015 | Zimmermann et al. [185] | EX | Parabolic dish | / | / | 500 | 2-axis | GaAs | Dense array | Manifold micrichannel | Water | / | / | / | Space heating; desalination; refrigeration | 15 | 45 | 60 |
| 2015 | Kronland et al. [188] | EX | Parabolic dish | Glass | / | 100 (NM) | 2-axis | / | Dense array | Aluminum fin-type heat sink | Water | 16 | 65 in tank | / | / | / | / | 45.5 |
| 2014; 2015; 2016 | Renno and Giacomo [189]; Renno and Petito [190]; Renno et al. [191] | TH | Parabolic dish | / | / | 900 | 2-axis | InGaP/InGaAs/Ge | Cells on the pipes | Pipes | Water-glycol | 20 | 82 – 110 in tank | / | Domestic hot water | 18 | 69 | / |
| 2015 | Gholami et al. [192] | TH | Parabolic dish | / | / | 600–800 | 2-axis | 3-junction | / | Tube | Water | 25 | ~65 | / | Domestic hot water | 38 | 48 | 85 |
| 2014 | Helmers et al. [193] | TH | Parabolic dish & homogenizer | / | 500 | | 2-axis | 3-junction | Dense array | Microchannel | Water | 80 | 240 | / | / | 24 | 51 | 75 |
| 1983 | Bar-lev et al. [194] | TH | Spherical dish | / | / | 25–200 | Tracking absorber | / | Two-section polygonal cone partially covered by cells | / | Water | / | <75 | / | / | / | / | / |
| 2016 | Hagfarah and Nazarinia [195] | T&E | Tower | / | / | 400–1000 | 2-axis | InGaP/InGaAs/Ge | Dense array | Microchannel | Water | 25 | 65 | / | / | / | / | / |
| 2015(2); 2016 | Han et al. [35,36]; Ju et al. [34] | TH | Tower | / | / | 500–2000 | 2-axis | InGaP/GaAs/Ge | Dense array | Microchannel | R134a | / | 77–124 | / | ORC power | / | / | 36.8–44 (power) |

[a] EX: experimental, TH: theoretical, T&E, theoretical and experimental, PA: patent.
[b] $C_o$: optical CR, $C_g$: geometrical CR; NM: not mentioned, treated as the geometrical CR; $C_g$ is considered as a primary factor on CPVT system classification if it is available in documents.
[c] $T_{in}$: inlet temperature, $T_{out}$: outlet temperature; $\Delta T$: temperature difference between the inlet and outlet of thermal system.
[d] $\eta_O$: overall efficiency, $\eta_E$: electrical efficiency, $\eta_T$: thermal efficiency. In case that both theoretical and experimental results are available in the literature, experimental results are adopted.

heat pump (AHP) is better than ones with a bottoming heat engine. For the PV/AHP hybrid system for refrigeration (single effect and double effect), the overall efficiency is up to 43%.

The feasibility of using a CPVT trigeneration system to satisfy the electricity and cooling demands of a server room was proved by Petrucci et al. [199]. Models of the main components, such as a single effect LiBr chiller and CPVT collectors, were developed in Simulink for different operating conditions. The results showed that the energy demand in August can be fully covered, and there is still surplus power to be supplied to adjacent rooms. However, in the final hours of the January afternoon, the power is not enough for at least 2 h.

Another research work of the CPVT cogeneration system discussed its application on space cooling [200]. The exergetic analysis of a 10 MW CPVT plant located in Algeria showed an overall conversion efficiency of 87.5%, in which the electrical efficiency is 25% and the thermal efficiency is 62.5%. The coolant water temperature of the CPVT system is up to 80 °C at 2000 suns. The economic analysis of the cogeneration system also showed how to optimize the CPVT power plant for a specific location.

Buonomano et al.'s [201] trigeneration CPVT system aims to provide electricity, space heating and cooling and domestic hot water for buildings. They analyzed the detailed performance of a parabolic dish CPVT system which is able to operate at up to 180 °C with two-effect absorptive cooling. Different from other investigations, diathermic oil was used as the HTF to improve the overall performance and permit its integration in high-temperature utilizations. Compared with the non-concentrating and the parabolic trough PVT systems, the dish CPVT collector in this work showed higher electrical and thermal efficiencies ($\eta_e$ = 19%–25%, $\eta_t$ = 60%) in a wide range of operating conditions.

A CPVT polygeneration system with single effect LiBr-$H_2O$ absorption chillers was simulated by a dynamic model [202]. The work also considered the use of electric chiller and gas-fired heater backup system. The optimized performance was obtained by a water to water auxiliary chiller. A case study of a building with both offices and dwellings in the meteorology of Milan and Naples was presented. The CPVT system shows an over 100% primary energy saving, which is better than the 74% of such savings in evacuated tube solar thermal collectors. The economic analysis also indicated that an electricity feed-in tariff unitary cost of higher than 0.15 €/kWh is still necessary. Another case study was for University Hospital District in Naples, Italy [203]. The studied system (Fig. 39) combined parabolic trough CPVT collectors, a single-effect LiBr-$H_2O$ absorption chiller, storage tanks and additional balance-of-plant devices. The demands data regarding cooling, heating and electricity were measured for a one-year operation. From both energy and economic points of views, the performance of the system was excellent. The results showed that all produced renewable energy can be consumed. Even without any public funding, the system can be profitable in a pay-back period around 12 years, and there is still a margin for improvement. Calise et al. [204] also showed that a similar type of polygeneration CPVT system was technically feasible for the university building. A double-stage LiBr-$H_2O$ absorption chiller, a parabolic dish concentrator and a triple-junction receiver were integrated into the system. The overall energetic and economic performance was evaluated, and also showed that a proper funding policy was necessary for commercialization. Compared with a similar flat-plate PVT system previously investigated by the authors [205], the CPVT system achieved better overall energy performance with comparable economic performance. The CPVT polygeneration system was also investigated for energy demands of small isolated communities in European Mediterranean countries [206,207]. This polygeneration system combined solar heating and cooling (single-stage LiBr-$H_2O$), CPVT, biomass-fired heater and multiple effect distillation (MED) for seawater desalination. The viability of the system was proved through accurate energetic, exergetic, thermoeconomic, and exergoeconomic analyses based on dynamic simulations. The factors that mostly affect the overall plant exergy efficiency were discussed, including the exergy destruction in the CPVT collector, biomass heater, and MED section. The system

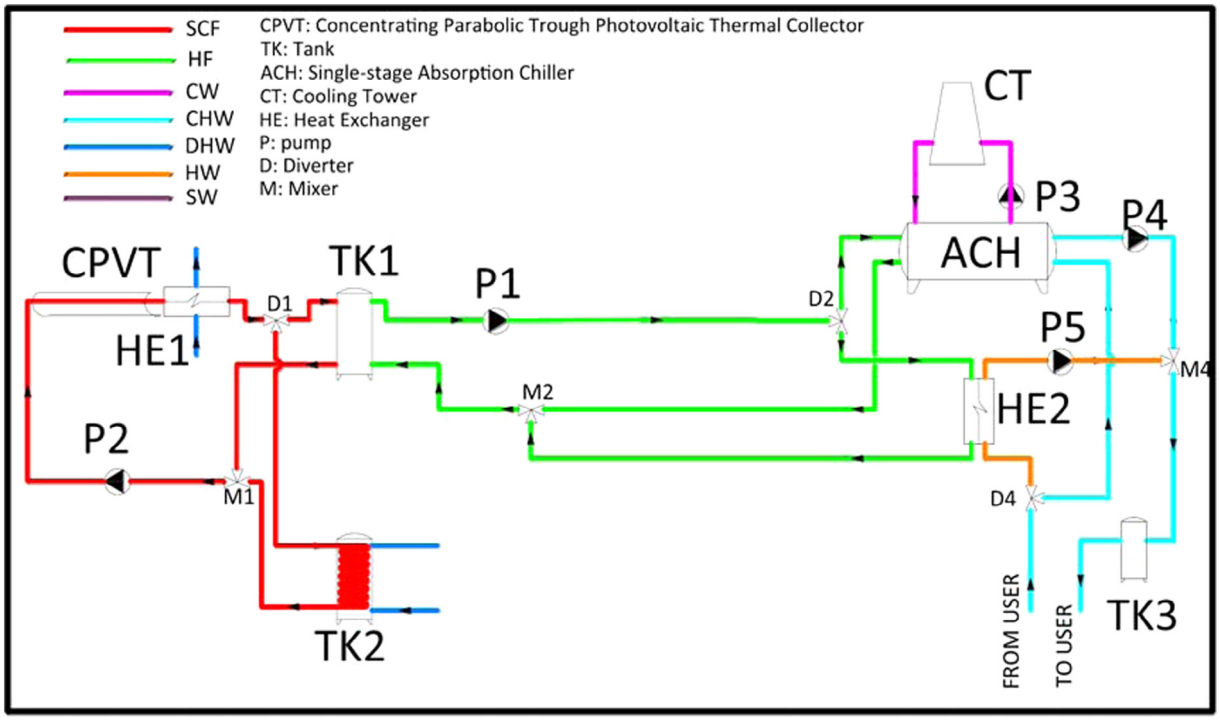



**Fig. 39.** (Color online) A polygeneration CPVT system for University Hospital District in Naples. Reprinted with permission from Ref. [203]. Copyright © 2014 Elsevier.

was deemed to be profitable in many European areas with present feed-in tariffs of PV technologies. Without funding, it would be scarcely competitive, and only suitable for disadvantaged areas, like small islands.

*2.4.2. WHR CPVT systems with heat pump*

The heat pump can also be integrated with WHR CPVT systems, such that the HTF temperature can be increased without sacrificing the PV efficiency. This kind of integration is more proper for LCPVTs, since to provide HTF with higher temperature would be a challenge. Xu et al. [208] fabricated a CPC-LCPVT integrating a heat pump system as shown in Fig. 40. The system simultaneously converted solar energy into electricity and collected solar heat efficiently to upgrade it for water heating. Refrigerant R134a flowed in the multi-port flat extruded aluminum tubes placed underneath the PV cells, absorbing solar heat and evaporating. The LCPVT-heat pump system achieved an average coefficient of performance (COP) of 4.8 for heating water from 30 to 70 °C on a sunny summer day.

*2.4.3. Absorption cooling*

The solar thermal cooling systems are usually found to be more expensive than conventional cooling, but when combined with the CPVT, the situation would be changed. Mittelman et al. [209] proposed a CPVT system that can produce electricity and high temperature thermal energy above 100 °C simultaneously. When coupled with a single-effect absorption chiller, it can be comparable or even better in costs under a wide range of conditions. Using InGaP/InGaAs/Ge solar cells as the PV receivers, and at the coolant outlet temperature of 50–150 °C [210], the overall electrical and thermal efficiencies are 20%–24% and 58%–59%, respectively.

*2.4.4. Air conditioning*

Latent loads (dehumidification) represent a significant portion of the air conditioning loads in hot and humid climates. Desiccant material based air conditioning is recognized to have significant technical, energy and environmental advantages over conventional systems. The required energy demand of desiccant air dehumidification is suitable to be provided by CPVT systems. The thermal energy can be used for continuous regeneration of the desiccant material, and the electrical energy can be used to drive other devices for air conditioning.

Al-Alili et al. [211,212] studied the application of CPVT hybrid system for air conditioning of buildings in hot and humid climates. As shown in Fig. 41, the system consisted of a solid desiccant wheel cycle (DWC) and a traditional vapor compression cycle (VCC). The DWC and VCC were driven by the thermal and electrical output respectively, such that the latent and sensible loads of air conditioning can be accommodated. The transient simulation results of the system in Abu Dhabi weather showed that the cooling COP is increased. Compared with the standalone VCC, the electricity demand reduces by 50%. In addition, the decoupled latent and sensible load are found to be effective in meeting the humidity and temperature requirements of buildings in hot and humid climates. The optimization of this system was carried out using the Pareto front multi-objective genetic algorithm [213]. The system cost was estimated based on the desired system performance. For electricity price of 0.12 $/kWh, the cost of the proposed system will be less than that of the standard VCC after 17.5 years of operation. An experiment on desiccant based air conditioning [214] was carried out to calibrate and validate the simulation.

Calise et al. [215] simulated the operation of a CPVT coupled air handling unit. The CPVT system [152] is capable of producing hot water at 80–100 °C, which is compatible with the 40–70 °C regeneration temperature of the silica-gel wheel for dehumidification. The generated electricity is used to drive the auxiliary devices, while the thermal energy is used to heat the regeneration air in summer and heat the process air in winter. The excessive electricity and heat are provided to the grid and to generate domestic hot water, respectively. The simulation was carried out in TRNSYS software, and was partially validated by the experimental data from the test facility in Benevento, Italy. The annual thermal and electri-

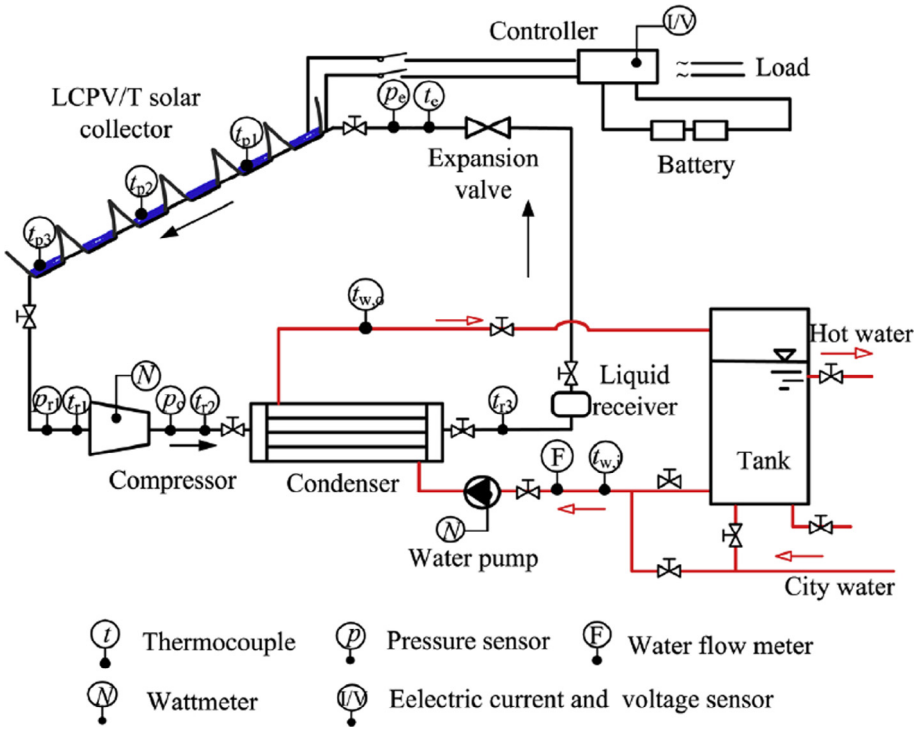



**Fig. 40.** (Color online) The CPC-LCPVT system with a heat pump. Reprinted with permission from Ref. [208]. Copyright © 2011 Elsevier.

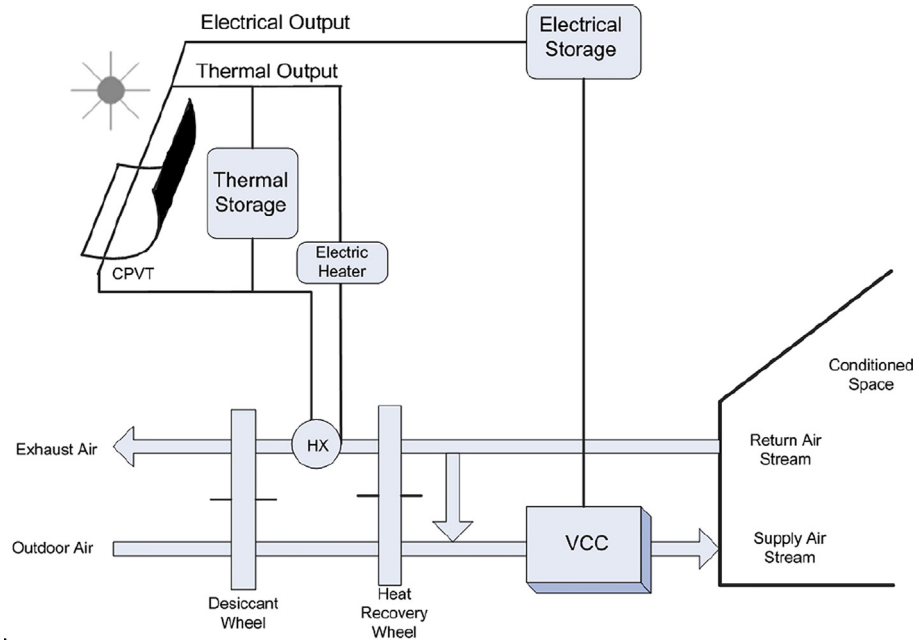



**Fig. 41.** (Color online) The air conditioning system based on a CPVT system. Reprinted with permission from Ref. [211]. Copyright © 2008 Elsevier.

cal efficiencies of the CPVT are 21.15% and 55.32%, respectively. It covers over 70% electricity demand, 60% of the regeneration energy in summer, and 30% of the process air heating energy in winter. Compared with a conventional air handling unit, the CPVT air conditioning system obtains a Primary Energy Saving of 81%–89%.

### 2.4.5. Desalination

WHR CPVT desalination systems exploit the waste heat of PV cells to desalinate water or use the generated electricity for desalination process. As thus, the combined plant can produce electricity and desalinated water.

The parabolic dish CPVT systems were applied for solar desalination. Ong et al. [216] developed a multi-effect membrane distillation (MEMD) system for isolated islands or coastal regions. Based on the cooling systems developed by IBM Research Zurich [186], the PV-receiver heat recovery at 75–80 °C was achieved for thermal energy storage and desalination with the membrane distillation (MD) technique. According to the measured and simulated results, the system converted about 85% of the solar irradiation into electricity and potable water.

Hughes et al. [217] presented a CPVT system for MD. Seawater was used to cool III-V junction solar cells, and then further heated in an additional evacuated tube thermal collector. The MD module was tested for a fluctuating inlet temperature ranging from 40 to 80 °C, as it would be in the real operating conditions. The transient performance of the MD module indicated that the effects of fluctuations in solar radiations were not significant, and the integration of the MD with the CPVT system was feasible.

Mittleman et al. [218] combined a multi-effect evaporation desalination (MEED) system with a CPVT system. A simulation was performed and showed that the overall plant efficiency is 77%, with a high capacity factor (CF) of over 79%. At a good solar site with around 2400 kWh/m$^2$ year beam radiation, 17 €/W$_p$ elec-

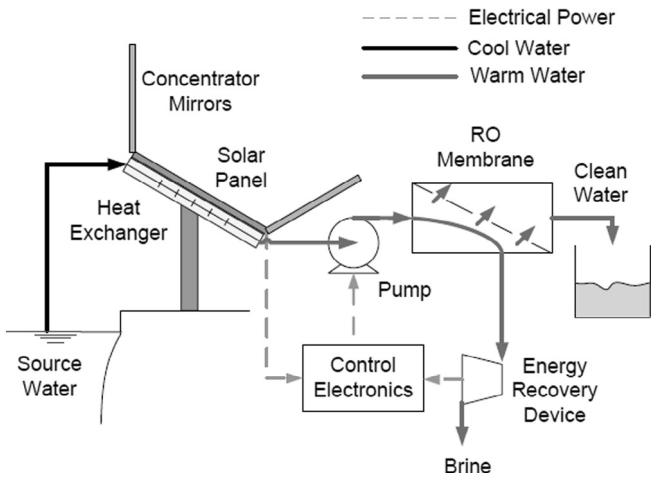



**Fig. 42.** The PV-powered RO desalination system with boosters. Reprinted with permission from Ref. [219]. Copyright © 2012 ASME.

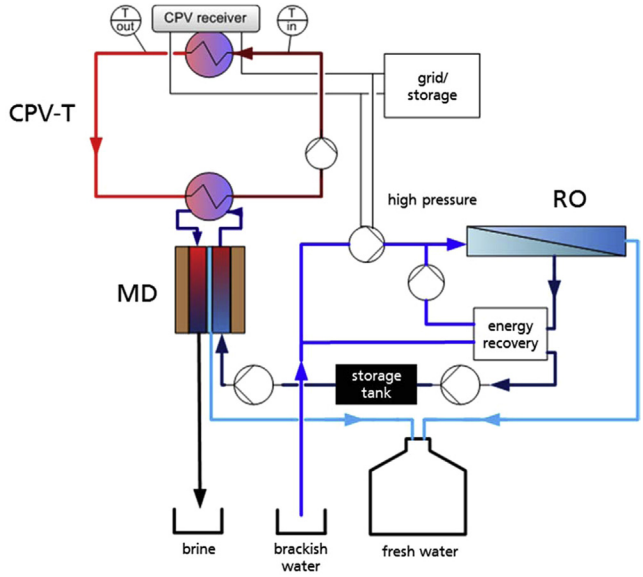



**Fig. 43.** (Color online) The MD and RO desalination system based on a CVPT system. Reprinted with permission from Ref. [220].

**Table 4**
Details of the researches on CPVT system applications.

| General information[a] | | | Concentrator[b] | | | | | PV subsystem | | Thermal subsystem[c] | | | | | | Efficiency[d] | | |
|---|---|---|---|---|---|---|---|---|---|---|---|---|---|---|---|---|---|---|
| Year | Author | Method | Type | Details | $C_o$ (suns) | $C_g$ (suns) | Tracking | Cells | Package | Structure | HTF | $T_{in}$ (°C) | $T_{out}$ (°C) | $\Delta T$ (°C) | Application | $\eta_E$ (%) | $\eta_T$ (%) | $\eta_O$ (%) |
| 2008 | Kribus and Mittelman [198] | TH | / | / | / | 50, 200, 1000 | 1-axis or 2-axis | InP/InGaAs/Ge | / | / | / | / | 50–350 (PV/CSP); 25–250 (PV/AHP) | / | PV/CSP; PV/AHP | / | / | PV/CSP (power): ~38 (200x), ~34 (50x); PV/AHP: ~45 (200x), ~39 (50x) |
| 2013 | Petrucci et al. [199] | TH | / | / | / | / | / | / | / | / | Water | / | 90 | / | Electricity, space heating, domestic hot water, single-effect absorption cooling | 18 | 62 | / |
| 2014 | Garcia-Heller et al. [200] | TH | Parabolic dish | / | / | 2000 (NM) | 2-axis | GaInP/GaAs/Ge | Dense array | Manifold microchannel | Water | 85 | 90 | / | Absorption cooling | 25 | 62.5 | 87.5 |
| 2013 | Buonomano et al. [201] | TH | Parabolic dish | / | / | 318 | 2-axis | InGaP/InGaAs/Ge | / | Microchannel | Diathermic oil | 30–200 | 40–210 | / | Electricity, space heating, domestic hot water, two-effect absorption cooling | 19–25 | 60 | / |
| 2014 | Buonomano et al. [203] | TH | Parabolic trough | / | / | ≤200 | 1-axis | / | / | Channel | Water | / | 70–90 | / | Electricity, space heating, domestic hot water, single-effect absorption cooling | 12.6–20.5 | 32.7–53.1 | / |
| 2013 | Buonomano et al. [202] | TH | Dish | / | / | 500 | 2-axis | GaAs | Dense array | Microchannel | Water | / | 85 | / | Electricity, space heating, domestic hot water, single-effect absorption cooling | / | / | / |
| 2013 | Calise et al. [204] | TH | Parabolic dish | / | / | 318 | 2-axis | 3-Junction | / | Channel | Pressurized water | / | 130–170 | / | Electricity, space heating, domestic hot water, double-effect absorption cooling | 13.3 | 32 | / |
| 2015(2) | Calise et al. [206,207] | TH | Parabolic trough | / | / | / | 1-axis | 3-Junction | / | Tube | Pressurized water | / | 85 in summer; 55 in winter | / | Electricity, space heating, domestic hot water, single-effect cooling, Multiple Effect Distillation | ~14 | ~32 | / |
| 2011 | Xu et al. [208] | EX | Symmetrical CPC | Mirror-finished aluminum plate | 1.6 | 3.52 | Stationary | / | Linear | Tube | R134a | 14.1–24.7 | / | <10 | Heat pump | 17.5 | / | / |
| 2006 | Mittelman et al. [209] | TH | / | / | / | ≤200 | 1-axis or 2-axis | 3-Junction | / | Cooling plate | Water | / | 59–159 | / | Single effect absorption cooling | 14 (159°C); 18 (59°C) | / | 79 |
| 2007 | Mittelman et al. [210] | TH | / | / | / | ≤200 | 1-axis or 2-axis | InGaP/InGaAs/Ge | / | Cooling plate | Water | / | 50–150 | / | Single effect absorption cooling | 20 (150°C); 23 (50°C) | 58 | / |
| 2008; 2012; 2013 | Al-Alili et al. [211–213] | TH | / | / | / | / | / | / | / | / | Water | / | / | / | Desiccant based air conditioning, electricity. | 16–17 | 63–64 | / |
| 2014 | Calise et al. [215] | TH | Parabolic trough | / | / | 10 | 1-axis | GaInP/GaAs/Ge | Linear | V-Channel | Water | / | 80–100 | / | Desiccant based air conditioning, electricity, domestic hot water | 21.15 | 55.32 | / |
| 2012 | Ong et al. [216] | T&E | Parabolic dish | / | / | 1000 (NM) | 2-axis | GaInP/GaAs/Ge | Dense array | Manifold microchannel | Water | 37–43 | 75–80 | / | Multi-effect membrane distillation | / | / | 85 |
| 2014 | Hughes et al. [217] | EX | Parabolic dish | / | / | 500 | 2-axis | III-V Multi-Junction | Dense array | CPVT cooling combined evacuated tube thermal collector | Sea water | / | 40–80 | / | Membrane distillation | / | / | / |
| 2009 | Mittleman et al. [218] | TH | Parabolic dish or parabolic trough | / | / | 200 (parabolic dish); 32 (parabolic trough) | 1-axis or 2-axis | InGaP/InGaAs/Ge or c-Si | / | Cooling plate | Water | / | 50–150 | / | Multi-effect evaporation distillation | 19 (150°C); 22 (50°C) | / | 80 |
| 2012 | Kelley et al. [219] | T&E | Flat reflector | Aluminum plate | ~1.5 | / | Stationary | / | Panel | / | Sea water | / | / | / | Reverse osmosis | / | / | / |
| 2016 | Wiesenfarth et al. [220] | EX | Parabolic dish | Glass | / | / | 2-axis | / | Dense array | / | Water | / | 90 | / | Membrane distillation & reverse osmosis | / | 79.2 | / |

[a] EX: experimental, TH: theoretical, T&E, theoretical and experimental, PA: patent.
[b] $C_o$: optical CR, $C_g$: geometrical CR; NM: not mentioned, treated as the geometrical CR; $C_g$ is considered as a primary factor on CPVT system classification if it is available in documents.
[c] $T_{in}$: inlet temperature, $T_{out}$: outlet temperature; $\Delta T$: temperature difference between the inlet and outlet of thermal system.
[d] $\eta_O$: overall efficiency, $\eta_E$: electrical efficiency, $\eta_T$: thermal efficiency. In case that both theoretical and experimental results are available in the literature, experimental results are adopted.

tricity price, and less than 3 €/$W_p$ collector cost, the 200x concentrated CPVT system achieves the lowest water cost even compared with the conventional reverse osmosis (RO) or PV + RO plant.

CPVT systems may also be combined with the reverse osmosis (RO) desalination. Kelley et al. [219] presented and tested a LCPVT system for PV-powered RO desalination unit (Fig. 42). It also exploited the complementary thermal energy of the solar panel and reverse osmosis unit. Using Mylar covered aluminum plates as the boosters, the optical system provided approximately 50% additional illumination. The simulation results of this concept were experimentally validated in a prototype. An increase of 57% in fresh water produced was achieved in the experiments using thermal management and solar concentrators.

Wiesenfarth et al. [220] combined the MD and RO water desalination to a CPVT system. As shown in Fig. 43, the thermal energy absorbed by the CPVT is used to produce fresh water through the MD process, and the generated electricity is partly used to run the pumps to overcome the osmotic pressure in the RO process. Since the specific energy consumption of the RO process increases with the water salinity rising, the MD process, of which the specific energy consumption is less sensitive to the water salinity, is used to further concentrate the brine from the RO process. The calculations showed that the total recovery ratio (the ratio between product and feed water) is 92% for the complete system. They also tested the thermal receiver of a parabolic dish CPVT, and the maximum thermal efficiency of the tested receiver achieved 79.2%.

#### *2.4.6. Summary of applications*

Details of the researches on the applications of WHR CPVT system are listed in Table 4. As shown before, the produced energy of WHR CPVT systems can be used for multiple purposes. The investigations concerning applications of WHR CPVT focused on complex thermal systems, such as desalination systems, absorption cooling systems, and air conditioning systems. As a contrast, the local/district heating, building, and agriculture applications require only a simple thermal system. On the other hand, parabolic troughs and dishes are considered as the concentrators in many researches, but the using of simple 1-axis tracking CPVT systems is a cost-effective solution for many scenes.

## 3. Current statues of WHR CPVT researches

Fig. 44 shows the count of documents on WHR CPVT researches. The count of research is reversed to its difficulty level. There are 73, 46, 31, and 19 researches for LCPVT, MCPVT, HCPVT, and Application, respectively. The count of research is doubled compared with the SBS CPVT researches [32]. The majority of researches on CPVT devices involve experiments, which is also different from the theoretical research method of most SBS CPVT researches. Especially for the LCPVT and MCPVT, the concentrators are much easier to be accessed or established, which facilitates experimental investigations. But for cogeneration CPVT applications, there are only several researches, since the CPVT systems are not matured enough to be applied in these fields.

Fig. 45 depicts the development of WHR CPVT systems. In 1981–1990, early studies showed the potentiality of WHR CPVT systems in energy saving, and several prototypes were tested. However, as the price decline of fossil fuel in the 1990s, the researches reduced in 1991–2000. Thereafter, the WHR CPVT regained the attention of researchers, and the count of research documents rapidly increased after 2009. The rapid increase in the researches of WHR CPVT may be due to the following reasons: (1) the fossil fuel price gradually increased after the Asian financial crisis in 1997, and the PV cell price rapidly reduced after 2009; (2) the maturity of related technologies, including optical concentrators and PV cells; and (3) the public concerns of global warming and environmental problems increasingly rose. It can also be observed that the research hotspot was gradually shifted from LCPVT to MCPVT and HCPVT. Studies on HCPVT rapidly increased in the 2013–2016 period.

The optics adopted in WHR CPVT researches are summarized in Fig. 46. LCPVT systems mainly use flat-plate reflectors and CPCs as the concentrator. These systems can be stationary such that the cost can be reduced. MCPVT systems adopt the linear concentrators, including the linear Fresnel lens/reflectors and parabolic troughs as the concentrator, and HCPVT systems mainly use the spot Fresnel lenses and parabolic dishes as the concentrator. The count of theoretical research is nearly the same as that of the experimental researches for each type of the concentrator. CPCs, parabolic troughs and parabolic dishes, which respectively corresponding to the LCPVT, MCPVT and HCPVT, are the top three optics adopted in WHR CPVT studies.

Fig. 47 shows the comparison of the HTF outlet temperature of the WHR and SBS CPVT systems. The HTF outlet temperature of WHR CPVT systems generally increases with the CR. However, it is not a distinct increase. The HTF of WHR LCPVT is ranging from 20 to 190 °C, while that of WHR HCPVT is ranging from 25 to 250 °C. The operating temperature of the thermal subsystem in WHR CPVT is restricted by PV cells. The high temperature will

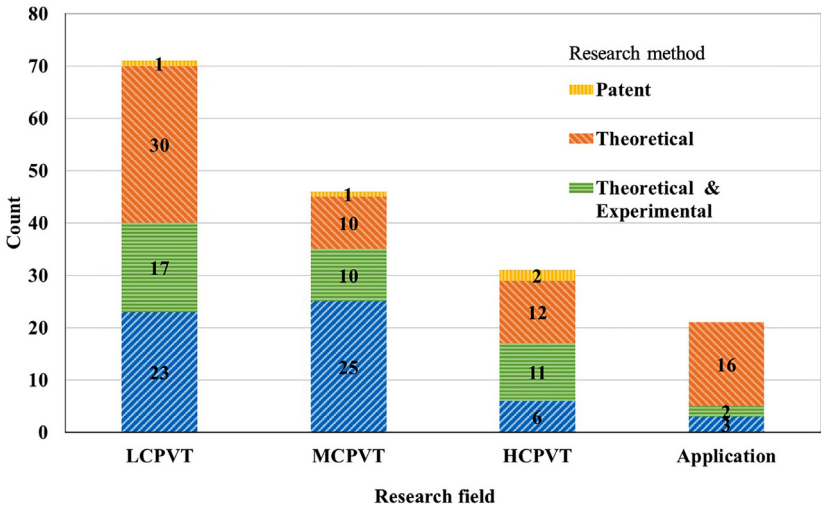



**Fig. 44.** (Color online) The count of WHR CPVT research documents according to research method and research field.

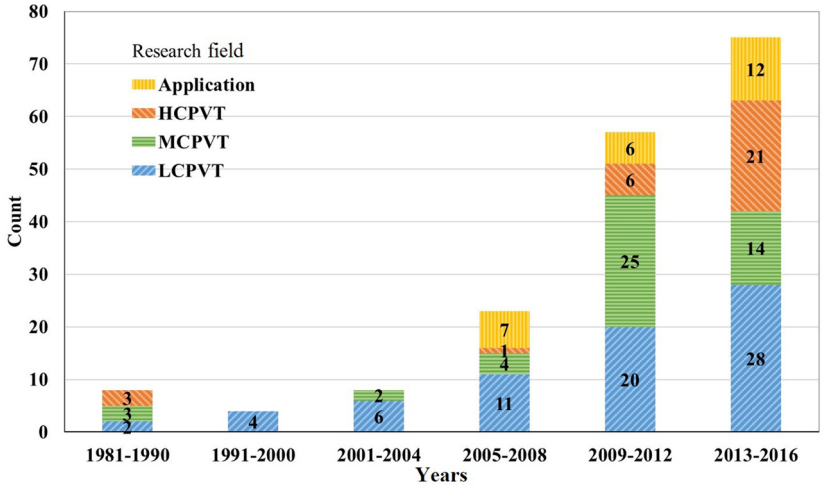



**Fig. 45.** (Color online) The count of WHR CPVT research documents according to year and research field.

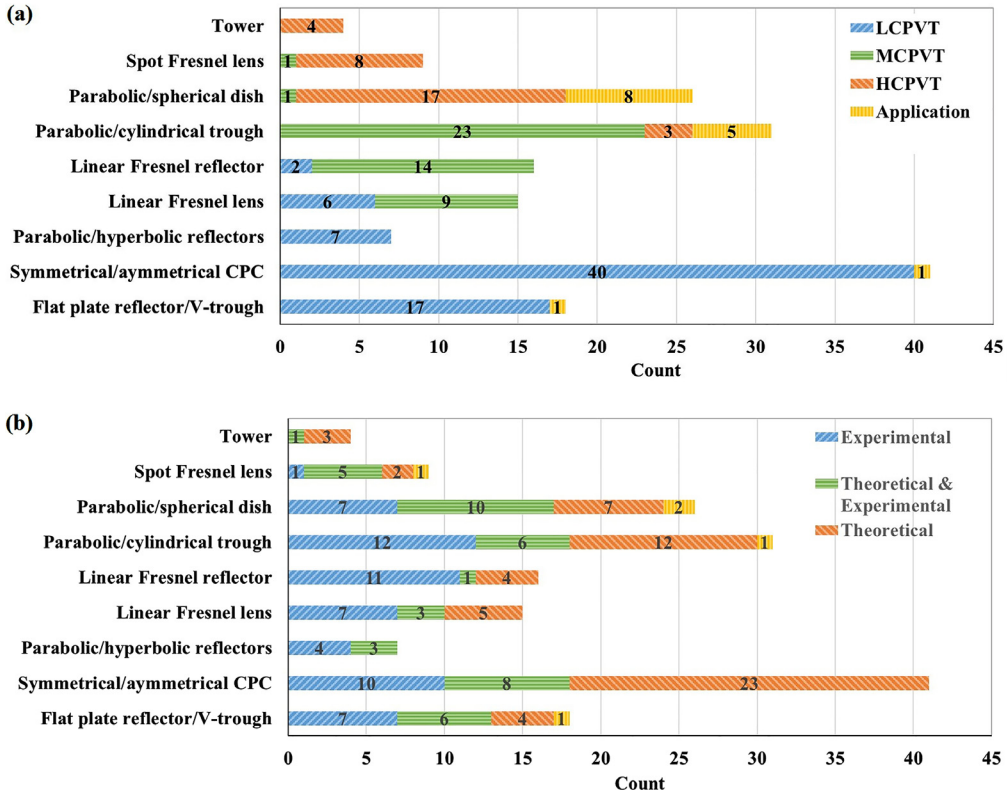



**Fig. 46.** (Color online) The count of WHR CPVT research documents according to: (a) optical concentrators and research field, (b) optical concentrators and research method.

increase the intrinsic carrier concentration and reduce the bandgap of PV cells. The conversion efficiency would be suffered because of the reduction in open-circuit voltage [221]. For commercially available solar cells, there exists a temperature limitation. The crystalline silicon solar cell efficiency would drop to 0 at 270 °C [222], and the multi-junction GaAs solar cells cannot operate at over 400 °C [37]. Moreover, the melting point of the solder alloy of PV module is usually ranging from 130 to 300 °C [223], and thus the PV modules are usually claimed to be operated below 120 °C. On the contrary, the thermally decoupled SBS CPVT systems have no such limitation as for the thermally coupled WHR CPVT. The HTF outlet temperature of SBS CPVT systems [32] could be much higher, reaching over 500 °C at CR over 100 suns. A linear regression of the outlet temperature also shows that the regressed HTF temperature in SBS CPVT systems increases more rapidly than WHR CPVT systems.

The applications of thermal energy according to the temperature are shown in Fig. 48. As WHR CPVT systems can provide thermal energy ranging from 20 to 250 °C, several thermal energy applications were discussed in researches, including the absorption cooling, desalination, local or district heating, Desiccant based air conditioning, crop drying, organic Rankine cycle (ORC) power, and so on. Whereas the generated electricity of PV cells can be used to drive the devices of a thermal system, supply power to the consumers, or directly connect to the grid. The essential thing is to seek out the consumers with combined electrical and thermal

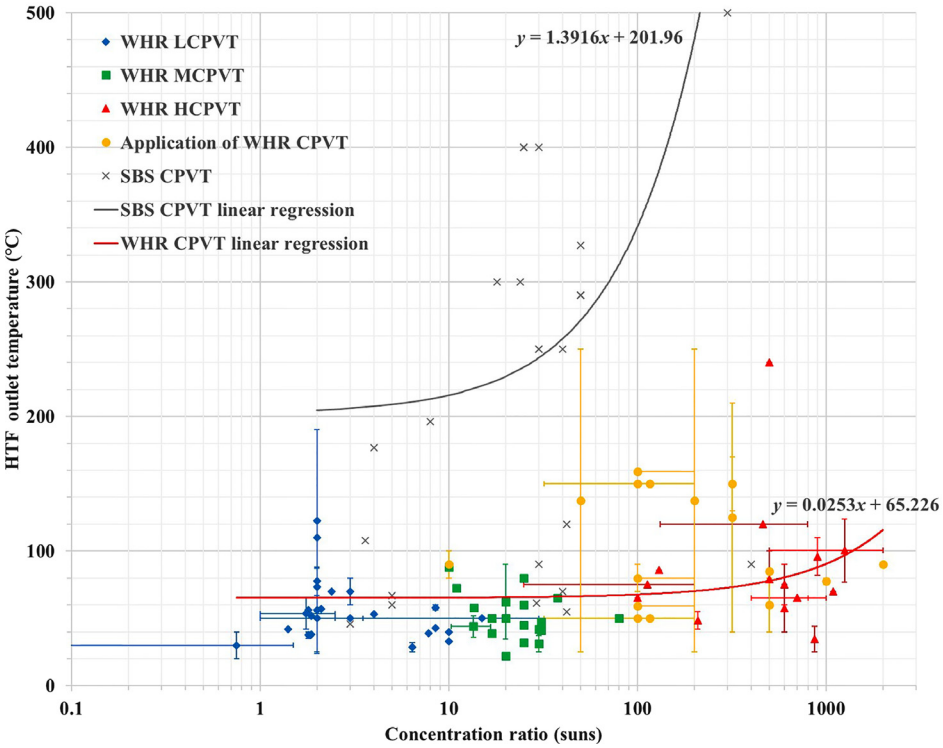



**Fig. 47.** (Color online) Comparison of the WHR CPVT and SBS CPVT: the HTF outlet temperature according to the concentration ratio and research field.




**Fig. 48.** (Color online) The Carnot efficiency according to different applications and temperature of the recovered thermal energy.

energy demand. The extracted thermal yield temperatures of the researches may be higher than the temperature range of its application. It is usually because of the secondary heat exchange. A higher thermal yield temperature means a better Carnot efficiency. If the thermal energy is appropriately used according to its temperature, the exergy efficiency will be higher, which will also help to reduce the costs.

For the thermal applications, there are several points to be explained. To be able to use water for hot tap water or heating, the temperature must be at least 40 °C. Local heating systems are operated at a quite low temperature, below 70 °C, to avoid salt crystallization in pipes or heat exchangers. In a district heating system, the hot water is distributed to the customer via a heat-supply network. A higher water temperature is necessary, but it is usually below 100 °C, because the pressurized hot water or steam would increase the complexity and costs. Various approaches can be used for water desalination, and the temperature ranges are listed as follows: for reversed osmosis, 25–45 °C; for multi-effect membrane distillation, 50–90 °C; for multi-stage evaporation or flash distillation, 80–120 °C. The solar thermal energy can also be used to drive an absorptive cooling process, producing chilled water for space cooling: for single-effect absorptive cooling, 50–150 °C; and for double-effect absorptive cooling, 120–185 °C. If the thermal yield temperature is much higher, an ORC (100–250 °C) or Rankine cycle (370–600 °C) would be a possible choice.

Fig. 49 shows the application fields of WHR CPVT systems studied in the documents. As mentioned before, the outlet temperature of WHR CPVT systems is limited by PV cells, and thus providing high-temperature thermal energy would sacrifice the PV efficiency. Therefore, most of the WHR CPVT systems are explored for low temperature applications. Except for the 47% application-not-specified researches, 55% (29% of the rest 53%) of the researches are concerned with the electricity supply, domestic hot water supply, and space heating of residential and commercial buildings. Combining with illumination for the buildings or greenhouses is also an optimal option, as different types of energy can be provided by a single WHR CPVT system. Other important application fields include the absorption cooling and water desalination. These researches require higher operating temperatures and more complex system configuration, but still keep a reasonable economic value [197] since the final product prices also increase.

A larger gap can be observed between the experimental and theoretical efficiencies in Fig. 50a and b. The experimental results showed that the average efficiencies of LCPVT, MCPVT and HCPVT systems are respectively 49.3%, 53.9% and 67.2%, while that of the theoretical results are respectively 70.0%, 75.3% and 75%. The efficiencies of experimental results are much lower than the theoretical ones, especially for the systems with lower CRs. That is possible because the systems with lower CRs were not elaborately designed and tested. High concentrated systems, which use high efficiency PV cells, 1-axis or 2-axis tracking systems, good thermal isolation, and precise control, would benefit the conversion efficiencies in real systems. It can also be observed from Fig. 50 that the systems with multi-junction solar cells will achieve better electrical efficiencies. The 3-junction (3J) solar cells are more accepted in researches of HCPVT devices and researches aimed for applications. In researches regarding LCPVT and MCPVT devices, silicon solar cells (a-Si, pc-Si and c-Si) are more commonly used.

## 4. Conclusions

WHR, SBS, EDF are research trends which are commonly utilized to refine the conversion efficiency of CPVT systems. Although the majority of these investigations focus on WHR CPVT approaches, there is still no detailed review on this topic. The researches and developments of WHR CPVT systems, including the feasibility analyses, conceptual designs, testing fabrications, theoretical and experimental performance evaluations, and the applied studies, are comprehensively reviewed in this paper. The WHR CPVT systems with low, medium and high CRs show different system configurations, characteristics, and research trends. In addition, the results extracted from the documents are also beneficial to understand the current technical improvement of the WHR CPVT approach, and identify the potential difficulties and barriers.

Nearly all kinds of concentrators are explored to be integrated into WHR CPVT systems. Development of LCPVT systems usually aims to reduce the cost by combining with stationary, robust, and low maintenance concentrators, while HCPVT systems aim to

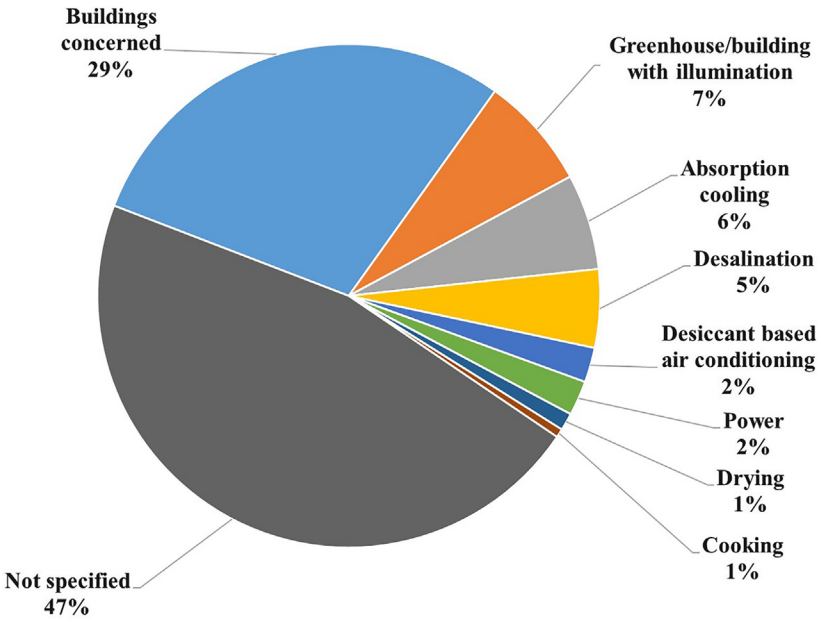



**Fig. 49.** (Color online) WHR CPVT researches concerned for different applications.

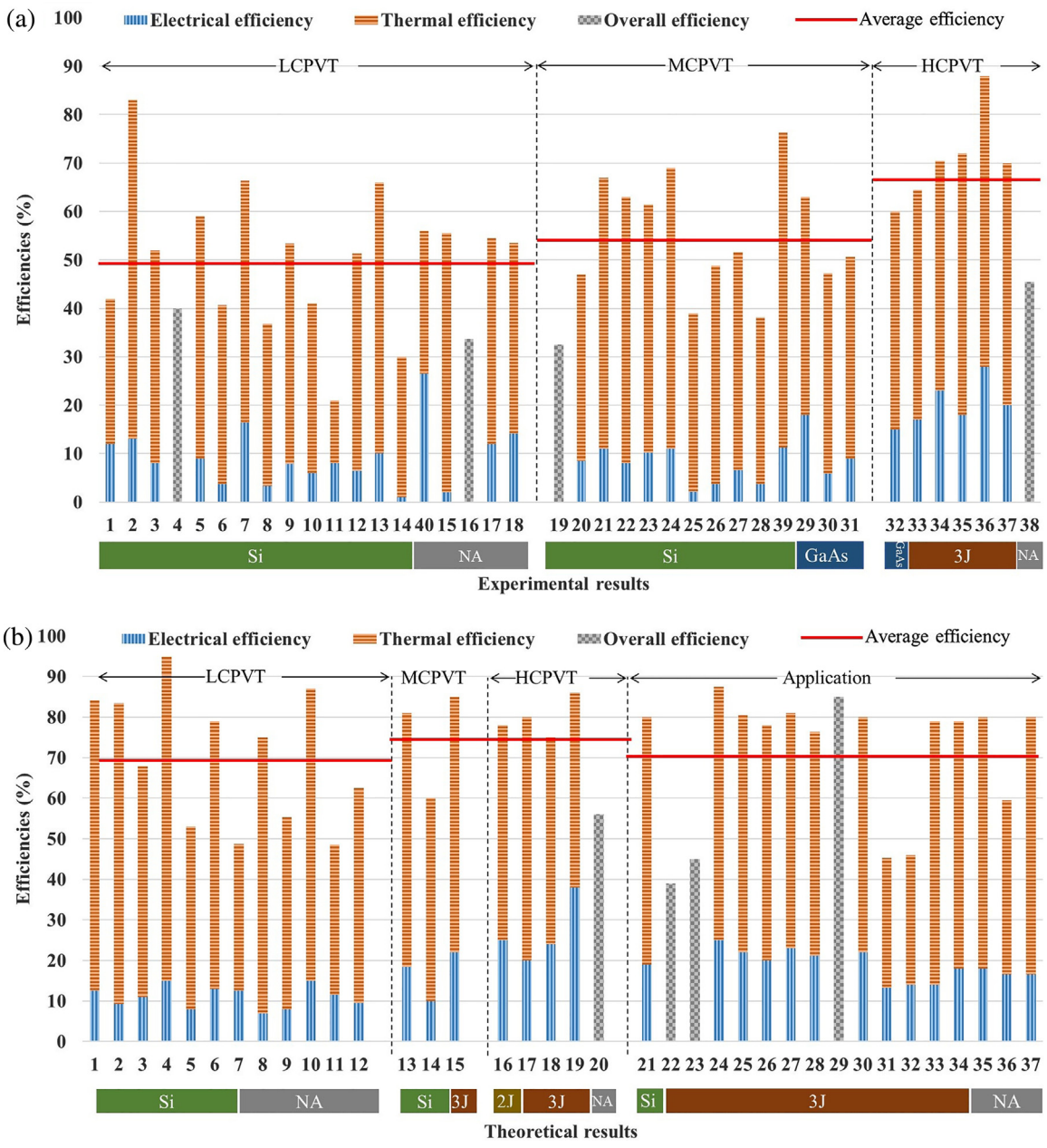



**Fig. 50.** (Color online) Electrical, thermal and overall efficiencies of WHR CPVT systems: (a) experimental results (b) theoretical results.

improve the conversion efficiencies as much as possible. This tendency can be observed especially in the use of solar cells and heat exchangers. From LCPVT to HCPVT, solar cells shift from silicon to III-V multijunction, and the microchannels are used as heat exchangers rather than conventional tubes. Moreover, various HTFs are tested, including ordinary fluids of air, water, and glycol, and non-traditional fluids of refrigerant, oil, molten salt, and PCM materials. Generally, the investigations conducted on WHR CPVT have covered a wide range of system configurations.

The WHR CPVT systems are investigated in order to be used in numerous applications. The generated electricity can be used off-grid or on-grid, and the thermal energy can be utilized for residential, commercial, and industrial purposes. For traditional or unpretentious utilizations, including the domestic hot water, local heating. The WHR CPVT systems do not have to achieve a relatively high temperature, but must take the customer's energy demand into consideration. On the contrary, the applications combining complex auxiliaries or systems, including district heating, steam cooking, crop drying, air conditioning, absorption cooling, desalination and organic Rankine cycle, require significantly for high temperatures. Hence, such systems can be introduced in the manufacturing of various products, which helps to broaden the market for diverse energy demands. However, these complex WHR CPVT systems are still far from the practical applications, and even prototypes are rarely tested.

The WHR CPVT systems are still not mature and successful in the market yet. There are several issues worth paying attention to in the future research and development.

(1) System designs and optimizations based on dynamic simulation and tests

Most of the researches on WHR CPVT design and optimization are based on steady-state models. However, the system design

and optimization highly depends on the time-related external conditions of a specified scene, such as the solar resource, meteorology, consumer demands, policy, and economy. Dynamic simulation and tests are essential for the design and optimization processes.

(2) Reliability and robustness research

Although there are many types of research which were conducted to verify the reliability and robustness of concentrators or flat-plate PVT receivers [224,225], investigations on this field of WHR CPVT system rarely appeared in the documents. The reason for this difference is supposed to be the difficulty in developing reliable and robust CPVT receiver. The operating conditions of the CVPT receiver are much tougher, especially under high concentrated and non-uniform illuminations. However, the long-term test on this research field is still necessary to prove that the WHR CPVT would be commercially available.

(3) CPVT receivers operating under high concentrated and non-uniform illumination

As mentioned before, the WHR CPVT systems usually operate under a deteriorated condition. The researches on high heat flux heat exchange technologies, including impinging jet flow, microchannel, phase change [226] would be helpful for the temperature control of the receiver. Whereas, the non-uniform illumination on PV module needs to be further investigated to reduce energy losses and alleviate the danger of potential damage. The researches on PV module's connection methods [196,227,228], heteromorphous PV modules, secondary optical elements and packaging [229] are significant in solving this problem.

(4) Proper application area based on the energy demand and economic analysis.

Since situations of the market diverse greatly in different areas and applications, it's necessary to extract proper application area of WHR CPVT from the basic data of the potential market. The application area and designs of a WHR CPVT system should take more influencing factors and constraints into consideration. Development of decision-making methodologies [230,231] for the system application would accelerate the commercialization process.

(5) Commercialization and standardization

A variety of different WHR CPVT systems have appeared in the market, but the lack of standard would lead to uncertainty and confusion of consumers. Thus, the development of other related standards is critical for the WHR CPVT systems. The standards on PVT, CSP, CPV, PV, and solar thermal systems [225,232,233] would be helpful for the initial standardization and commercialization of the WHR CPVT systems.

(6) Novel WHR CPVT development

As mentioned before, the WHR CPVT concept can be combined with SBS or EDF concepts to develop novel high efficiency ploygeneration systems. Beside that there are also many other technologies can be combined with the WHR CPVT, such as TPV, thermoelectrics, photocatalytic process, etc. These inspired novel designs may lead to a new regime for the development of WHR CPVT approach.

## Conflict of interest

The authors declare that they have no conflict of interest.

## Acknowledgments

This work was supported by the National Natural Science Foundation of China (51406051 and 51522602), the Beijing Municipal Science and Technology Project (Z161100002616039), and the Fundamental Research Funds for the Central Universities (2016MS20).

## References

[1] World energy assessment. United Nations Development Programme; 2000.
[2] International energy outlook 2016 with projections to 2040. U.S. Energy Information Administration; 2016.
[3] Renewables 2017 global status report. Paris: REN21 Secretariat; 2017.
[4] Solar heat worldwide 2017. IEA Solar Heating & Cooling Programme; 2017.
[5] Philipps SP, Bett AW, Horowitz K, Kurtz S. Current status of concentrator photovoltaic (CPV) technology. Fraunhofer ISE/NREL report; 2015.
[6] Wenham SR. Applied photovoltaics: Routledge; 2011.
[7] Makki A, Omer S, Sabir H. Advancements in hybrid photovoltaic systems for enhanced solar cells performance. Renew Sust Energ Rev 2015;41:658–84.
[8] Maghanki MM, Ghobadian B, Najafi G, Galogah RJ. Micro combined heat and power (MCHP) technologies and applications. Renew Sust Energ Rev 2013;28:510–24.
[9] Raj NT, Iniyan S, Goic R. A review of renewable energy based cogeneration technologies. Renew Sust Energ Rev 2011;15:3640–8.
[10] Ibrahim A, Othman MY, Ruslan MH, Mat S, Sopian K. Recent advances in flat plate photovoltaic/thermal (PV/T) solar collectors. Renew Sust Energ Rev 2011;15:352–65.
[11] Zondag HA. Flat-plate PV-Thermal collectors and systems: a review. Renew Sust Energ Rev 2008;12:891–959.
[12] Michael JJ, Iniyan S, Goic R. Flat plate solar photovoltaic–thermal (PV/T) systems: a reference guide. Renew Sust Energ Rev 2015;51:62–88.
[13] Aste N, del Pero C, Leonforte F. Water flat plate PV–thermal collectors: a review. Sol Energy 2014;102:98–115.
[14] Tripanagnostopoulos Y. Aspects and improvements of hybrid photovoltaic/thermal solar energy systems. Sol Energy 2007;81:1117–31.
[15] Chemisana D. Building integrated concentrating photovoltaics: a review. Renew Sust Energ Rev 2011;15:603–11.
[16] Pérez-Higueras P, Muñoz E, Almonacid G, Vidal PG. High concentrator photovoltaics efficiencies: present status and forecast. Renew Sust Energ Rev 2011;15:1810–5.
[17] Imenes AG, Mills DR. Spectral beam splitting technology for increased conversion efficiency in solar concentrating systems: a review. Sol Energ Mat Sol C. 2004;84:19–69.
[18] Chow TT. A review on photovoltaic/thermal hybrid solar technology. Appl Energy 2010;87:365–79.
[19] Sharaf OZ, Orhan MF. Concentrated photovoltaic thermal (CPVT) solar collector systems: part II – Implemented systems, performance assessment, and future directions. Renew Sust Energ Rev 2015;50:1566–633.
[20] Sharaf OZ, Orhan MF. Concentrated photovoltaic thermal (CPVT) solar collector systems: part I – Fundamentals, design considerations and current technologies. Renew Sust Energ Rev 2015;50:1500–65.
[21] Zhang L, Jing D, Zhao L, Wei J, Guo L. Concentrating PV/T hybrid system for simultaneous electricity and usable heat generation: a review. Int J Photoenergy 2012;2012:869753.
[22] Chow TT, Tiwari GN, Menezo C. Hybrid solar: a review on photovoltaic and thermal power integration. Int J Photoenergy 2012;2012:307287.
[23] Zhang X, Zhao X, Smith S, Xu J, Yu X. Review of R&D progress and practical application of the solar photovoltaic/thermal (PV/T) technologies. Renew Sust Energ Rev 2012;16:599–617.
[24] Hasan MA, Sumathy K. Photovoltaic thermal module concepts and their performance analysis: a review. Renew Sust Energ Rev 2010;14:1845–59.
[25] Shan F, Tang F, Cao L, Fang G. Performance evaluations and applications of photovoltaic–thermal collectors and systems. Renew Sust Energ Rev 2014;33:467–83.
[26] Tyagi VV, Kaushik SC, Tyagi SK. Advancement in solar photovoltaic/thermal (PV/T) hybrid collector technology. Renew Sust Energ Rev 2012;16:1383–98.
[27] Pikk P, Annuk A. Overview of photovoltaic-thermal collector cooling technologies in northern latitudes. 2012.
[28] Dupeyrat P, Helmers H, Fortuin S, Kramer K. Recent advances in the development and testing of hybrid pv-thermal collectors. In: Proceedings of ISES solar world congress 2011. p. 4548–59.
[29] Avezov R, Akhatov J, Avezova N. A review on photovoltaic-thermal (PV-T) air and water collectors. Appl Solar Energy 2011;47:169–83.
[30] Singh B, Othman MY. A review on photovoltaic thermal collectors. J Renew Sustain Energy 2009;1:062702.
[31] Charalambous PG, Maidment GG, Kalogirou SA, Yiakoumetti K. Photovoltaic thermal (PV/T) collectors: a review. Appl Therm Eng 2007;27:275–86.
[32] Ju X, Xu C, Han X, Du X, Wei G, Yang Y. A review of the concentrated photovoltaic/thermal (CPVT) hybrid solar systems based on the spectral beam splitting technology. Appl Energy 2017;187:534–63.
[33] Meng X, Xia X, Sun C, Li Y, Li X. A novel free-form Cassegrain concentrator for PV/T combining utilization. Sol Energy 2016;135:864–73.
[34] Ju X, Xu C, Du X, Yang Y, Wang Z. One kind of CPV solar thermal combined cycle power generation system. Google Patents; 2015.
[35] Han X, Zhao G, Xu C, Ju X, Du X, Yang Y. Parametric analysis of a hybrid solar concentrating photovoltaic/concentrating solar power (CPV/CSP) system. Appl Energy 2017;189:520–33.
[36] Han X, Xu C, Ju X, Du X, Yang Y. Energy analysis of a hybrid solar concentrating photovoltaic/concentrating solar power (CPV/CSP) system. Sci Bull 2015;60:460–9.
[37] Branz HM, Regan W, Gerst KJ, Borak JB, Santori EA. Hybrid solar converters for maximum exergy and inexpensive dispatchable electricity. Energy Environ Sci 2015.

[38] Branz HM. Full-spectrum optimized conversion and utilization of sunlight (FOCUS) program. 20th solar power and chemical energy systems conference (SolarPACES 2014) Beijing, China, 2014.
[39] DeJarnette D, Otanicar T, Brekke N, Hari P, Roberts K, Saunders AE, et al. Plasmonic nanoparticle based spectral fluid filters for concentrating PV/T collectors. In: Proc SPIE 9175, high and low concentrator systems for solar energy applications IX. San Diego, CA, USA: International Society for Optics and Photonics; 2014. p. 917509.
[40] Al-Baali AA. Improving the power of a solar panel by cooling and light concentrating. Sol Wind Technol 1986;3:241–5.
[41] Haddad S, Touafek K, Tabet I, Amirat Y. Investigation of a concentrating photovoltaic thermal collector (CPVT) system. In: 2016 eleventh international conference on ecological vehicles and renewable energies (EVER). p. 1–6.
[42] Garg HP, Agarwal RK, Kumar Bhargava A. The effect of plane booster reflectors on the performance of a solar air heater with solar cells suitable for a solar dryer. Energy Convers Manage 1991;32:543–54.
[43] Ziapour BM, Palideh V, Mokhtari F. Performance improvement of the finned passive PVT system using reflectors like removable insulation covers. Appl Therm Eng 2016;94:341–9.
[44] He W, Zhou J, Chen C, Ji J. Experimental study and performance analysis of a thermoelectric cooling and heating system driven by a photovoltaic/thermal system in summer and winter operation modes. Energy Convers Manage 2014;84:41–9.
[45] Du B, Hu E, Kolhe M. Performance analysis of water cooled concentrated photovoltaic (CPV) system. Renew Sust Energ Rev 2012;16:6732–6.
[46] Chaabane M, Mhiri H, Bournot P. Performance optimization of water-cooled concentrated photovoltaic system. Heat Transfer Eng 2015;1–6.
[47] Robles-Ocampo B, Ruíz-Vasquez E, Canseco-Sánchez H, Cornejo-Meza RC, Trápaga-Martínez G, García-Rodriguez FJ, et al. Photovoltaic/thermal solar hybrid system with bifacial PV module and transparent plane collector. Sol Energ Mat Sol C 2007;91:1966–71.
[48] Ibrahim EE-S, Khalil T. An experimental study of a composite photovoltaic/thermal collector with a tracking concentrator system. World Appl Sci J 2014;31:988–92.
[49] Gurel AE. Exergetic assessment of a concentrated photovoltaic thermal (CPV/T) system. Int J Exergy 2016;21:127–35.
[50] Tripanagnostopoulos Y, Nousia T, Souliotis M, Yianoulis P. Hybrid photovoltaic/thermal solar systems. Sol Energy 2002;72:217–34.
[51] Tripanagnostopoulos Y, Souliotis M, Battisti R, Corrado A. Energy, cost and LCA results of PV and hybrid PV/T solar systems. Prog Photovolt: Res Appl 2005;13:235–50.
[52] Tripanagnostopoulos Y, Georgostathis P, Iliopoulou A. Optical study of new designs for CPVT systems. International conference on concentrating-PV Darmstadt, Germany, 2009.
[53] Kostić LT, Pavlović TM, Pavlović ZT. Optimal design of orientation of PV/T collector with reflectors. Appl Energy 2010;87:3023–9.
[54] Huang BJ, Lin TH, Hung WC, Sun FS. Performance evaluation of solar photovoltaic/thermal systems. Sol Energy 2001;70:443–8.
[55] Kostic LT, Pavlovic TM, Pavlovic ZT. Influence of reflectance from flat aluminum concentrators on energy efficiency of PV/Thermal collector. Appl Energy 2010;87:410–6.
[56] Garg HP, Agarwal RK, Joshi JC. Experimental study on a hybrid photovoltaic-thermal solar water heater and its performance predictions. Energy Convers Manage 1994;35:621–33.
[57] Künnemeyer R, Anderson TN, Duke M, Carson JK. Performance of a V-trough photovoltaic/thermal concentrator. Sol Energy 2014;101:19–27.
[58] Gilbert R. Low concentrating photovoltaic thermal solar collector. Google Patents; 2010.
[59] Hedayatizadeh M, Ajabshirchi Y, Sarhaddi F, Safavinejad A, Farahat S, Chaji H. Thermal and electrical assessment of an integrated solar photovoltaic thermal (PV/T) water collector equipped with a compound parabolic concentrator (CPC). Int J Green Energy 2013;10:494–522.
[60] Cheng X, Xu X, Liang X. Analysis of a concentrating photovoltaic/thermal solar system. In: Goswami DY, Zhao YW, editors. Proceedings of ISES solar world congress 2007: solar energy and human settlement. p. 1386–90.
[61] Garg HP, Adhikari RS. Performance analysis of a hybrid photovoltaic/thermal (PV/T) collector with integrated CPC troughs. Int J Energy Res 1999;23:1295–304.
[62] Garg HP, Adhikari RS. Optical design calculations for CPCs. Energy 1998;23:907–10.
[63] Redpath DAG, Singh H, Tierney C, Dalzell P. An experimental comparison of two solar photovoltaic-thermal (PVT) energy conversion systems for production of heat and power. Energy Power 2012;2:46–50.
[64] Othman MYH, Yatim B, Sopian K, Abu Bakara MN. Performance analysis of a double-pass photovoltaic/thermal (PV/T) solar collector with CPC and fins. Renew Energy 2005;30:2005–17.
[65] Alfegi EMA, Sopian K, Othman MYH, Yatim BB. Transient mathematical model of both side single pass photovoltaic thermal air collector. J Eng Appl Sci 2007;2.
[66] Alfegi MEA, Sopian K, Othman MYH, Yatim BB. Experimental investigation of single pass, double duct photovoltaic thermal (PV/T) air collector with CPC and fins. Am J Appl Sci 2008;5:866–71.
[67] Elsafi AM, Gandhidasan P. Comparative study of double-pass flat and compound parabolic concentrated photovoltaic–thermal systems with and without fins. Energy Convers Manage 2015;98:59–68.
[68] Sun J, Shi M. Numerical study on optical and electric-thermal performance for solar concentrating PV/T air system. Sci China Ser E 2009;52:3514–20.
[69] Sun J, Shi M. Numerical simulation of electric-thermal performance of a solar concentrating photovoltaic, thermal system. Asia-Pacific Power and Energy. Engineering Conference 2009;2009:672–5.
[70] Sun J, Wang Y. Numerical simulation of heat transfer of a concentrating solar photovoltaic system. In: Asia-Pacific power and energy engineering conference. p. 1–4.
[71] Atheaya D, Tiwari A, Tiwari GN, Al-Helal IM. Analytical characteristic equation for partially covered photovoltaic thermal (PVT) compound parabolic concentrator (CPC). Sol Energy 2015;111:176–85.
[72] Atheaya D, Tiwari A, Tiwari GN. Exergy analysis of photovoltaic thermal (PVT) compound parabolic concentrator (CPC) for constant collection temperature mode. Sol Energy 2016;135:222–31.
[73] Atheaya D, Tiwari A, Tiwari GN, Al-Helal IM. Performance evaluation of inverted absorber photovoltaic thermal compound parabolic concentrator (PVT-CPC): constant flow rate mode. Appl Energy 2016;167:70–9.
[74] Tripathi R, Tiwari GN, Al-Helal IM. Thermal modelling of N partially covered photovoltaic thermal (PVT) – Compound parabolic concentrator (CPC) collectors connected in series. Sol Energy 2016;123:174–84.
[75] Tripathi R, Tiwari GN, Dwivedi VK. Overall energy, exergy and carbon credit analysis of N partially covered Photovoltaic Thermal (PVT) concentrating collector connected in series. Sol Energy 2016;136:260–7.
[76] Tripathi R, Tiwari S, Tiwari GN. Energy analysis of partially covered number (N) of photovoltaic thermal-compound parabolic concentrator collectors connected in series at constant collection temperature mode. In: 2016 international conference on emerging trends in electrical electronics & sustainable energy systems (ICETEESES). p. 12–7.
[77] Tripathi R, Tiwari GN. Energetic and exergetic analysis of N partially covered photovoltaic thermal-compound parabolic concentrator (PVT-CPC) collectors connected in series. Sol Energy 2016;137:441–51.
[78] Jiang L, Lan C, Kim Y, Ma Y, Winston R. An evacuated PV/thermal hybrid collector with the tube/XCPC design. In: Proceedings of world renewable energy forum 2012 (WREF 2012). p. 88–94.
[79] Jiang L, Winston R. Solar receiver with integrated optics. Proceedings of SPIE – nonimaging optics: efficient design for illumination and solar concentration IX, 2012. p. 84850D.
[80] Jiang L, Kim S, Winston R. A vacuum PV/thermal hybrid collector with CPC-tube design; 2012.
[81] Li G, Gang P, Su Y, Xi Z, Jie J. Preliminary study based on building-integrated compound parabolic concentrators (CPC) PV/thermal technology. In: Zeng D, editor. 2011 2nd international conference on advances in energy engineering. p. 343–50.
[82] Proell M, Reuss M, Schoelkopf W, et al. Maximum efficiency of low concentrating PV-T collectors and optical boundary conditions. In: Proceedings of ISES solar world congress. p. 2631–8.
[83] Proell M, Hilt M. The significance of the fluid to PV thermal coupling in a CPC PVT collector. Energy Procedia 2014;57:3120–9.
[84] Al Imam MFI, Beg RA, Rahman MS, Khan MZH. Performance of PVT solar collector with compound parabolic concentrator and phase change materials. Energy Build 2016;113:139–44.
[85] Brogren M, Nostell P, Karlsson B. Optical efficiency of a PV–thermal hybrid CPC module for high latitudes. Sol Energy 2001;69(Supplement 6):173–85.
[86] Brogren M. Optical efficiency of low-concentrating solar energy systems with parabolic reflectors [PhD Thesis]. Acta Universitatis Upsaliensis; 2004.
[87] Xie H, Wei J, Wang Z, Liu Z, Gao Y, Ma Q, et al. Design and performance study of truncated CPC by eliminating multiple reflections of solar radiation in hybrid CPV/T system: highest and lowest truncation position. Sol Energy 2016;136:217–25.
[88] Xie H, Wei J, Wang Z, Yang G, Ma Q. Design and performance research on eliminating multiple reflections of solar radiation within compound parabolic concentrator (CPC) in hybrid CPV/T system. Sol Energy 2016;129:126–46.
[89] Li G, Pei G, Yang M, Ji J, Su Y. Optical evaluation of a novel static incorporated compound parabolic concentrator with photovoltaic/thermal system and preliminary experiment. Energy Convers Manage 2014;85:204–11.
[90] Li G, Pei G, Ji J, Su Y. Outdoor overall performance of a novel air-gap-lens-walled compound parabolic concentrator (ALCPC) incorporated with photovoltaic/thermal system. Appl Energy 2015;144:214–23.
[91] Li G, Pei G, Ji J, Yang M, Su Y, Xu N. Numerical and experimental study on a PV/T system with static miniature solar concentrator. Sol Energy 2015;120:565–74.
[92] Cui W, Zhao L, Wu W, Wang K, Jen T-C. Asme. Energy efficiency of a quasi CPC concentrating solar PV/T system. In: Proceedings of the ASME 2010 international mechanical engineering congress and exposition. p. 1071–6.
[93] Nilsson J, Håkansson H, Karlsson B. Electrical and thermal characterization of a PV-CPC hybrid. Sol Energy 2007;81:917–28.
[94] Gomes J, Diwan L, Bernardo R, Karlsson B. Minimizing the impact of shading at oblique solar angles in a fully enclosed asymmetric concentrating PVT collector. Energy Procedia 2014;57:2176–85.
[95] Ricardo B, Henrik D, Niko G, Christian G, Luis C, Chabu M. Measurements of the electrical incidence angle modifiers of an asymmetrical photovoltaic/thermal compound parabolic concentrating-collector. Engineering 2013;5:37.
[96] Fernandes CAF, Torres JPN, Gomes J, Costa Branco PJ, Nashih SK. Stationary solar concentrating photovoltaic-thermal collector-cell string layout. In: IEEE

International power electronics and motion control conference (PEMC) Varna, Bulgaria. p. 1275–82.
[97] Chaabane M, Charfi W, Mhiri H, Bournot P. Performance evaluation of concentrating solar photovoltaic and photovoltaic/thermal systems. Sol Energy 2013;98:315–21.
[98] Brogren M, Wennerberg J, Kapper R, Karlsson B. Design of concentrating elements with CIS thin-film solar cells for façade integration. Sol Energ Mat Sol C 2003;75:567–75.
[99] Brogren M, Karlsson B. Low-concentrating water-cooled PV-thermal hybrid systems for high latitudes. In: 2002 29th IEEE photovoltaic specialists conference (PVSC). p. 1733–6.
[100] Davidsson H, Perers B, Karlsson B. Performance of a multifunctional PV/T hybrid solar window. Sol Energy 2010;84:365–72.
[101] Pihl E, Thapper C, Nilsson J. Evaluation of the concentrating PVT systems MaReCo and Solar8; 2006.
[102] Bernardo LR, Perers B, Ha Kansson H, Karlsson B. Evaluation of the concentrating PVT system Solar 8. Proceedings of Eurosun 2008 Lisbon, Portugal, 2008.
[103] Bernardo LR, Perers B, Hakansson H, Karlsson B. Performance evaluation of low concentrating photovoltaic/thermal systems: a case study from Sweden. Sol Energy 2011;85:1499–510.
[104] Tripanagnostopoulos Y, Siabekou C, Tonui JK. The Fresnel lens concept for solar control of buildings. Sol Energy 2007;81:661–75.
[105] Tripanagnostopoulos Y, Souliotis M, Tonui J, Kavga A. Irradiation aspects for energy balance in greenhouses. In: International conference on sustainable greenhouse systems (Greensys2004). p. 733–40.
[106] Chemisana D, Ibáñez M, Rosell JI. Characterization of a photovoltaic-thermal module for Fresnel linear concentrator. Energy Convers Manage 2011;52:3234–40.
[107] Chemisana D, Lamnatou C, Tripanagnostopoulos Y. The effect of Fresnel lens – solar absorber systems in greenhouses. Acta Hortic 2012;952:425–32.
[108] Chemisana D, Lamnatou C, Tripanagnostopoulos Y. Fresnel solar concentrators for agriculture applications. In: International conference of agricultural engineering CIGR (AgEng2012). p. C-2195.
[109] Kong C, Xu Z, Yao Q. Outdoor performance of a low-concentrated photovoltaic–thermal hybrid system with crystalline silicon solar cells. Appl Energy 2013;112:618–25.
[110] Li M, Ji X, Li G, Wei S, Li Y, Shi F. Performance study of solar cell arrays based on a trough concentrating photovoltaic/thermal system. Appl Energy. 2011;88:3218–27.
[111] Adeilla S, Sellami N, Tapas M. Experimental performance of concentrating photovoltaic thermal module. In: 7th international renewable energy congress Hammamet, Tunisia. p. 1–6.
[112] Swinkels GLAM, Sonneveld PJ, van Tuijl BAJ, Janssen HJJ, de Zwart HF. A concentrator system for BI-CPVT with static linear Fresnel lenses. In: 26th European photovoltaic solar energy conference and exhibition. p. 4179–83.
[113] Kerzmann TL, Schaefer LA. An energy analysis of a linear concentrating photovoltaic system with an active cooling system. In: High and low concentrator systems for solar electric applications V. p. 121–6.
[114] Xu Y, Wang CY, Hua YM, Zhang YM. Studies on a low concentration photovoltaic/thermal system with constant volume refrigeration. Key Eng Mater: Trans Tech Publ 2012:776–83.
[115] Sharan SN, Mathur SS, Kandpal TC. Analysis of an actively cooled photovoltaic-thermal solar concentrator receiver system using a fin-type absorber. Solar Wind Technol 1986;3:281–5.
[116] Sharan SN, Kandpal TC. Testing of a prototype combined photovoltaic-thermal linear fresnel concentrator-receiver system. Energy Convers Manage 1992;33:37–9.
[117] Sonneveld PJ, Swinkels GLAM, van Tuijl BAJ, Janssen HJJ, Campen J, Bot GPA. Performance of a concentrated photovoltaic energy system with static linear Fresnel lenses. Sol Energy 2011;85:432–42.
[118] Sonneveld PJ, Swinkels GLAM, Van Tuijl BAJ, Janssen H, De Zwart HF. Up scaling and test results of an advanced Fresnel greenhouse. In: International symposium on advanced technologies and management towards sustainable greenhouse ecosystems (Greensys2011). p. 531–7.
[119] Sonneveld PJ, Swinkels GLAM, van Tuijl BAJ, Janssen HJJ, de Zwart HF. Static linear Fresnel lenses as LCPV system in a greenhouse. In: 7th international conference on concentrating photovoltaic systems: CPV-7. AIP Publishing; 2011. p. 158–62.
[120] Kerzmann T, Schaefer L. Flow rate optimization of a linear concentrating photovoltaic system. J Sol Energy-t Asme 2013;135:021009.
[121] Kerzmann T, Schaefer L. System simulation of a linear concentrating photovoltaic system with an active cooling system. Renew Energy 2012;41:254–61.
[122] Jaffré D, Gualdi F, Sicre M, El Ouamari R, Dollet A, Baud G, et al. Design and characterization of a curved linear Fresnel lens concentrating photovoltaic and thermal system. In: AIP conference proceedings. p. 173–6.
[123] Feng C, Zheng H, Wang R, Ma X. Performance investigation of a concentrating photovoltaic/thermal system with transmissive Fresnel solar concentrator. Energy Convers Manage 2016;111:401–8.
[124] Rosell JI, Vallverdu X, Lechon MA, Ibanez M. Design and simulation of a low concentrating photovoltaic/thermal system. Energy Convers Manage 2005;46:3034–46.
[125] Vivar M, Everett V, Fuentes M, Blakers A, Tanner A, Le Lievre P, et al. Initial field performance of a hybrid CPV-T microconcentrator system. Prog Photovolt: Res Appl 2013;21:1659–71.
[126] Everett V, Harvey J, Surve S, Thomsen E, Walter D, Vivar M, et al. Evaluation of electrical and thermal performance of a linear hybrid CPV-T micro-concentrator system. In: AIP conference proceedings. p. 262–5.
[127] Everett V, Walter D, Harvey J, Vivar M, Van Scheppingen R, Surve S, et al. A linear Fresnel hybrid PV/thermal micro-concentrator system for rooftop Integration. In: 25th European photovoltaic solar energy conference and exhibition/5th world conference on photovoltaic energy conversion. p. 3937–41.
[128] Everett V, Greaves M, Harvey J, Lievre PL, Surve S, Tanner A, et al. Evaluation of performance and reliability for components of a linear hybrid micro-concentrator system. In: AIP conference proceedings. p. 317–20.
[129] Vivar M, Everett V, Fuentes M, Thomsen E, Harvey J, Ebert M, et al. Results from the first ANU-chromasun CPV-T microconcentrator prototype in Canberra. In: 8th international conference on concentrating photovoltaic systems: CPV-8. AIP Publishing; 2012. p. 114–7.
[130] Walter D, Everett V, Blakers A, Vivar M, Harvey J, Muric-Nesic J, et al. A 20-sun hybrid PV-Thermal linear micro-concentrator system for urban rooftop applications. 2010 35th IEEE photovoltaic specialists conference (PVSC). IEEE; 2010. p. 000831–6.
[131] Everett V, Walter D, Harvey J, Vivar M, Van Scheppingen R, Surve S, et al. A closed loop tracking system for a linear Fresnel hybrid PV/thermal micro-concentrator system. In: 25th European photovoltaic solar energy conference and exhibition/5th world conference on photovoltaic energy conversion. p. 1063–5.
[132] Chatterjee A, Bernal E, Seshadri S, Mayer O, Greaves M, Dimroth F, et al. Linear Fresnel reflector based solar radiation concentrator for combined heating and power. In: AIP conference proceedings. p. 257.
[133] Chemisana D, Rosell JI. Design and optical performance of a nonimaging Fresnel transmissive concentrator for building integration applications. Energy Convers Manage 2011;52:3241–8.
[134] Chemisana D, Rosell JI, Riverola A, Lamnatou C. Experimental performance of a Fresnel-transmission PVT concentrator for building-façade integration. Renew Energy 2016;85:564–72.
[135] Sonneveld PJ, Swinkels GLAM, van Tuijl BAJ, Janssen H. Design of a NIR-concentrator system integrated in a greenhouse. In: Kittas C, Katsoulas N, Bartzanas T, editors. International symposium on advanced technologies and management towards sustainable greenhouse ecosystems (Greensys2011). p. 523–9.
[136] Swinkels GLAM, Sonneveld PJ, van Tuijl BAJ, Janssen HJJ. A spectral selective lamellae concentrator system as BI-CPV/T System. In: Proceedings of the 26th European photovoltaic solar energy conference and exhibition (26th EU PVSEC). p. 3791–4.
[137] Sonneveld PJ, Swinkels GLAM, Bot GPA, Flamand G. Feasibility study for combining cooling and high grade energy production in a solar greenhouse. Biosyst Eng 2010;105:51–8.
[138] Gibart C. Study of and tests on a hybrid photovoltaic-thermal collector using concentrated sunlight. Sol Cells 1981;4:71–89.
[139] Coventry JS, Franklin E, Blakers A. Thermal and electrical performance of a concentrating PV/Thermal collector: results from the ANU CHAPS collector. 40th ANZSES conference: Newcastle, Australia; 2002.
[140] Coventry J. Simulation of a concentrating PV/thermal collector using TRNSYS. 40th ANZSES conference. Newcastle, Australia; 2002.
[141] Coventry JS. Performance of a concentrating photovoltaic/thermal solar collector. Sol Energy 2005;78:211–22.
[142] Smeltink JFH, Blakers AW. 40kW PV Thermal roof mounted concentrator system. In: 2006 IEEE 4th world conference on photovoltaic energy conversion. IEEE; 2006. p. 636–9.
[143] Li M, Li GL, Ji X, Yin F, Xu L. The performance analysis of the trough concentrating solar photovoltaic/thermal system. Energy Convers Manage 2011;52:2378–83.
[144] Xu Y, Li M, Wang L, Lin W, Zhang X, Xiang M, et al. The effect of concentrated light intensity on output performance of solar cell arrays. Acta Phys Sin-ch Ed 2009;58:8067–76.
[145] Li M, Ji X, Li GL, Yang ZM, Wei SX, Wang LL. Performance investigation and optimization of the Trough Concentrating Photovoltaic/Thermal system. Sol Energy 2011;85:1028–34.
[146] Ji X, Li M, Lin W, Wang W, Wang L, Luo X. Modeling and characteristic parameters analysis of a trough concentrating photovoltaic/thermal system with GaAs and super cell arrays. Int J Photoenergy 2012;2012:782560.
[147] Tan L, Ji X, Li M, Leng C, Luo X, Li H. The experimental study of a two-stage photovoltaic thermal system based on solar trough concentration. Energy Convers Manage 2014;86:410–7.
[148] Ji X, Tan L, Li M, Tang R, Wang Y, Song X, et al. Improvement of energy comprehensive utilization in a solar trough concentrating PV/T system. J Energ Eng. 2016;142.
[149] Niedermeyer WP. Parabolic trough solar collector for fluid heating and photovoltaic cells. Google Patents; 2008.
[150] Gerwing DH. GHG reduction and economics of scaleable concentrating solar co-generation systems. In: 2006 IEEE EIC climate change conference. p. 567–74.
[151] Calise F, Vanoli L. Parabolic trough photovoltaic/thermal collectors: design and simulation model. Energies 2012;5:4186–208.
[152] Calise F, Palombo A, Vanoli L. A finite-volume model of a parabolic trough photovoltaic/thermal collector: energetic and exergetic analyses. Energy. 2012;46:283–94.

[153] Reatti A, Kazimierczuk MK, Catelani M, Ciani L. Linear solar PV/T concentrator monitoring system and derivation of performance index. In: 2015 IEEE international instrumentation and measurement technology conference (I2MTC). p. 1285–90.
[154] Cappelletti A, Reatti A, Martelli F. Numerical and experimental analysis of a CPV/T receiver suitable for low solar concentration factors. In: Corsini A, Rispoli F, DeSantoli L, editors. 70th conference of the Italian Thermal Machines Engineering Association (Ati2015). p. 724–9.
[155] Cappelletti A, Catelani M, Ciani L, Kazimierczuk MK, Reatti A. Practical issues and characterization of a photovoltaic/thermal linear focus 20x solar concentrator. Ieee T Instrum Meas 2016;65:2464–75.
[156] Geng WG, Gao L, Ma XX, Ma XL, Yu ZY, Li XY. Honeysuckle drying by using hybrid concentrator photovoltaic-thermal (PV/T) dryer: an experimental study. In: Tang X, Chen X, Dong Y, Wei X, Yang Q, editors. Advances in energy science and technology. p. 132–6.
[157] Sonneveld PJ, Swinkels GLAM, Campen J, van Tuijl BAJ, Janssen HJJ, Bot GPA. Performance results of a solar greenhouse combining electrical and thermal energy production. Biosyst Eng 2010;106:48–57.
[158] Manokar AM, Winston DP, Vimala M. Performance analysis of parabolic trough concentrating photovoltaic thermal system. In: International conference on emerging trends in engineering, science and technology (Icetest – 2015). p. 485–91.
[159] Su Y, Kulacki FA, Davidson JH. Experimental and numerical investigations on a solar tracking concentrated photovoltaic–thermal system with a novel non-dimensional lattice Boltzmann method. Sol Energy 2014;107:145–58.
[160] Radwan A, Ookawara S, Ahmed M. Analysis and simulation of concentrating photovoltaic systems with a microchannel heat sink. Sol Energy 2016;136:35–48.
[161] Sharan SN, Mathur SS, Kandpal TC. Analysis of a combined photovoltaic-thermal system consisting of a linear solar concentrator and a tubular absorber. Energy Convers Manage 1987;27:55–9.
[162] Sharan SN, Mathur SS, Kandpal TC. Analytical performance evaluation of combined photovoltaic-thermal concentrator-receiver systems with linear absorbers. Energy Convers Manage 1987;27:361–5.
[163] Araki K, Yano T, Kuroda Y. 30 kw concentrator photovoltaic system using dome-shaped Fresnel lenses. Opt Express 2010;18:53–63.
[164] O'Leary MJ, Clements LD. Thermal-electric performance analysis for actively cooled, concentrating photovoltaic systems. Sol Energy 1980;25:401–6.
[165] Del Col D, Bortolato M, Padovan A, Quaggia M. Experimental and numerical study of a parabolic trough linear cpvt system. Energy Procedia 2014;57:255–64.
[166] Quaia S, Lughi V, Giacalone M, Vinzi G. Technical-economic evaluation of a Combined Heat And Power Solar (CHAPS) generator based on concentrated photovoltaics. In: 2012 international symposium on power electronics, electrical drives, automation and motion (SPEEDAM). IEEE; 2012. p. 1130–5.
[167] Rumyantsev VD. Terrestrial concentrator PV systems. Springer Ser Opt Sci 2007;130:151.
[168] Mbewe DJ, Card HC, Card DC. A model of silicon solar cells for concentrator photovoltaic and photovoltaic/thermal system design. Sol Energy 1985;35:247–58.
[169] Arab Re, Awad Y, Grumazescu M. Concentrated photovoltaic and thermal system. Google Patents; 2011.
[170] Rumyantsev VD, Andreev VM, Chekalin AV, Davidyuk NY, Sadchikov NA. HCPV modules of SMALFOC design in versions for PV and PV/T operation. In: 2014 40th IEEE photovoltaic specialists conference (PVSC). p. 2720–3.
[171] Imtiaz Hussain M, Lee GH. Experimental and numerical studies of a U-shaped solar energy collector to track the maximum CPV/T system output by varying the flow rate. Renew Energy 2015;76:735–42.
[172] Imtiaz Hussain M, Lee GH. Parametric performance analysis of a concentrated photovoltaic co-generation system equipped with a thermal storage tank. Energy Convers Manage 2015;92:215–22.
[173] Hussain MI, Ali A, Lee GH. Multi-module concentrated photovoltaic thermal system feasibility for greenhouse heating: model validation and techno-economic analysis. Sol Energy 2016;135:719–30.
[174] Renno C, Petito F. Experimental and theoretical model of a concentrating photovoltaic and thermal system. Energy Convers Manage 2016;126:516–25.
[175] Xu N, Ji J, Sun W, Huang W, Li J, Jin Z. Numerical simulation and experimental validation of a high concentration photovoltaic/thermal module based on point-focus Fresnel lens. Appl Energy 2016;168:269–81.
[176] Kribus A, Kaftori D, Mittelman G, Hirshfeld A, Flitsanov Y, Dayan A. A miniature concentrating photovoltaic and thermal system. Energy Convers Manage 2006;47:3582–90.
[177] Chayet H, Kost O, Moran R, Lozovsky I. Efficient, low cost dish concentrator for a CPV based cogeneration system. In: AIP conference proceedings: AIP. p. 249–52.
[178] Chayet H, Lozovsky I, Kost O, Loeckenhoff R, Rasch K-D. High efficiency, low cost parabolic dish system for cogeneration of electricity and heat. In: AIP conference proceedings: AIP. p. 175–8.
[179] Moran R, Chayet H, Kost O. Solar electricity generation system. Google Patents; 2012.
[180] Lockenhoff R, Kubera T, Rasch KD. Water cooled TJ dense array modules for parabolic dishes. In: AIP conference proceedings: AIP. p. 43–6.
[181] Polonsky G, Shelef G, Flitsanov Y, Wiesenfarth M, Steiner M, Helmers H, et al. Efficiency of dense-array CPVT module with front-side interconnected cells. In: AIP conference proceedings. p. 180–4.
[182] Helmers H, Boos A, Jetter F, Heimsath A, Wiesenfarth M, Bett AW. Outdoor test setup for concentrating photovoltaic and thermal (CPVT) systems. In: 7th international conference on concentrating photovoltaic systems (CPV-7). p. 175–9.
[183] Helmers H, Kramer K. Multi-linear performance model for hybrid (C)PVT solar collectors. Sol Energy 2013;92:313–22.
[184] Helmers H, Thor WY, Schmidt T, van Rooyen DW, Bett AW. Optical analysis of deviations in a concentrating photovoltaics central receiver system with a flux homogenizer. Appl Optics 2013;52:2974–84.
[185] Zimmermann S, Helmers H, Tiwari MK, Paredes S, Michel B, Wiesenfarth M, et al. A high-efficiency hybrid high-concentration photovoltaic system. Int J Heat Mass Tran 2015;89:514–21.
[186] Escher W, Brunschwiler T, Michel B, Poulikakos D. Experimental Investigation of an Ultrathin Manifold Microchannel Heat Sink for Liquid-Cooled Chips. J Heat Trans-t ASME 2010;132:081402–81410.
[187] Escher W, Michel B, Poulikakos D. A novel high performance, ultra thin heat sink for electronics. Int J Heat Fluid Fl 2010;31:586–98.
[188] Kronland MJ, Leak NB, Randall JE, Womack CD, ElSawy AE. An investigation into combined concentrated photovoltaic and fluidic thermal extraction in harnessing the power of the sun. In: 2015 5th international youth conference on energy (IYCE). p. 1–5.
[189] Renno C, De Giacomo M. Dynamic simulation of a CPV/T system using the finite element method. Energies 2014;7:7395.
[190] Renno C, Petito F. Choice model for a modular configuration of a point-focus CPV/T system. Energy Build 2015;92:55–66.
[191] Renno C, Miranda S, Petito F. Inefficiencies analysis of a point-focus CPV/T system. Int J Green Energy 2016;13:918–29.
[192] Gholami H, Sarwat AI, Hosseinian H, Khalilnejad A. Evaluation of optimal dual axis concentrated photovoltaic thermal system with active ventilation using Frog Leap algorithm. Energy Convers Manage 2015;105:782–90.
[193] Helmers H, Bett AW, Parisi J, Agert C. Modeling of concentrating photovoltaic and thermal systems. Prog Photovolt Res Appl 2014;22:427–39.
[194] Bar-Lev A, Waks S, Grossman G. Analysis of a combined thermal-photovoltaic solar system based on the spherical reflector/tracking absorber concentrator. J Sol Energ-t Asme 1983;105:322–8.
[195] Hagfarah A, Nazarinia M. Fundamental study for the power tower's high concentrated photovoltaic/thermal-combined thermal receiver. Proceedings of the ASME 10th international conference on energy sustainability, 2016. p. V001T04A4.
[196] Siaw F-L, Chong K-K, Wong C-W. A comprehensive study of dense-array concentrator photovoltaic system using non-imaging planar concentrator. Renew Energy 2014;62:542–55.
[197] Escher W, Paredes S, Zimmermann S, Ong CL, Ruch P. Michel B. Thermal management and overall performance of a high concentration PV. In: AIP conference proceedings. p. 239–43.
[198] Kribus A, Mittelman G. Potential of polygeneration with solar thermal and photovoltaic systems. J Sol Energy-t Asme 2008;130:011001.
[199] Petrucci L, Fabbri G, Boccaletti C, Cardoso AJM. Powering and cooling of a server room using a hybrid trigeneration system. Int J Comp Theory Eng 2013;5:263–7.
[200] Garcia-Heller V, Paredes S, Ong CL, Ruch P, Michel B. Exergoeconomic analysis of high concentration photovoltaic thermal co-generation system for space cooling. Renew Sust Energ Rev 2014;34:8–19.
[201] Buonomano A, Calise F, d'Accadia MD, Vanoli L. A novel solar trigeneration system based on concentrating photovoltaic/thermal collectors. Part 1: design and simulation model. Energy. 2013;61:59–71.
[202] Buonomano A, Calise F, Palombo A. Solar heating and cooling systems by CPVT and ET solar collectors: a novel transient simulation model. Appl Energy 2013;103:588–606.
[203] Buonomano A, Calise F, Ferruzzi G, Vanoli L. A novel renewable polygeneration system for hospital buildings: design, simulation and thermo-economic optimization. Appl Therm Eng 2014;67:43–60.
[204] Calise F, d'Accadia MD, Palombo A, Vanoli L. Dynamic simulation of a novel high-temperature solar trigeneration system based on concentrating photovoltaic/thermal collectors. Energy. 2013;61:72–86.
[205] Calise F, d'Accadia MD, Vanoli L. Design and dynamic simulation of a novel solar trigeneration system based on hybrid photovoltaic/thermal collectors (PVT). Energy Convers Manage 2012;60:214–25.
[206] Calise F, Dentice d'Accadia M, Piacentino A. Exergetic and exergoeconomic analysis of a renewable polygeneration system and viability study for small isolated communities. Energy 2015.
[207] Calise F, Dentice d'Accadia M, Piacentino A. A novel solar trigeneration system integrating PVT (photovoltaic/thermal collectors) and SW (seawater) desalination: dynamic simulation and economic assessment. Energy 2014;67:129–48.
[208] Xu G, Zhang X, Deng S. Experimental study on the operating characteristics of a novel low-concentrating solar photovoltaic/thermal integrated heat pump water heating system. Appl Therm Eng 2011;31:3689–95.
[209] Mittelman G, Kribus A, Dayan A. Cogeneration with concentrating photovoltaic systems. In: 2005 international solar energy conference. p. 477–83.
[210] Mittelman G, Kribus A, Dayan A. Solar cooling with concentrating photovoltaic/thermal (CPVT) systems. Energy Convers Manage 2007;48:2481–90.
[211] Al-Alili A, Hwang Y, Radermacher R, Kubo I, Rodgers P. High efficiency solar cooling technique. In: The second international energy 2030 conference. p. 239–51.

[212] Al-Alili A, Hwang Y, Radermacher R, Kubo I. A high efficiency solar air conditioner using concentrating photovoltaic/thermal collectors. Appl Energy 2012;93:138–47.
[213] Al-Alili A, Hwang Y, Radermacher R. Optimization study of a hybrid solar air conditioner. ASME 2013 7th international conference on energy sustainability collocated with the ASME 2013 heat transfer summer conference and the ASME 2013 11th international conference on fuel cell science, engineering and technology. Minneapolis, Minnesota, USA: American Society of Mechanical Engineers; 2013. p. V001T01A8–VT01A8.
[214] Al-Alili A, Hwang Y, Radermacher R. A hybrid solar air conditioner: experimental investigation. Int J Refrig 2014;39:117–24.
[215] Calise F, Dentice d'Accadia M, Roselli C, Sasso M, Tariello F. Desiccant-based AHU interacting with a CPVT collector: simulation of energy and environmental performance. Sol Energy 2014;103:574–94.
[216] Ong CL, Escher W, Paredes S, Khalil ASG, Michel B. A novel concept of energy reuse from high concentration photovoltaic thermal (HCPVT) system for desalination. Desalination 2012;295:70–81.
[217] Hughes AJ, O'Donovan TS, Mallick TK. Experimental evaluation of a membrane distillation system for integration with concentrated photovoltaic/thermal (CPV/T) energy. Energy Procedia 2014;54:725–33.
[218] Mittelman G, Kribus A, Mouchtar O, Dayan A. Water desalination with concentrating photovoltaic/thermal (CPVT) systems. Sol Energy 2009;83:1322–34.
[219] Kelley L, Bilton AM, Dubowsky S. Asme. Enhancing the performance of photovoltaic powered reverse osmosis desalination systems by active thermal management. In: Proceedings of the ASME 2011 international mechanical engineering congress and exposition. p. 427–36.
[220] Wiesenfarth M, Went J, Bösch A, Dilger A, Kec T, Kroll A, et al. CPV-T mirror dish system combined with water desalination systems. AIP conference proceedings, 2016. 1766:020008.
[221] Wilcox JR. Solar cell temperature dependent efficiency and very high temperature efficiency limits [PhD Thesis]. Purdue University; 2013.
[222] Skoplaki E, Palyvos JA. On the temperature dependence of photovoltaic module electrical performance: a review of efficiency/power correlations. Sol Energy 2009;83:614–24.
[223] Shiomi K, Ishio M, Fujita T. Electrode wire for solar battery. Google Patents; 2005.
[224] Perers B, Furbo S, Han J, Kong W, Stergiakis S. Long term testing and evaluation of PV modules with and without Sunarc antireflective coating of the cover glass. Energy Procedia 2015;70:311–7.
[225] Hofmann P, Dupeyrat P, Kramer K, Hermann M, Stryi-Hipp G. Measurements and benchmark of PV-T collectors according to EN12975 and development of a standardized measurement procedure. Proceedings EuroSun, 2010. p. 28.9–1.10.
[226] Royne A, Dey CJ, Mills DR. Cooling of photovoltaic cells under concentrated illumination: a critical review. Sol Energ Mat Sol C 2005;86:451–83.
[227] Segev G, Kribus A. Performance of CPV modules based on vertical multi-junction cells under non-uniform illumination. Sol Energy 2013;88:120–8.
[228] Ben Or A, Appelbaum J. Performance analysis of concentrator photovoltaic dense-arrays under non-uniform irradiance. Sol Energ Mat Sol C 2013;117:110–9.
[229] Escher W, Rami G, Ahmed K, Stephan P, Bruno M. Advanced liquid cooling for concentrated photovoltaic electro thermal co generation. In: 2010 3rd international conference on thermal issues in emerging technologies theory and applications (ThETA 2010) Cairo, Egypt. p. 9–17.
[230] Abdelhamid M, Singh R, Qattawi A, Omar M, Haque I. Evaluation of on-board photovoltaic modules options for electric vehicles. IEEE J Photovolt 2014;4:1576–84.
[231] Abdelhamid M. Comparison of an analytical hierarchy process and fuzzy axiomatic design for selecting appropriate photovoltaic modules for onboard vehicle design. I J Mod Eng 2014;15:23–35.
[232] Kramer K, Helmers H. The interaction of standards and innovation: hybrid photovoltaic–thermal collectors. Sol Energy 2013;98:434–9.
[233] Vivar M, Clarke M, Pye J, Everett V. A review of standards for hybrid CPV-thermal systems. Renew Sust Energ Rev 2012;16:443–8.